

1 **Author's response:**

2 We thank both reviewers for their careful reading of the manuscript and valuable comments  
3 improve the manuscript. A copy of our response, as well as detailed (track changes) manuscript  
4 improvements are given below.

5

6 **Anonymous Referee #1.**

7 **The authors have performed a very detailed analysis of the fundamental kinetics of HOBr uptake**  
8 **kinetics into tropospheric aerosol, both as a function of acidity and halide ion (bromide, chloride)**  
9 **content. In some respects I like this paper, but in others I feel it needs a lot of work. Starting with**  
10 **the good, I agree with the basic hypothesis that under some pH conditions, the general acid**  
11 **assisted mechanism is a more general representation of the reaction kinetics than a simple**  
12 **termolecular representation. There is merit to the paper to point this issue out, which is not**  
13 **currently acknowledged in atmospheric models. Also, there is merit to attempting to reconcile the**  
14 **disparity in the laboratory reaction kinetics presented, which the paper does by illustrating that**  
15 **some of the slow HOBr/chloride kinetics of Pratte and Rossi may be due to chloride displacement**  
16 **at high acidity.**

17 We thank the Reviewer for these positive comments regarding the scope of the manuscript.

18

19 **That being said, there are a number of weaknesses to the paper. First and foremost, it is far too**  
20 **long (starting with the Abstract!) and extremely hard to read. A major rewrite is necessary to**  
21 **make the paper publishable, with a lot of the detailed mechanistic analysis shortened and going**  
22 **into Supplementary Information, and instead clear, major points are left in the manuscript.**  
23 **Currently, the paper is not approachable by an atmospheric modeler, which I see as one of the**  
24 **goals of this type of analysis.**

25 Both reviewers commented on the manuscript style, and the revised version is simplified and  
26 shortened. Details of the revised manuscript outline are summarised at the end of this response.

27 The goal of this manuscript is to point out a major limitation to the approach used by existing  
28 models to simulate reactive bromine chemistry in the troposphere, to provide a new framework  
29 based on a sound mechanistic basis which reconciles reported laboratory data, and to illustrate the  
30 potential implications of the new approach regarding BrO chemistry in marine and volcanic  
31 environments. A long-term aim is to provide and implement a new parameterisation for HOBr  
32 kinetics to improve atmospheric models of BrO chemistry for which this manuscript provides the  
33 first stage.

34

35 **Second, the paper needs to address a number of laboratory papers that looked at the kinetics of**  
36 **HOBr reacting with HCl and HBr in acidic sulfuric acid solutions (notably, Hanson and**  
37 **Ravishankara, GRL, 1995; Waschewsky and Abbatt, JPC-A, 1999) if the model is to be fully**  
38 **evaluated, i.e. how does the model match up against these data. Or, is the acidity too high in**

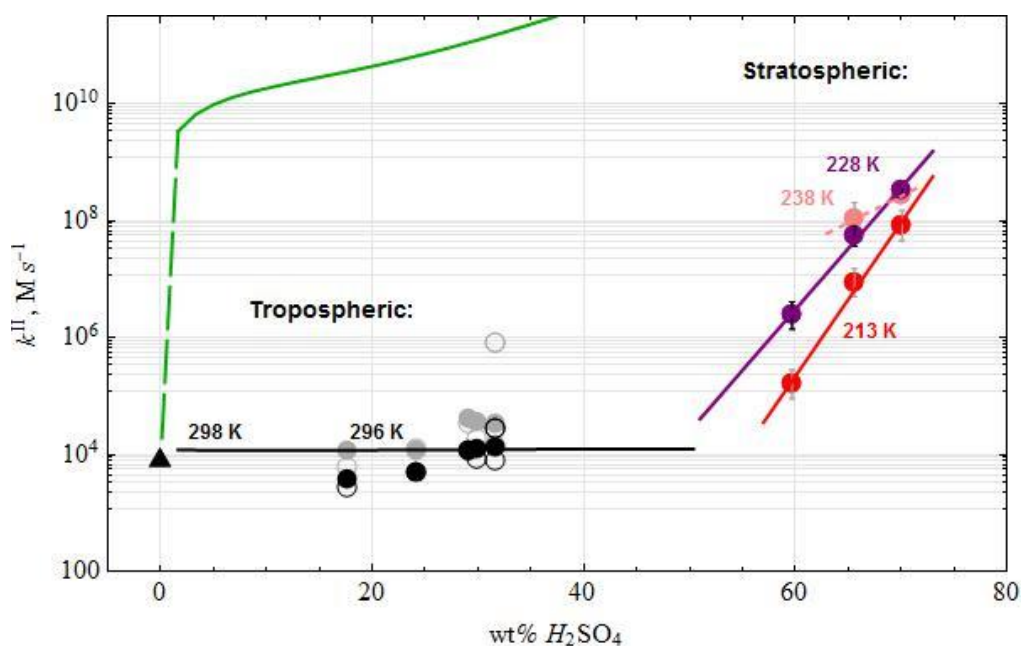
39 **these experiments to make the model not appropriate (i.e. the reaction proceeds at very high**  
40 **acidity through protonation of HOBr initially and not via interaction of HOBr with the halide ion)?**

41 Here we focused on a parameterisation of HOBr reactive uptake in the troposphere. We had indeed  
42 considered our analysis in the context of experimental data for HOBr reactive uptake with HX on  
43 sulphuric acid aerosol at low temperatures (stratospherically relevant) i.e. high wt%H<sub>2</sub>SO<sub>4</sub>, but had  
44 excluded this from the final version of the manuscript in order to improve clarity and brevity.

45 For example, experiments by Waschewsky and Abbatt (1999) were performed at low temperature  
46 (213-238 K) at very high wt%H<sub>2</sub>SO<sub>4</sub> (59.7-70.1 wt%), and identified strong acidity-dependency of the  
47  $k^{\text{II}}$  rate constant and also a temperature dependency. Values for  $k^{\text{II}}$  for HOBr+Cl<sup>-</sup> from these  
48 experiments are between 10<sup>6</sup> and 10<sup>9</sup> s<sup>-1</sup>. The likely mechanism under such low temperature and  
49 high wt%H<sub>2</sub>SO<sub>4</sub> is not the general acid assisted mechanism but rather likely involves first protonation  
50 of HOBr followed by reaction of H<sub>2</sub>OBr<sup>+</sup> with X<sup>-</sup> (i.e. in agreement with the reviewer's suggestion  
51 above).

52 Conversely, in their experiments at higher temperatures (293 K), Eigen and Kustin (1961) found that  
53 such a mechanism via a first stage protonation to be insignificant under their experimental  
54 conditions relevant for the troposphere, and instead the kinetics were found to be consistent with  
55 general acid-assisted mechanism with a first stage that involves nucleophilic attack by the halide ion.  
56 In the experiments of Pratte and Rossi (2006) at 296 K, we calculate using E-AIM that the H<sub>2</sub>SO<sub>4</sub> wt%  
57 is less than 35 wt% i.e. substantially less than that of the experiments of Waschewsky and Abbatt  
58 (1999).

59 Thus, there are two different mechanisms for reactive uptake of HOBr under different atmospheric  
60 conditions. With the limited experimental data currently available it is not possible to derive a full  
61 parameterisation that includes the transition between both mechanisms. Nevertheless, we consider  
62 that the general-assisted mechanism may largely apply under T, RH conditions relevant for the  
63 troposphere, whilst the protonation mechanism likely applies in the stratosphere. The new  
64 parameterisation predicts  $k^{\text{II}}$  for HOBr+Cl<sup>-</sup> saturates at ~10<sup>4</sup> s<sup>-1</sup> i.e. yields  $k^{\text{II}}$  rate constants for  
65 tropospheric conditions that are lower than that reported in experiments under stratospheric  
66 conditions (10<sup>6</sup> and 10<sup>9</sup> s<sup>-1</sup>). In contrast, the existing termolecular approach to the kinetics where  $k^{\text{II}}$   
67 increases with increasing acidity predicts  $k^{\text{II}}$  increases rapidly with acidity to > 10<sup>10</sup> s<sup>-1</sup> for all aerosol  
68 with wt%H<sub>2</sub>SO<sub>4</sub> > 5 wt%, i.e. predicts  $k^{\text{II}}$  for sulphate aerosol under tropospheric conditions that  
69 exceeds that reported for sulphate aerosol under stratospheric conditions. This is illustrated in the  
70 Figure 1 below.



71

72 Figure 1.

73 Comparison of  $k^{\text{II}}$  estimates for HOBr + Cl<sup>-</sup> under tropospheric and stratospheric conditions. The new  
 74 parameterisation for the second order rate constant for HOBr in the troposphere according to the  
 75 general acid assisted mechanism is shown as a black line alongside experimental data (circles refer  
 76 to the reanalysed data from Pratte and Rossi, 2006, triangle to experimental data from Liu and  
 77 Margarem 2001).  $k^{\text{II}}$  values reported for experiments (Wachewsy and Abbatt, 1999) under  
 78 stratospheric conditions (low-temperature, high wt% $\text{H}_2\text{SO}_4$ ) are shown in purple (228 K), red (213 K),  
 79 pink (238 K). Note the 238 K data (pink) is consistent with the 228 K gradient (purple line) within  
 80 experimental uncertainty. Also shown (green Line) is  $k^{\text{II}}$  for HOBr + Cl<sup>-</sup> under tropospheric conditions  
 81 calculated according to the termolecular approach as used in models to date.

82 Note that an apparent gradient in the re-evaluated Pratte and Rossi (2006) data is related to the fact  
 83 that the new parameterisation only partially captures the reported RH-dependency in the uptake  
 84 coefficients of Pratte and Rossi (2006), which may be due to a range of reasons as discussed in the  
 85 text.

86

87 **Third, the general idea that HOBr kinetics might be so slow on small particles in the marine**  
88 **boundary layer because of their high acidity and subsequent halide loss that this leads to**  
89 **accumulation of bromide in these particles seems somewhat contradictory to me, i.e. if the**  
90 **bromide is building up to high levels, why is the uptake coefficient too slow to remove it? I view**  
91 **this suggestion as largely speculative and that a full box model needs to be implemented to test**  
92 **the hypothesis.**

93 The marine environment contains both supra- and sub-micron particles, the latter of which typically  
94 are very rich in H<sub>2</sub>SO<sub>4</sub>. For example the submicron particles (with average enrichment factor 5) in  
95 Keene et al. (2009) Figure 3 have on average 12 nmol/m<sup>3</sup> nss SO<sub>4</sub><sup>2-</sup> whilst the concentration of Br- is  
96 very low (hard to estimate from the graph but perhaps approximately ~ 2 nmol/m<sup>3</sup>). Observations  
97 report bromine to be depleted (relative to Sodium) in the supra-micron aerosol yet simultaneously  
98 enhanced (relative to Sodium) in the sub-micron aerosol, see Sander et al. (2003).

99 We hypothesise that low HOBr reactive uptake on these submicron particles prevents the particles  
100 from becoming Br-depleted. Furthermore, in the presence of both supra-micron particles  
101 undergoing Br-depletion, our proposed mechanism enables accumulation of bromine (relative to  
102 sodium) in the submicron particles – i.e. a positive enrichment factor. The reviewer raises concern  
103 that this relative enhancement of bromide would act to increase the uptake coefficient. It is true  
104 that the sub-micron bromine content must remain sufficiently low that  $\gamma_{\text{HOBr}}$  remains low, however  
105 this does not preclude a positive enrichment factor according the proposed mechanism: absolute  
106 concentrations of Br in H<sub>2</sub>SO<sub>4</sub>-rich submicron particles can nevertheless remain very low even at  
107 higher enrichment factors. Therefore, we do not see a serious contradiction. The text in the revised  
108 manuscript is both shortened, and includes a comment there must be an upper limit to the degree  
109 of Br enrichment in these particles, in accordance with the reviewer's query.

110 We acknowledge that our hypothesis is, however, rather speculative. A full test will require future  
111 development of a detailed atmospheric chemistry (box) model that is capable of simulating reactive  
112 halogen chemistry using our revised parameterisation, and also simulates the temporally evolving  
113 halogen & acidity compositions of both supra- and submicron aerosol particles.

114 **Given the length of the paper, I recommend pulling out all the discussion of uptake coefficients**  
115 **under marine and volcanic conditions, and putting them instead into another paper with a full box**  
116 **model simulation, so that the ideas of HCl release and HBr uptake can be assessed.**

117 The revised manuscript is outlined at the end of the section. Reviewer 2 finds that the conclusions  
118 drawn for section 5 are generally reasonable (albeit too longwinded) and that the material  
119 demonstrates new information regarding the release of BrOx in marine BL and Volcanic plume  
120 environment. Therefore we propose to keep the basic elements of this discussion in the revised  
121 manuscript, but written much more succinctly. By adapting and moving certain sections to  
122 supplementary material, and removing repetitive statements, the new manuscript length is reduced  
123 by about a third.

124 **Finally, when the halide concentrations get so low, I am not convinced that the formalism**  
125 **presented in Equation 2 is appropriate, i.e. this equation assumes that HOBr is the limiting reagent**  
126 **and that the halide ion is in excess. If that is not the case, as may occur if there is a lot of halide**  
127 **displacement and with low concentrations of bromide, the use of an HOBr uptake coefficient for**  
128 **atmospheric modeling is not useful, and it would be better to describe the kinetics in terms of**  
129 **either HCl or HBr uptake, with HOBr in a semi-steady-state in solution. The authors need to justify**  
130 **their decision to express all the kinetics in terms of HOBr uptake.**

131 This is a valid question. It has not featured particularly in studies of bromine chemistry in the  
132 troposphere given the assumption of a termolecular rate constant for reaction of HOBr, and the  
133 implicit assumption that reaction with Cl-(aq) dominates and is always fast under acidic conditions.  
134 The concept is familiar in stratospheric studies of reactive bromine chemistry.

135 HOBr is a product in the autocatalytic BrO chemistry cycles. Thus, at the moment when BrO  
136 chemistry is commencing, we can assume HOBr concentrations are extremely low hence rate  
137 limiting. Therefore the HOBr reactive uptake parameterisations as shown for both HOBr+Br- and  
138 HOBr+Cl- are valid.

139 In an evolved situation a substantial degree of Br-(aq) has been converted into reactive bromine  
140 species such as BrO and HOBr. If HOBr concentrations are high enough, it may be that Br- or Cl-  
141 become limiting rather than HOBr, particularly in the situation where the aqueous-phase  
142 concentrations of these species are reduced (via acid-displacement or the dilution effect). Under  
143 such situations, the uptake calculations must be modified as the reviewer outlines.

144 Again, it is difficult to fully quantify this evolution which will require future development of a  
145 detailed atmospheric chemistry (box) model that is capable of simulating reactive halogen chemistry  
146 using our revised parameterisation and the temporally evolving supra- and submicron aerosol  
147 particles compositions.

148 Nevertheless, some conclusions can still be drawn.

149 As reactive bromine species (including HOBr) are formed at the expense of Br- (or HBr), there will  
150 ultimately be a transition towards HOBr limited system. This limitation becomes important when  
151  $H_{\text{HOBr}}^* \cdot [\text{HOBr}_{(\text{g})}] > H_{\text{HBr}}^* \cdot [\text{HBr}_{(\text{g})}]$  or equivalently  $H_{\text{HOBr}}^* \cdot [\text{HOBr}_{(\text{g})}] > [\text{Br}_{(\text{aq})}]$ .

152 The solubility of HOBr,  $H_{\text{HOBr}}^*$  is  $6.1 \times 10^3 \text{ Matm}^{-1}$  (in water) or  $4 \times 10^2 \text{ Matm}^{-1}$  (in sulphuric acid,  
153 assumed RH independent given lack of experimental data), at 298 K, see Section 3.2. The  $H_{\text{HBr}}^*$  is  
154 calculated by  $1.3 \times 10^9 / K_a \cdot (1 + K_a / [\text{H}^+])$ , with  $K_a = 10^9 \text{ M}$ . This equates to  $1.3 \cdot 10^7 \text{ Matm}^{-1}$  at pH = -2, or  
155  $1.3 \cdot 10^{11} \text{ Matm}^{-1}$  at pH = 2. Thus the solubility of HBr is much greater than that of HOBr, and it can be  
156 assumed the reaction kinetics remains HOBr limited under most conditions, even when a significant  
157 fraction of bromine is converted into reactive forms. For the specific case of highly acidified sea-salt  
158 particles where  $[\text{Br}_{(\text{aq})}]$  are diluted by the acid volume, it can also be noted that the  $\text{HOBr}_{(\text{aq})}$   
159 concentrations will be similarly diluted.

160  
161 Similarly the reactive uptake of HOBr reacting with Cl- could become HOBr limited if  $H_{\text{HOBr}}^* \cdot [\text{HOBr}_{(\text{g})}]$   
162  $> [\text{Cl}_{(\text{aq})}^-]$ . In our simple model of acidified sea-salt aerosol (which is not necessarily directly applicable  
163 to the more complex marine environment), Cl-(aq) concentration is initially high (~ 4 mol/L) but  
164 declines to ~  $4 \cdot 10^{-4} \text{ mol L}^{-1}$  at high  $\text{H}_2\text{SO}_4$ -acidification. Assuming an atmospheric HOBr abundance of

165 20 pptv, the aqueous-phase concentration of HOBr in the aerosol would be  $[\text{HOBr}] \cdot H_{\text{HOBr}}^* = 8 \cdot 10^{-9}$   
166  $\text{mol L}^{-1}$  (acid) or  $1.2 \cdot 10^{-7} \text{ mol L}^{-1}$  (water). The reaction kinetics are still HOBr limited.

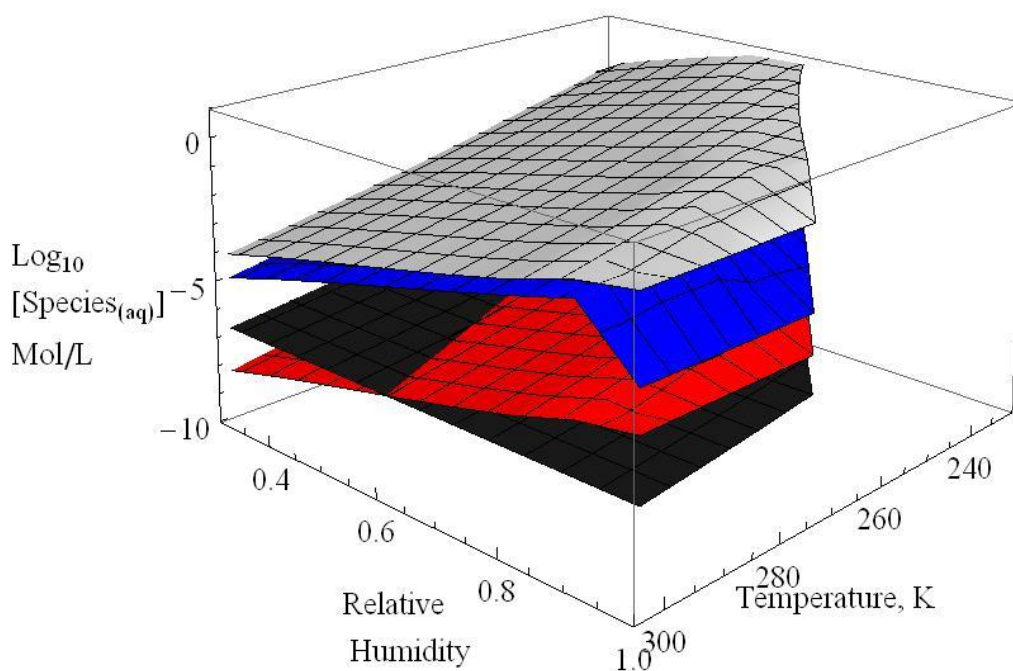
167 Thus, whilst numerical model simulations are necessary for a full quantification, this analysis  
168 suggests the assumption that the kinetics is HOBr limited is generally valid.

169 Regarding the volcanic plume implications in the troposphere, the uptake coefficient exhibited  
170 temperature dependence due to the greater solubility of HOBr and halogens in acid aerosol at low  
171 temperatures (it was assumed that the reaction rate constant is temperature independent within  
172 the troposphere, given lack of experimental data to provide any temperature-dependent  
173 parameterisation).

174  
175 The temperature dependence of the HOBr solubility follows a logarithmic equation (equation 8 of  
176 the manuscript). For HCl and HBr the aerosol concentrations were calculated using E-AIM but also  
177 exhibit logarithmic dependence with temperature. Figure 2 below shows the aqueous-phase  
178 concentrations of  $\text{Cl}^-_{(\text{aq})}$  and  $\text{Br}^-_{(\text{aq})}$  in the volcanic aerosol (assuming 1 ppmv  $\text{SO}_2$  plume strength) in  
179 grey and blue respectively ( $[\text{Cl}^-_{(\text{aq})}]$  exceeds  $[\text{Br}^-_{(\text{aq})}]$ ). An upper limit for the  $\text{HOBr}_{(\text{aq})}$  concentration is  
180 shown in black assuming complete conversion of all volcanic bromine into HOBr only (i.e. no other  
181 forms of reactive bromine present), calculated using the  $H^*$  for HOBr of equation 8. This upper limit  
182 is thus an overestimate but useful for illustration. The upper limit for the  $\text{HOBr}_{(\text{aq})}$  concentration is  
183 substantially less than the halide ions, indicating that the reactive uptake chemistry is indeed HOBr  
184 limited. This remains true even when a substantial proportion of volcanic HBr is converted into  
185 reactive forms. However, if volcanic bromine is severely depleted to a value of  $7 \cdot 10^{-5} \cdot [\text{Cl}^-_{(\text{aq})}]$  as  
186 shown in red, then the  $\text{Br}^-_{(\text{aq})}$  concentrations becomes rate limiting (rather than HOBr) for low RH  
187 and high temperatures. A more comprehensive test will require incorporation of the chemistry into  
188 a numerical model.

189  
190 For the revised manuscript, the discussion of the 'evolved' volcanic scenario is in any case removed,  
191 as we agree it should rather be investigated using a full chemistry model.

192



193

194 Figure 2. Aqueous-phase concentrations (Mol/L) in a volcanic plume of plume strength 1 ppmv SO<sub>2</sub>  
 195 for Cl<sup>-</sup><sub>(aq)</sub> and Br<sup>-</sup><sub>(aq)</sub> in gray and blue. An upper limit for the concentration of HOBr<sub>(aq)</sub> is shown in  
 196 black (assuming all volcanic bromine as HOBr). In red is shown the evolved scenario of the original  
 197 manuscript where the concentration of Br<sup>-</sup><sub>(aq)</sub> if bromine is depleted to  $7 \cdot 10^{-5} \cdot [\text{Cl}^-_{(\text{aq})}]$ .

198

199 **Small point: The diffusion coefficient listed on page 2729, line 26 has the wrong units.**

200 Corrected. In the revised ms this text is moved to Supplementary Material. The units are corrected  
 201 to diffusion coefficient  $D_r, \text{HOBr} = 1.42 \cdot 10^{-5} \text{ cm}^2 \text{ s}^{-1}$ .

202

203 **Referee #2, Tony Cox.**

204 **Scope: The heterogenous oxidation of halide ions in atmospheric aerosols is complex chemically**  
 205 **and despite efforts over past years a number of outstanding questions remain. It is nevertheless**  
 206 **an important aspect of atmospheric chemistry which needs attention. This paper presents a new**  
 207 **analysis of available data from laboratory and field experiments, which significantly improves our**  
 208 **understanding of the heterogeneous chemistry as it relates to the atmospheric chemistry of**  
 209 **bromine compounds and to the oxidising capacity of the troposphere. The analysis shows that**  
 210 **revised kinetics of the aqueous phase HOBr + X- reaction that includes acid saturation effects**  
 211 **indicates current numerical models substantially overestimate the rate of HOBr uptake on acidic**  
 212 **halogen-rich particles.**

213 **Scientific quality:** The paper is comprehensive, extends previous conceptions of the heterogenous  
214 chemistry, and reaches important new quantitative conclusions on the kinetics and mechanisms of  
215 the reactions, as investigated in laboratory and field experiments. It also discusses the significance  
216 of the results for atmospheric chemistry in the marine boundary layer and in volcanic plumes,  
217 where halogen chemistry plays an important role. The analysis is thorough and makes good use of  
218 existing up-to-date literature on kinetics and thermochemical data pertaining to the gas-aerosol  
219 reactions, to obtain fundamental parameters allowing representation in models of the rates of  
220 overall chemical processes involving Br- and Cl-containing species in the atmosphere. A weak  
221 point in calculating uptake coefficients is the reliance on the accommodation coefficient of 0.6  
222 from Wachsmuth et al. in the analysis. This is a reasonable assumption, as is the reliance on the E-  
223 AIM model for electrolyte concentrations in the aerosol. On this basis I recommend publication of  
224 the work.

225 We thank the Reviewer for these positive comments regarding the scope and scientific quality of the  
226 manuscript.

227 **Presentation:** Although the presentation is well structured, mostly clear, it is hardly concise. The  
228 abstract contains all the achievements but includes too much detail and hence is inappropriately  
229 long. A summary giving the novel mechanistic aspects, the key numerical results and the main  
230 conclusions relating to the marine BL chemistry and volcanic would suffice. The structure of the  
231 paper is good overall, but the arguments tend to be obscured by too many caveats and too much  
232 repetition. This makes the paper more like a tutorial and could be improved by simplification and  
233 less qualification of the important points and conclusions. Personally I prefer use of the passive  
234 tense rather than the use of active first person for general description.

235 Both reviewers commented that improvements were needed to the manuscript clarity and length.  
236 These have been undertaken in the revised version of the manuscript (an outline is provided at the  
237 end of this response). The text (including the abstract) is reduced through moving detailed  
238 methodology to Supplementary Materials, and removing unnecessary repetitive paragraphs. In the  
239 revision, we also increased the use of passive tense and reduced the use of active first person.

240 **The background material in the introduction (section 2) and the methodology (section 3) seems to**  
241 **be up-to-date and error free. I particularly like the use of the e-AIM model for calculation of**  
242 **aerosol composition, crucial for quantifying the rate of uptake controlled by reaction of HOBr in**  
243 **solutions containing X- ion. Both these sections which are based on material in contemporary**  
244 **literature, could be presented more concisely, with emphasis on details which are specific to the**  
245 **present study.**

246 The revised manuscript introduction and methods focuses more specifically on issues relevant to the  
247 reactive uptake of HOBr and its representation in numerical models, and the reported findings from  
248 experiments quantifying the uptake coefficient or reaction rate. In particular, some specific details of  
249 solubility and diffusion constant parameterisations, and the E-AIM set-up are moved from the  
250 methodology to Supplementary material.

251 **In section 4 the results of the kinetic analysis are presented. In section 4.1 the key equations are**  
252 **(11) and (15)-(18). The derivation could be omitted in the main text – case for supplementary**



253 **material. In section 4.4 the explanation of the discrepancy between the earlier results for**  
254 **gamma(HOBr) is dealt with. The reconciliation is not perfect but considering the assumptions and**  
255 **uncertainty in both studies the results are convincing. However the argument is hard to pull**  
256 **together because of repetition (eg on p2742 to p2743) and qualification (p2744) – could be**  
257 **improved.**

258 The derivation has been moved to Supplementary Material in the revised manuscript. Section 4  
259 focuses on evaluating the underlying rate constants to derive  $k^{\text{II}}$  parameterisations, and calculation  
260 of reactive uptake coefficients using the  $k^{\text{II}}$  parameterisation for aerosol under reported  
261 experimental conditions. The details of the E-AIM calculations for aerosol composition, and the  
262 qualification discussion (e.g. HCl displacement predicted by E-AIM in comparison to aerosol  
263 composition assumed by Pratte and Rossi, 2006) is now included in Supplementary Material, to  
264 avoid repetition.

265 **In section 5 - atmospheric implications – Generally the material demonstrates new information**  
266 **regarding the release of BrOx in marine BL and Volcanic plume environment. The conclusions**  
267 **drawn are reasonable. However the text contains superfluous material (eg l. 16 – l.18, p 2747; l.14**  
268 **– l.19, p 2748). ; l.7 – l.12, p 2750), and would benefit from emphasizing the key conclusions.**

269 In the revised manuscript, this section 5 has been shortened to emphasize the key conclusions, see  
270 provisional outline at the end of this document. In particular, sections 5.2-5.3 have been merged to  
271 make the text shorter, and section 5.4 and 5.5 are also combined with implications stated more  
272 succinctly. To improve clarity, superfluous material and details (e.g. information related to E-AIM  
273 methods) is now contained in Supplementary Material.

274 **Queries and Corrections p. 2734 l.6 in conventional kinetics jargon equation 12 results from steady**  
275 **state for [HOBrX<sup>-</sup>] in eq 11 not equilibrium**

276 Is now corrected to read: ‘...assuming  $[\text{HOBrX}^{\text{-}}_{(\text{aq})}]$  is in steady-state, leads to Eq. (12)’. The text  
277 containing this sentence is also moved to Supplementary Material.

278 **p. 2736 l.4: a definition of relative stability constants’ would be helpful here**

279 Details and full argumentation is given in the discussion of Eigen and Kustin (1961). The sentence is  
280 modified to:

281 These experiments quantified the rate of reaction in the termolecular regime only, although Eigen  
282 and Kustin (1962) used a consideration of relative stability constants (e.g. for equilibrium molarity of  
283 ternary compounds  $\text{X}_3^-$  or  $\text{X}_2\text{OH}^-$  relative to  $\text{X}^-$ ,  $\text{X}_2$  or  $\text{XOH}$ ) across the halogen series: HOCl+Cl,  
284 HOBr+Br and HOI+I to attempt to estimate underlying rate constants.

285 **p. 2738 l.13 and l.19: units of  $k_0$  should be s<sup>-1</sup>, not M<sup>-1</sup>s<sup>-1</sup>; R19 is first order!**

286 We agree there was a mistake in the units in this part of the text. Has been corrected.

287 **p. 2741 l.22 and p2742 l.8 harmonise assumed radius and diameter for these particles**

288 We now refer to our calculations in radius throughout, i.e. change 2  $\mu\text{m}$  diameter to 1  $\mu\text{m}$  radius in  
289 Line 22 but keep the reported lab experiment data as 'diameter' how it was reported. This section of  
290 text is now in the Supplementary Material.

291 **p.2744 l.8 - 9: |Do you mean 'an HOBr diffusion coefficient'? If so give units ( $\text{cm}^2\text{s}^{-1}$  I presume)**

292 Yes. This has been corrected, and with units as stated.

### 293 **Comments on Figures**

294 **Figure 1: annotation of Br<sup>-</sup> and Cl<sup>-</sup> together with more contrasting color distinction would make**  
295 **clearer;**

296 Annotation for HOBr + Br<sup>-</sup> and HOBr + Cl<sup>-</sup> is added in the revised manuscript, and the colours  
297 improved.

298 **Figure 2: Graphs are too small for easy registration of content**

299 Graphs are larger in the revised manuscript. Note this figure goes into Supplementary Material.

300 **Figure 3 Dotted line too faint; caption too long – move some of comment material into main text**  
301 **(eg last sentence)**

302 Last sentence is removed from figure caption, and caption is shortened in the revised version.

303 **Figure 4. Needs clear labelling of Cl<sup>-</sup> data and Br<sup>-</sup> data on figure; misspelt 'grey' on line 2 of**  
304 **caption. Graphs would be clearer if bigger**

305 'Gray' corrected to 'Grey'.

306 Cl<sup>-</sup> data and Br<sup>-</sup> data is labelled on the y-axis. The revised figures are a larger size.

307 **Figure 5. Graphs altogether too small; cannot see lines, colours, labels or axis numerals!**

308 Size and clarity is improved in the revised version.

309 **Figure 6. Graphs altogether too small; cannot see lines, labels or axis numerals; 4 graphs of larger**  
310 **size would be sufficient to give the message.**

311 Size and clarity is improved in the revised version. Only 4 plots are presented. The 'evolved' scenario  
312 is omitted from the manuscript and only the strongest and weakest plume cases shown.

313

### 314 **Improved manuscript structure and clarity:**

315 Both reviewers request that the manuscript clarity be improved and the text length shortened.

316 Efforts towards a revised version have been undertaken which reduces the manuscript text by about  
317 one third, through both removal of superfluous text and moving of some material into

318 Supplementary Material. Provisional outlines of the revised manuscript and supplementary material  
319 are provided below.

320

321 **The revised manuscript structure (similar to that proposed in response to reviewers) now includes:**

322 Abstract (~330 words, much shorter than original version)

323 1. Introduction

324 2. Method and experimental data

325 2.1 Quantifying the reactive uptake coefficient,  $\gamma_{\text{HOBr}}$

326 2.2 Reported experimental studies on the reactive uptake of HOBr onto liquid aerosol

327 - Further methods details are now in Supp. Mat.

328 3. Results (note the derivation of  $k_{\text{II}}$  has now been moved to Supp. Mat.)

329 3.1 The second order rate constant for aqueous-phase reaction of HOBr with halide ions

330 3.2 Estimating the underlying rate constants ( $k_1$ ,  $k_{-1}$ ,  $k_0$ ,  $k_{\text{H}}$ ) for HOBr+Br<sup>-</sup> and HOBr+Cl<sup>-</sup>

331 3.3 A new parameterisation for  $k_{\text{II}}$  for HOBr+Br and HOBr+Cl (refers to Figure 1)

332 3.4 Comparison of model with experimental uptake coefficient data (refers to Table 4). Note that a  
333 proportion of the original text describing/repeating E-AIM methods has been moved to Supp. Mat.

334 3.4.1 High uptake coefficient on HCl-acidified sea-salt aerosol

335 3.4.2 Low uptake coefficient on H<sub>2</sub>SO<sub>4</sub>-acidified sea-salt aerosol with RH dependence

336 4. Implications for BrO chemistry in marine and volcanic environments

337 4.1 Declining uptake coefficients on progressively H<sub>2</sub>SO<sub>4</sub>-acidified sea-salt aerosol

338 4.2 Implications for BrO chemistry in the marine boundary layer (this section contains the 2 merged  
339 and shortened sections of original manuscript)

340 4.3 Reactive uptake of HOBr on volcanic aerosol (this section contains the 2 merged and shortened  
341 sections of the original manuscript)

342 5. Conclusions

343

344 **The Supplementary Material includes:**

345 1. Derivation of the equation of  $k^{\text{II}}$  according to the general acid assisted mechanism.

346 2. Calculation of HOBr reactive uptake coefficients (detailed methodology)

347 3. Application of E-AIM to predict aerosol composition

348 3.1 Application of E-AIM to reported experimental conditions:

349 3.1.1 HCl-acidified sea-salt aerosol of Wachewsky and Abbatt, 1998

350 3.1.2 H<sub>2</sub>SO<sub>4</sub>-acidified sea-salt aerosol of Pratte and Ross, 2006

351 3.2 Application of E-AIM to a progressively H<sub>2</sub>SO<sub>4</sub>-acidified marine aerosol (+ Figure illustrating

352 composition of acidified sea-salt aerosol)

353 3.3 Application of E-AIM to volcanic aerosol (+ Figure illustrating volcanic aerosol composition)

354

355

356 **References:**

357 Keene W. C., Long M. S., Pszenny A. A. P., Sander R., Maben J. R., Wall A. J., O'Halloran T. L., Kerkweg

358 A., Fischer E. V., and Schrem O.: Latitudinal variation in the multiphase chemical processing of

359 inorganic halogens and related species over the eastern North and South Atlantic Oceans, *Atmos.*

360 *Chem. Phys.*, 9, 7361–7385, 2009.

361 Sander R., Keen W. C., Pszenny A. A. P., Arimoto R., Ayers G. P., Baboukas E., Caine J. M., Crutzen P.

362 J., Duce R. A., Hönninger G., Huebert B. J., Maenhaut W., Mihalopoulos N., Turekian V. C., and Van

363 Dingenen R.: Inorganic bromine in the marine boundary layer: a critical review, *Atmos. Chem. Phys.*,

364 3, 1301-1336, 2003.

365

366 **Re-evaluating the reactive uptake of HOBr in the troposphere with**  
367 **implications for the marine boundary layer and volcanic plumes**

368

369 **Tjarda J. Roberts<sup>1</sup>, Line Jourdain<sup>1</sup>, Paul T. Griffiths<sup>2</sup>, and Michel Pirre<sup>1</sup>**

370

371 [1] {LPC2E, UMR 7328, CNRS-Université d'Orléans, 3A Avenue de la Recherche  
372 Scientifique, 45071 Orleans, Cedex 2, France }

373 [2] {Centre for Atmospheric Science, Cambridge University, Chemistry Department,  
374 Lensfield Road, Cambridge, CB2 1EW, UK }

375

376 | Correspondence to: T. J. Roberts (Tjarda.Roberts@cnrs-orleans.fr)

377

378

379 **Abstract**

380 The reactive uptake of HOBr onto halogen-rich aerosols promotes conversion of  $\text{Br}^-_{(\text{aq})}$  into gaseous  
381 reactive bromine (incl. BrO) with impacts on tropospheric oxidants and mercury deposition.  
382 However, experimental data quantifying HOBr reactive uptake on tropospheric aerosols is limited,  
383 and reported values vary in magnitude. This study introduces a new evaluation of HOBr reactive  
384 uptake coefficients in the context of the general acid assisted mechanism. We emphasise that the  
385 termolecular kinetic approach assumed in numerical model studies of tropospheric reactive bromine  
386 chemistry to date is strictly only valid for a specific pH range and, according to the general acid  
387 assisted mechanism for HOBr, the reaction kinetics becomes bimolecular and independent of pH at  
388 high acidity.

389 ~~This study re-examines the reaction kinetics of HOBr across a range of aerosol acidity conditions,~~  
390 ~~focusing on chemistry within the marine boundary layer and volcanic plumes.~~

391 ~~We highlight that the termolecular approach to HOBr reaction kinetics, used in numerical model~~  
392 ~~studies to date, is strictly only valid over a specific pH range. This study reconciles for the first time~~  
393 ~~the different reactive uptake coefficients reported from laboratory experiments. Here we re-~~  
394 ~~evaluate the reaction kinetics of HOBr according to the general acid-assisted mechanism. The rate of~~  
395 ~~reaction of HOBr with halide ions becomes independent of pH at high acidity yielding an acid-~~  
396 ~~independent second-order rate constant,  $k^{\text{II}}$ . The limit of acid-saturation is poorly constrained by~~  
397 ~~available experimental data, although a reported estimate for  $\text{HOBr} + \text{Br}^-_{(\text{aq})} + \text{H}^+_{(\text{aq})}$  is  $k^{\text{II}}_{\text{sat}} = 10^8 - 10^9 \text{ M}^{-1}$~~   
398  ~~$\text{s}^{-1}$ , at  $\text{pH} \leq \sim 1$ . By consideration of halide nucleophilic strength and re-evaluation of reported uptake~~  
399 ~~coefficient data on  $\text{H}_2\text{SO}_4$ -acidified sea-salt aerosol, we suggest the reaction of  $\text{HOBr}_{(\text{aq})} + \text{Cl}^-_{(\text{aq})} + \text{H}^+_{(\text{aq})}$~~   
400 ~~may saturate to become acid-independent at  $\text{pH} \leq 6$ , with  $k^{\text{II}}_{\text{sat}} \sim 10^4 \text{ M}^{-1} \text{ s}^{-1}$ . This rate constant is~~  
401 ~~multiple orders of magnitude lower (a factor of  $10^3$  at  $\text{pH} = 3$  and a factor of  $10^5$  at  $\text{pH} = 0$ ) than that~~  
402 ~~currently assumed in numerical models of tropospheric BrO chemistry, which are based on the~~  
403 ~~termolecular approach.~~

404 ~~Reactive uptake coefficients,  $\gamma_{\text{HOBr}}$ , were calculated as a function of composition using the revised~~  
405 ~~HOBr kinetics, with  $k^{\text{I}} = k^{\text{II}} \cdot [\text{X}^-_{(\text{aq})}]$ , and  $\text{X} = \text{Br}$  or  $\text{Cl}$ .  $\gamma_{\text{HOBr}}$  initially increases with acidity but~~  
406 ~~subsequently declines with increasing  $\text{H}_2\text{SO}_4$ -acidification of sea-salt aerosol. The HOBr+Cl<sup>-</sup> uptake~~  
407 ~~coefficient declines due to acid displacement of  $\text{HCl}_{(\text{g})}$ , reducing  $[\text{Cl}^-_{(\text{aq})}]$ . The HOBr+Br<sup>-</sup> uptake~~  
408 ~~coefficient also declines at very high  $\text{H}_2\text{SO}_4$ :Na ratios due to dilution of  $[\text{Br}^-_{(\text{aq})}]$ . The greatest~~  
409 ~~reductions in HOBr uptake coefficients occur for small particle sizes, across which the probability of~~  
410 ~~diffusion of  $\text{HOBr}_{(\text{aq})}$  without reaction is highest. Our new uptake calculations are consistent with all~~

411 ~~reported experimental data thus resolve previously reported discrepancies within a unified uptake~~  
412 ~~coefficient framework.~~

413 The ~~re-evaluation following implications for BrO chemistry in the marine boundary layer are~~  
414 ~~highlighted: we confirm<sub>s</sub> HOBr reactive uptake is rapid on moderately acidified sea-salt supramicron~~  
415 ~~aerosol (and slow on alkaline aerosol), but~~-but~~ predict<sub>s</sub> very low reactive uptake coefficients on~~  
416 ~~highly-acidified submicron particles. This is due to acid-saturated kinetics combined with low halide~~  
417 ~~concentrations induced by both acid-displacement reactions and the dilution effects of H<sub>2</sub>SO<sub>4(aq)</sub>. A~~  
418 ~~mechanism is thereby proposed for reported Br-enhancement (relative to Na) in H<sub>2</sub>SO<sub>4</sub>-rich~~  
419 ~~submicron particles in the marine environment. Further, the fact that HOBr reactive uptake on~~  
420 ~~H<sub>2</sub>SO<sub>4</sub>-acidified supra-micron particles is driven by HOBr+Br<sup>-</sup> (rather than HOBr+Cl<sup>-</sup>), indicates self-~~  
421 ~~limitation via decreasing  $\gamma_{\text{HOBr}}$  once aerosol Br<sup>-</sup> is converted into reactive bromine, very low HOBr~~  
422 ~~reactive uptake coefficients on the highly acidified submicron marine aerosol fraction. This re-~~  
423 ~~evaluation is in contrast to the high HOBr reactive uptake previously assumed to occur on all~~  
424 ~~acidified sea-salt aerosol. Instead, our uptake evaluation indicates that particle bromide in the~~  
425 ~~submicron aerosol fraction is not easily depleted by HOBr uptake, and furthermore can be~~  
426 ~~augmented by deposition of gas-phase bromine released from the supramicron particles. We~~  
427 ~~present this mechanism as a first explanation for the observed (but previously unexplained) Br-~~  
428 ~~enhancement (relative to Na) in submicron particles in the marine environment. Further, we find~~  
429 ~~HOBr reactive uptake on acidified sea-salt aerosol is driven by reaction of HOBr+Br<sup>-</sup> rather than~~  
430 ~~HOBr+Cl<sup>-</sup> ( $\gamma_{\text{HOBr+Br}^-} > \gamma_{\text{HOBr+Cl}^-}$ ) once HCl displacement has occurred. Thus, the reduction in  $\gamma_{\text{HOBr+Br}^-}$  as~~  
431 ~~BrO chemistry progresses (noting  $\gamma_{\text{HOBr+Br}^-}$  is a function of aerosol Br<sup>-</sup><sub>(aq)</sub> concentration which declines~~  
432 ~~as aerosol bromide is converted into gaseous-phase reactive bromine) will have greater importance~~  
433 ~~in slowing overall HOBr reactive uptake as BrO chemistry evolves than has been assumed previously.~~  
434 ~~We suggest both the above factors may explain the reported overprediction of BrO cycling in the~~  
435 ~~marine environment by numerical models to date.~~

436 First predictions of HOBr reactive uptake on sulphate particles in ~~halogen-rich tropospheric~~ volcanic  
437 plumes are ~~also presented~~. High (accommodation limited) HOBr+Br<sup>-</sup> uptake coefficient in  
438 concentrated (> 1  $\mu\text{mol/mol/ppmv}$  SO<sub>2</sub>) plume environments supports ~~potential for rapid BrO~~  
439 ~~formation in plumes throughout the troposphere. However, under all conditions, reduced~~ However,  
440 ~~the HOBr+Cl<sup>-</sup> uptake coefficient exhibits an inverse temperature trend which becomes more~~  
441 ~~pronounced as the plume disperses. The HOBr+Br<sup>-</sup> coefficient also declines with temperature in~~  
442 ~~dilute (~ppbv SO<sub>2</sub>) plumes. We infer that BrO chemistry can readily be sustained in downwind~~  
443 ~~plumes entering the mid- to upper troposphere. HOBr reactive uptake may reduce the rate of BrO~~

Formatted: Subscript

Formatted: Subscript

Formatted: Subscript

Formatted: Subscript

Formatted: Subscript

444 ~~cycling, e.g. either from continuous degassing from elevated volcano summits (e.g. Etna, 3.3 km asl)~~  
445 ~~or episodic eruptions (e.g. Eyjafjallajökull, Iceland). However, low HOBr reactive uptake coefficients~~  
446 ~~may limit sustained BrO cycling in dilute plumes in the in the lower troposphere.~~

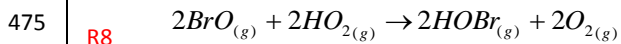
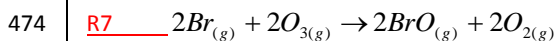
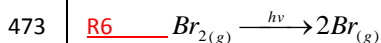
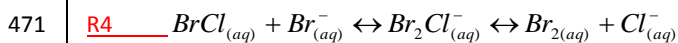
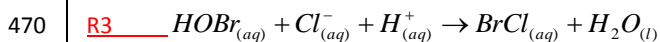
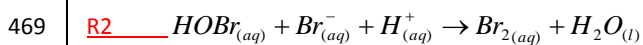
447 In summary, our ~~revised re-evaluation of~~ HOBr kinetics ~~provides a new framework for interpretation~~  
448 ~~of experimental data and suggests the reactive uptake of HOBr on H<sub>2</sub>SO<sub>4</sub>-acidified particles that is~~  
449 ~~substantially over-estimated in includes acid saturation indicates that~~ current numerical models of  
450 BrO chemistry in the troposphere ~~substantially overestimate the rate of HOBr reactive uptake on~~  
451 ~~acidic halogen rich particles, with implications for BrO chemistry in both the marine environment~~  
452 ~~and volcanic plumes, as well as the wider troposphere.~~

453



454 **1. Introduction**

455 The reactive uptake of HOBr onto halogen-containing aerosols to release Br<sub>2</sub> enables propagation of  
 456 the chain reaction leading to autocatalytic BrO formation, the so-called 'bromine explosion', (Vogt et  
 457 al., 1996), first proposed following the discovery of ozone depletion events in the polar boundary  
 458 layer (Barrie et al. 1988). Rapid and substantial (10's ppbv) ozone depletion occurs upon the  
 459 formation of just 10's pptv BrO due to cycling between Br and BrO, with further Br-mediated impacts  
 460 on environmental mercury in the conversion of Hg<sup>0</sup> to more reactive and easily deposited form Hg<sup>II</sup>  
 461 (Schroeder et al., 1998). Tropospheric BrO chemistry has since been recognised outside the polar  
 462 regions, with BrO identified above salt pans (Hebestreit et al., 1999), in the marine boundary layer  
 463 (Read et al. 2008), and is suggested to have a significant impact on the chemistry of the free  
 464 troposphere (e.g. von Glasow et al., 2004). In particular, recent evidence of rapid BrO formation in  
 465 acidic volcanic plumes (10's pptv to ppbv on a timescale of minutes) has highlighted volcanic halogen  
 466 emissions as a source of reactive bromine entering the troposphere (Bobrowski et al., 2003).



476  
 477 Key to reactive halogen formation is the cycle R1-R8 which results in autocatalytic formation of BrO.  
 478 Accommodation of HOBr<sub>(g)</sub> to aerosol (R1), followed by reaction with Br<sub>(aq)</sub><sup>-</sup> or Cl<sub>(aq)</sub><sup>-</sup> and H<sub>(aq)</sub><sup>+</sup> results  
 479 in a di-halogen product (R2,R3). The reaction of HOBr with Cl<sub>(aq)</sub><sup>-</sup> (R3) is typically considered the

Formatted: Font: Bold

Formatted: Subscript

Formatted: Superscript

Formatted: Subscript

Formatted: Superscript

Formatted: Subscript

Formatted: Superscript

Formatted: Subscript

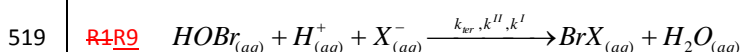
480 dominant reaction pathway (albeit an assumption that may not apply in highly acidified aerosol as  
481 we show in this study) given sea-salt aerosol contains  $[\text{Br}_{(\text{aq})}^-] \ll [\text{Cl}_{(\text{aq})}^-]$  by a factor of 700 (or greater  
482 once reactive bromine formation has commenced), and the termolecular rate constants for R2 and  
483 R3 are of comparable magnitudes (Liu and Margareem, 2001, Beckwith et al., 1996). However,  $\text{Br}_2$  is  
484 commonly the observed product, as confirmed by laboratory experiments by Fickert et al. (1999).  
485 The product conversion from  $\text{BrCl}$  to  $\text{Br}_2$  is explained by aqueous-phase equilibria (R4) that  
486 interconvert  $\text{BrCl}$  into  $\text{Br}_2$  (via  $\text{Br}_2\text{Cl}$ ) before gaseous release (R5). According to equilibrium constants  
487 reported by Wang et al. (1994), conversion of  $\text{BrCl}$  to  $\text{Br}_2$  is favoured at room temperature in aerosol  
488 provided  $\text{Br}_{(\text{aq})}^-:\text{Cl}_{(\text{aq})}^- > \sim 10^{-4}$ , as for example in sea-salt aerosol where  $\text{Br}_{(\text{aq})}^-:\text{Cl}_{(\text{aq})}^- \approx 1.5 \cdot 10^{-3}$ . The  
489 dihalogen species then partition into the gas-phase, R5. The exsolution of dihalogens from the  
490 aerosol to the gas-phase also limits the occurrence of reverse reactions that might reform  $\text{HOBr}$ .  
491 Once in the gas-phase,  $\text{Br}_2$  is photolysed to produce 2 Br radicals, R6, which may react with ozone to  
492 form  $\text{BrO}$ , R7.  $\text{HOBr}$  is reformed via the reaction of  $\text{BrO}$  with  $\text{HO}_2$ , (R8), whereupon it may react again  
493 with halogen-containing aerosol to further propagate the cycle, each time doubling the  
494 concentration of reactive bromine.

495

496 ~~To this respect, N~~umerical models have been developed to better understand the formation of  $\text{BrO}$   
497 and evaluate impacts on atmospheric oxidants throughout the troposphere and on mercury cycling  
498 in the environment. ~~For the different tropospheric environments, the models~~ Models capture the  
499 salient features of  $\text{BrO}$  formation and impacts (e.g. on ozone depletion and Hg deposition events) in  
500 the different tropospheric environments (~~for example see~~ reviews by Simpson et al. (2007) and  
501 Saiz-Lopez A. and von Glasow R., (2012) ~~and references therein~~). Nevertheless, a number of  
502 uncertainties remain. For example, models tend to overestimate  $\text{Br}_x$  cycling in the marine  
503 environment (Sander et al., 2003; Smoydzin and von Glasow, 2007; Keene et al., 2009). Models  
504 predict a depletion in the inorganic bromine content of all acidified marine aerosols, as consequence  
505 of  $\text{HOBr}$  reactive uptake to form  $\text{Br}_2$  and its release into the gas-phase. However, an aerosol bromine  
506 deficit is only observed in the slightly acidified supramicron fraction, whilst aerosol bromine is found  
507 to be enhanced (relative to that expected based on  $\text{Br}:\text{Na}$  ratios in sea-salt, using sodium as a sea-  
508 salt tracer) in the highly acidified sub-micronmeter fraction. This phenomenon has not been  
509 explained to date (Sander et al., 2003). Numerical models have also attempted to simulate reactive  
510 halogen chemistry in volcanic plume environments. Models initialised with a high-temperature  
511 source region, are able to reproduce the rapid formation of  $\text{BrO}$  in the near-source plume  
512 (Bobrowski et al., 2007a, Roberts et al., 2009, Von Glasow 2010), as well as ozone depletion (Kelly et

513 al., 2013), but a source of model uncertainty is the representation of heterogeneous halogen  
514 chemistry on volcanic aerosol, which may differ from that reported from experiments on sea-salt  
515 aerosol.

516 All these studies rely on laboratory experiments to quantify rate constants of the reactions, with a  
517 key process in the formation of reactive bromine being the reaction of HOBr<sub>(aq)</sub> with halide ion X<sup>-</sup><sub>(aq)</sub>  
518 (Cl<sup>-</sup><sub>(aq)</sub> or Br<sup>-</sup><sub>(aq)</sub>) and H<sup>+</sup><sub>(aq)</sub>. R2,R3, which can be written generically as R9.



520 Experimental studies (e.g. Fickert et al., 1999) show the reaction of HOBr<sub>(aq)</sub> is promoted when  
521 alkaline sea-salt aerosols becomes acidified, either by natural (e.g. methane sulphonic acid) or  
522 anthropogenic (e.g. sulphuric acid) sources of acidity. However, laboratory experiments have  
523 reported uptake coefficients on acidified sea-salt aerosol, >0.2 (Abbatt and Wachewsky, 1998) and  
524 10<sup>-2</sup> (Pratte and Rossi, 2006), a discrepancy that has not been explained to date. In addition, no  
525 experiments have been performed to quantify uptake of HOBr on volcanic aerosol under  
526 tropospheric conditions.

527 Numerical model studies of reactive bromine chemistry currently implement ~~R1-R9~~ using three-body  
528 reaction kinetics, i.e. assumed the reaction rate is directly proportional to H<sup>+</sup><sub>(aq)</sub> concentration (e.g.  
529 von Glasow, 2002), or using uptake coefficients calculated on this assumption (IUPAC evaluations,  
530 e.g. Ammann et al., 2013). We highlight, however, that earlier literature on the general acid-assisted  
531 mechanism for this and similar reactions (e.g. Eigen and Kustin, 1962, Nagy et al., 1988) identify that  
532 the pH dependence of the reaction rate is more complex, with acid-saturation of the kinetics at high  
533 acidity.

534 This study re-evaluates HOBr reactive uptake in the context of the general acid assisted mechanism  
535 for the first time. The plan of the paper is as follows. In Section 2 the method for calculating the  
536 reactive uptake coefficient is recalled with the approach based on the general acid assisted  
537 mechanism explained. The data used to evaluate the new uptake coefficient calculations are  
538 presented. In Section 3 pH-dependent second-order rate constants (k<sup>II</sup>) are derived for both  
539 HOBr+Br<sup>-</sup> and HOBr+Cl<sup>-</sup> in the context of the general assisted mechanism, using reported literature  
540 data for the underlying rate constants, and a thermodynamic model to predict aerosol composition  
541 under experimental conditions. Using the new parameterisation for k<sup>II</sup>, reactive uptake coefficients  
542 for HOBr + Br<sup>-</sup> and HOBr + Cl<sup>-</sup> are calculated and compared to reported laboratory data for HCl-  
543 acidified sea-salt aerosol (Wachewsky and Abbatt, 1998) and H<sub>2</sub>SO<sub>4</sub>-acidified sea-salt aerosol (Pratte  
544 and Rossi, 2006). We provide new quantification of HOBr+Br<sup>-</sup> and HOBr+Cl<sup>-</sup> uptake coefficients on

Formatted: Superscript

545 H<sub>2</sub>SO<sub>4</sub>-acidified sea-salt aerosol in the marine environment, and sulphuric acid aerosol in volcanic  
546 plumes dispersing into the troposphere. In section 4, reactive uptake coefficients are calculated for  
547 HOBr on H<sub>2</sub>SO<sub>4</sub>-acidified sea-salt aerosol in the marine environment, and on sulphuric acid aerosol in  
548 volcanic plumes entering the troposphere, and implications discussed for BrO chemistry in these  
549 environments.

550 ~~First we evaluate the second-order rate constants for the reaction of HOBr+Br<sup>-</sup> and HOBr+Cl<sup>-</sup> from~~  
551 ~~reported literature data with use of a thermodynamic model to predict aerosol composition under~~  
552 ~~experimental conditions. Secondly, we evaluate the uptake coefficients for HOBr onto HCl-acidified~~  
553 ~~and H<sub>2</sub>SO<sub>4</sub>-acidified aerosol. We provide new quantification of HOBr+Br<sup>-</sup> and HOBr+Cl<sup>-</sup> uptake~~  
554 ~~coefficients on H<sub>2</sub>SO<sub>4</sub>-acidified sea-salt aerosol in the marine environment, and sulphuric acid~~  
555 ~~aerosol in volcanic plumes dispersing into the troposphere. Implications for our understanding of~~  
556 ~~reactive halogen chemistry in the troposphere and improvements to numerical modelling are~~  
557 ~~discussed.~~

558

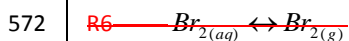
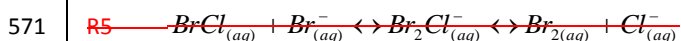
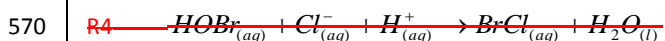
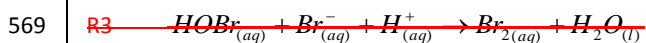
559

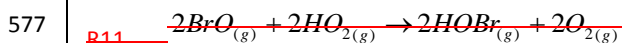
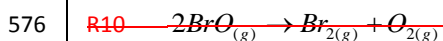
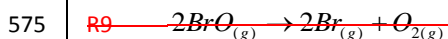
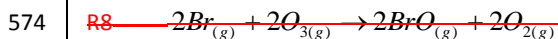
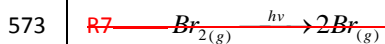
## 560 2. Method and experimental data

### 561 ~~2. The reactive uptake of HOBr~~

#### 562 ~~2.1 Reactive bromine chemistry in the troposphere~~

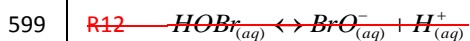
563 ~~Reactions R2-R11 illustrate the autocatalytic mechanism for BrO formation in the troposphere, in the~~  
564 ~~so-called 'bromine explosion'. The mechanism requires halogens, aerosol and sunlight to be present,~~  
565 ~~and acts to convert Br<sup>-</sup><sub>(aq)</sub> (or HBr) into reactive bromine (that includes BrO, HOBr, BrONO<sub>2</sub>, BrNO<sub>2</sub>,~~  
566 ~~Br<sub>2</sub>, BrCl, Br). The reaction of HOBr with X<sup>-</sup><sub>(aq)</sub> in the aerosol phase is a key step in the propagation of~~  
567 ~~the reaction cycles and the release of reactive halogens to the gas-phase.~~





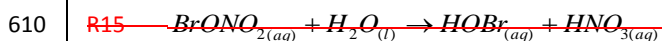
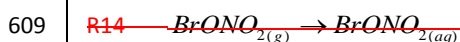
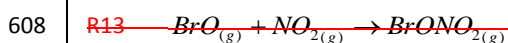
578 ~~The reactive uptake of HOBr involves accommodation of HOBr<sub>(aq)</sub> to aerosol and reaction with Cl<sup>-</sup><sub>(aq)</sub> or~~  
579 ~~Br<sup>-</sup><sub>(aq)</sub> to form BrCl<sub>(aq)</sub> or Br<sub>2(aq)</sub> (R2-4). The reaction of HOBr with Cl<sup>-</sup><sub>(aq)</sub> (R4) is typically considered the~~  
580 ~~dominant reaction pathway (albeit an assumption that may not apply in highly acidified aerosol as~~  
581 ~~we show in this study) given sea salt aerosol contains [Br<sup>-</sup><sub>(aq)</sub>] << [Cl<sup>-</sup><sub>(aq)</sub>] by a factor of 700 (or greater~~  
582 ~~once reactive bromine formation has commenced), and the termolecular rate constants for R3 and~~  
583 ~~R4 are of comparable magnitudes (Liu and Margareum, 2001, Beckwith et al., 1996). However, Br<sub>2</sub> is~~  
584 ~~commonly the observed product, as confirmed by laboratory experiments by Fickert et al. (1999).~~  
585 ~~The product conversion from BrCl to Br<sub>2</sub> is explained by aqueous phase equilibria (R5) that~~  
586 ~~interconvert BrCl into Br<sub>2</sub> (via Br<sub>2</sub>Cl<sup>-</sup>) before gaseous release (R6). According to equilibrium constants~~  
587 ~~reported by Wang et al. (1994), conversion of BrCl to Br<sub>2</sub> is favoured at room temperature in aerosol~~  
588 ~~provided Br<sup>-</sup><sub>(aq)</sub>:Cl<sup>-</sup><sub>(aq)</sub> > ~10<sup>-4</sup>, as for example in sea salt aerosol where Br<sup>-</sup><sub>(aq)</sub>:Cl<sup>-</sup><sub>(aq)</sub> ~ 1.5·10<sup>-3</sup>. The~~  
589 ~~dihalogen species then partition into the gas phase, R6. The exsolution of dihalogens from the~~  
590 ~~aerosol to the gas phase also limits the occurrence of reverse reactions that might reform HOBr.~~  
591 ~~Once in the gas phase, Br<sub>2</sub> is photolysed to produce 2 Br radicals, R7, which may react with ozone to~~  
592 ~~form BrO, R8. Ozone is catalytically destroyed only if BrO recycle to Br atoms without production of~~  
593 ~~ozone. This occurs through cycles e.g. by the self reaction of BrO (R9 and R10). HOBr is reformed via~~  
594 ~~the reaction of BrO with HO<sub>2</sub>, (R11), whereupon it may react again with halogen containing aerosol~~  
595 ~~to further propagate the cycle, each time doubling the concentration of reactive bromine.~~

596 ~~Reactive uptake of HOBr consumes H<sup>+</sup><sub>(aq)</sub> thus acidity is required for prolonged BrO formation~~  
597 ~~chemistry to occur. Moreover, under alkaline conditions, dissolved HOBr largely dissociates to form~~  
598 ~~less reactive BrO<sup>-</sup><sub>(aq)</sub> (R12: the pKa of HOBr being 8.59 (Nagy and Ashby, (2007))).~~



600 ~~Alongside reactive uptake of HOBr, uptake of BrONO<sub>2</sub> (a product of the reaction of BrO and NO<sub>2</sub>,~~  
601 ~~R13) onto aerosol can also act to promote reactive bromine formation, whereupon hydrolysis~~

602 generates HOBr and HNO<sub>2</sub>. R14, R15. Once formed, HOBr may then react immediately with aqueous-  
 603 phase halogens to produce dihalogens or may be released from the aerosol phase as HOBr  
 604 (whereafter it might still undergo heterogeneous chemistry or undergo photolysis). Experimental  
 605 studies indicate evidence for both HOBr and dihalogens as products from the heterogeneous  
 606 reaction of BrONO<sub>2</sub>. Here, the focus is on quantifying HOBr reaction kinetics as a major driver of  
 607 reactive bromine formation.



611

612 **2.12 Quantifying the reactive uptake of HOBr reactive uptake coefficient,  $\gamma_{HOBr}$**

Formatted: Font: Not Bold

613 The reactive uptake of HOBr<sub>(g)</sub> can be quantified by E1 (with further modification required for large  
 614 particles due to the limitation of gas-phase diffusion<sub>7</sub>) in terms of the reactive uptake coefficient,  
 615  $\gamma_{HOBr}$ , where  $v_{HOBr}$  is the mean molecular velocity of HOBr<sub>(g)</sub>, cm s<sup>-1</sup>, and *Area*, is the surface area  
 616 density of the aqueous phase, cm<sup>2</sup>/cm<sup>3</sup>.

617  $\gamma_{HOBr}$  is a fractional number that quantifies the likelihood of reaction given a collision of HOBr<sub>(g)</sub> with  
 618 a particle, and can be calculated following the resistor-model framework (E2) that describes the  
 619 accommodation to the aerosol, and the reaction and diffusion in or across the aerosol particle.  $\gamma_{HOBr}$   
 620 is a function of several parameters, including accommodation coefficient,  $\alpha_{HOBr}$ , the solubility of  
 621 HOBr,  $H^*$ , the aqueous-phase diffusion rate,  $D_1$ , the gas constant  $R$ , Temperature,  $T$ , the mean  
 622 molecular velocity,  $v_{HOBr}$ , and the first-order rate constant for the reaction of HOBr<sub>(aq)</sub>,  $k^I$ . The  
 623 parameter  $l$  is a function of  $D_1$  and  $k^I$ ,  $l = (D_1/k^I)^{0.5}$ .

624 E1 
$$-\frac{d[HOBr_{(g)}]}{dt} = \gamma_{HOBr} \cdot \frac{v_{HOBr}}{4} \cdot [HOBr_{(g)}] \cdot Area$$

625 E2 
$$\frac{1}{\gamma_{HOBr}} = \frac{1}{\alpha_{HOBr}} + \frac{v_{HOBr}}{4 \cdot H^*_{HOBr} \cdot R \cdot T \cdot \sqrt{D_{1,HOBr} \cdot k^I}} \cdot \frac{1}{\coth\left[\frac{r}{l}\right] - \frac{l}{r}}$$

626 E3 
$$-\frac{d[HOBr_{(aq)}]}{dt} = k^I \cdot [HOBr_{(aq)}]$$

627 E4 
$$k^I = k_{ter} \cdot [X_{(aq)}^-] \cdot [H_{(aq)}^+]$$

628 E5  $k^I = k^{II} \cdot [X_{(aq)}^-]$

629 To date, numerical models have adopted two approaches to simulate the reactive uptake of HOBr.  
630 Detailed process models (e.g. MISTRA; von Glasow et al. (2002), MECCA; Sander et al. (2011)) tend  
631 to model HOBr gas-aerosol partitioning to and from the aerosol directly, with the reaction of HOBr  
632 inside the aerosol simulated using E3 and termolecular kinetics (E4). On the other hand, global  
633 models (e.g. in studies by von Glasow et al., (2004), Yang et al., (2005), Breider et al., (2010), Parella  
634 et al. (2012)) tend to simulate HOBr reactive uptake as one step, E1, quantified by the uptake  
635 coefficient,  $\gamma_{\text{HOBr}}$ . The IUPAC evaluation recommends uptake coefficient to be calculated using E2  
636 and the termolecular approach to HOBr kinetics, E4. In global models, a fixed uptake coefficient,  
637  $\gamma_{\text{HOBr}}$ , is typically used for computational reasons.

638 However, as we highlight in this study, the termolecular kinetics approach (E4) is only valid within a  
639 limited pH range. Here we instead ~~use E2 and evaluate~~ the reaction kinetics of HOBr<sub>(aq)</sub> in terms of a  
640 second-order rate constant, E5, where  $k^{\text{II}}$  is a variable function of pH according to the general acid  
641 assisted reaction mechanism for HOX+Y<sup>(+H<sup>+</sup>)</sup> ~~constrained by available laboratory data. Details on~~  
642 ~~the mechanism and derivation of  $k^{\text{II}}$  are given in Section 1 of Supplementary maerial and (section~~  
643 ~~Section 43.1).~~ Despite being well-documented (Eigen and Kustin, 1962; Kumar and Margarem, 1987;  
644 Nagy et al. 1988; Gerritsen and Margarem, 1990, Wang and Margarem, 1994) this mechanism has  
645 not been implemented in any numerical model studies of reactive halogen chemistry to date. ~~Based~~  
646 ~~on this approach we re-evaluate the reactive uptake coefficients for HOBr with  $k^{\text{I}}$  defined using E5 in~~  
647 ~~terms of  $k^{\text{II}}$  instead of  $k_{\text{ter}}$ , with a parameterisation for  $k^{\text{II}}$  developed in the context of the general acid~~  
648 ~~assisted mechansim. We compare our new approach to reported estimates of HOBr reactive uptake~~  
649 ~~coefficients from laboratory experiments as outlined below.~~

650 ~~To calculate reactive uptake coefficients (E2), we also need to determine the aerosol composition,~~  
651 ~~specifically halide concentration,  $[X_{(aq)}^-]$  and the acidity. Indeed,  $[X_{(aq)}^-]$  is needed for E5 and~~  
652 ~~subsequently E2, and the acidity is also needed to determine  $k^{\text{II}}$  in the context of the general~~  
653 ~~assisted mechanism (see the expression in Section 3.1) and subsequently E5 and E2. This was~~  
654 ~~achieved using the E-AIM (Extended- Aerosol Inorganic model) and Henry's constants (for more~~  
655 ~~details see Section 3 of Supplementary Material). Given high ionic strength of the solutions studied,~~  
656 ~~concentrations were converted to activities using activity coefficients provided by E-AIM.~~

657 ~~Finally, we assume in E2 an accommodation coefficient of 0.6 (Wachsmuth et al., 2002), with~~  
658 ~~solubility and diffusion coefficients for HOBr in water and sulphuric acid derived from Frenzel et al.~~  
659 ~~(1998), Iraci et al. (2005), and Klassen et al (1998). A radius of 0.1 or 1  $\mu\text{m}$  was assumed, reflecting~~

Formatted: Superscript

Formatted: Superscript

Formatted: Superscript

660 [the presence of both sub- and supra-micron particles in volcanic and marine environments. Further](#)  
661 [details are provided in Section 2 of Supplementary Materials.](#)

662 [We compare our new approach to reported estimates of HOBr reactive uptake coefficients from](#)  
663 [laboratory experiments as outlined below.](#)

664

### 665 **2.3.2 Reported experimental studies on the reactive uptake of HOBr onto liquid aerosol**

666 A number of laboratory experiments (Table 1) have quantified the reactive uptake of HOBr onto  
667 acidified sea-salt aerosol under tropospheric conditions (as well as on solid particles, not considered  
668 here).

669 The accommodation coefficient for HOBr onto super-saturated  $\text{NaBr}_{(\text{aq})}$  aerosol was determined by  
670 Wachsumth et al. (2002) to be  $\alpha_{\text{HOBr}} = 0.6 \pm 0.2$  at 298 K.

671 Experiments using acidified sea-salt particles made by nebulizing a 5 M NaCl and 0.5 M HCl solution  
672 under conditions representative of the troposphere found the reactive uptake coefficient for the  
673 reaction ( $\text{HOBr} + \text{Cl}^-$ ) to be very high ( $\gamma_{\text{HOBr}} > 0.2$ ) on deliquesced aerosol ( $\text{RH} > 75\%$ ,  $T = 298 \text{ K}$ ),  
674 (Abbatt and Waschewsky, 1998). Conversely, experiments by Pratte and Rossi (2006) on  $\text{H}_2\text{SO}_4$ -  
675 acidified sea-salt aerosol with  $\text{H}_2\text{SO}_4:\text{NaCl}$  molar ratio = 1.45:1 at 296 K measured a substantially  
676 lower HOBr uptake coefficient,  $\gamma_{\text{HOBr}} \sim 10^{-2}$ , with a dependence on relative humidity ( $\gamma_{\text{HOBr}} \sim 10^{-3}$   
677 below 70% RH). This large ( $10^1$ - $10^2$ ) discrepancy has not been resolved to date. Uptake of HOBr on  
678 pure sulfate aerosol at 296 K is found to be low ( $\gamma_{\text{HOBr}} \sim 10^{-3}$ ), Pratte and Rossi (2006).

679 Aqueous-phase rate constants for the reaction of  $\text{HOBr} + \text{X} + \text{H}^+$  have also been reported: for  $\text{HOBr} + \text{Br}^-$   
680  $_{(\text{aq})}$ , Eigen and Kustin (1952) and Beckwith et al. (1996) report termolecular rate constants of  $k_{\text{ter}} =$   
681  $1.6 \cdot 10^{10} \text{ M}^{-2} \text{ s}^{-2}$  over a pH range of 2.7-3.6 and 1.9-2.4 at 298 K, respectively. For  $\text{HOBr} + \text{Cl}^-$   $_{(\text{aq})}$ , Liu and  
682 Margarem (2001) report a three-body rate constant of  $2.3 \cdot 10^{10} \text{ M}^{-2} \text{ s}^{-2}$  in buffered aerosol at pH = 6.4  
683 and 298K. Pratte and Rossi (2006) derived first-order rate constants for the reaction of  $\text{HOBr}_{(\text{aq})}$  from  
684 their uptake experiments, finding  $k^1 \sim 10^3 \text{ s}^{-1}$ .

685 The IUPAC subcommittee for gas kinetic data evaluation currently recommends an uptake  
686 coefficient parameterisation utilising accommodation coefficient  $\alpha_{\text{HOBr}} = 0.6$  (Wachsmuth et al.,  
687 2002), and first-order rate constant  $k^1 = k_{\text{ter}} \cdot [\text{H}^+_{(\text{aq})}] \cdot [\text{X}^-_{(\text{aq})}]$ , with  $k_{\text{ter}} = 2.3 \cdot 10^{10} \text{ M}^{-2} \text{ s}^{-2}$  (Liu and  
688 Margarem, 2001) for  $\text{HOBr} + \text{Cl}^-$  and  $k_{\text{ter}} = 1.6 \cdot 10^{10} \text{ M}^{-2} \text{ s}^{-2}$  (Beckwith et al., 1996) for  $\text{HOBr} + \text{Br}^-$ .  
689 Assuming a  $\text{Cl}^-_{(\text{aq})}$  concentration of 5.3 M typical of sea-water and low uptake coefficients in alkaline  
690 sea-salt aerosol (IUPAC evaluation, see website, e.g. Ammann et al., 2013), this parameterisation



691 yields a high uptake coefficient,  $\gamma_{\text{HOBr}} \sim 0.6$ , on acidified sea-salt aerosol, and is in agreement with  
692  $\gamma_{\text{HOBr}} \geq 0.2$  reported by Abbatt and Waschewsky (1998) while overestimating the uptake coefficient  
693 as reported by Pratte and Rossi (2006) by a factor of  $\sim 20$ .

694 Here we present new uptake calculations based on the general acid assisted mechanism rather than  
695 termolecular kinetics in an attempt to consolidate these contrasting reported uptake coefficients  
696 within a single framework for the first time, and explain differences between model predictions and  
697 field observations of reactive bromine in the marine environment, as well as making first predictions  
698 of HOBr reactive uptake coefficients in volcanic plumes.

699 |

700 **3-Method**

701 **3.1 A new parameterisation for the rate constant for HOBr + X<sup>-</sup><sub>(aq)</sub>**

702 Critical to this re-evaluation of  $\gamma_{\text{HOBr}}$  is the parameterisation of the rate of reaction of HOBr with Br-  
703 or Cl- in terms of a second-order rate constant,  $k^{\ddagger}$ , that is a function of particle acidity, in line with  
704 the general acid assisted mechanism (Eigen and Kustin, 1962). The first-order rate constant,  $k^{\dagger}$  can  
705 then be determined as the product of the second-order rate constant,  $k^{\ddagger}$ , and the concentration of  
706 halide ion X<sup>-</sup><sub>(aq)</sub>:  $k^{\dagger} = k^{\ddagger} [X_{(aq)}^-]$ . This contrasts to previous approaches that assumed termolecular  
707 kinetics with  $k^{\dagger} = k_{\text{ter}} [X_{(aq)}^-] [H_{(aq)}^+]$ .

708 Parameterisations for  $k^{\ddagger}$  were derived as a function of acidity using kinetic theory of the general acid  
709 assisted mechanism, and available laboratory data. To determine the aerosol composition,  
710 specifically halide concentration,  $[X_{(aq)}^-]$ , and acidity, we use the E-AIM (Extended Aerosol Inorganic)  
711 model and Henry's constants (see below). Given high ionic strength of the solutions studied,  
712 concentrations were converted to activities using activity coefficients provided by E-AIM.

714 **3.2 Definition of other parameters in the uptake equation, for sulphuric acid and sea salt aerosol**

715 Further parameters to calculate the uptake coefficient for HOBr (E2) were defined as follows. The  
716 accommodation coefficient,  $\alpha_{\text{HOBr}}$ , was set to 0.6, following experimental findings by Wachsmuth et  
717 al. (2002) who measured accommodation limited uptake onto NaBr<sub>(aq)</sub> particles under very low  
718 HOBr<sub>(g)</sub> concentrations. It is assumed that this accommodation coefficient is also representative for  
719 acidified NaCl<sub>(aq)</sub> or H<sub>2</sub>SO<sub>4(aq)</sub> particles in the troposphere. Temperature, T = 298 K unless otherwise  
720 stated, the ideal gas constant R = 8.206 · 10<sup>-2</sup> L atm K<sup>-1</sup> mol<sup>-1</sup>. The particle radius, r, was set to r = 1 or  
721 r = 0.1 μm, noting the occurrence of both supra- and submicron aerosol in the marine environment  
722 and volcanic plumes. The diffusive length scale, l, describes the typical distance over which  
723 reaction occurs, with  $l = (D_{\text{HOBr}}/k)^{0.5}$ .

724 This study focuses primarily on HOBr reactive uptake under acidic aerosol conditions. In order to  
725 account for the dissociation of HOBr under alkaline conditions, we used a modified HOBr rate  
726 constant to reflect the dissociation of HOBr<sub>(aq)</sub> into BrO<sup>-</sup> at high pH. We also assumed BrO<sup>-</sup><sub>(aq)</sub> is  
727 unreactive to X<sup>-</sup><sub>(aq)</sub>. Thus,  $k^{\ddagger} = k^{\ddagger} [Cl_{(aq)}^-] [H_{(aq)}^+] / ([H_{(aq)}^+] + K_a)$ , where the acid dissociation constant is  $K_a$   
728 = 2.6 · 10<sup>-9</sup> mol/L (given a pKa for HOBr of 8.59, Nagy and Ashby, 2007), and where the term  
729  $[H_{(aq)}^+] / ([H_{(aq)}^+] + K_a)$  reflects the fraction of dissolved HOBr<sub>(aq)</sub> in that remains in the form HOBr.

730 ~~Two parameterisations for the aqueous-phase diffusion constant for HOBr,  $D_{i,HOBr}$ ,  $m^2 s^{-1}$ , and the~~  
 731 ~~solubility of HOBr,  $H^*$ ,  $mol L^{-1} atm^{-1}$ , for salt solutions and sulphuric acid solutions are used. The~~  
 732 ~~former applies for weakly acidified sea-salt aerosol (and is the approach used in studies to date),~~  
 733 ~~whereas we consider the latter more appropriate for highly  $H_2SO_4$ -acidified sea-salt aerosol and~~  
 734 ~~volcanic aerosol.~~

735 ~~We use  $D_{i,HOBr} = 1.42 \cdot 10^{-5} m^2 s^{-1}$  reported by Frenzel et al. (1998) for HOBr diffusion in salt solutions at~~  
 736 ~~291 K, which we apply directly in this study at 298 K. For HOBr diffusion in sulphuric acid solutions,~~  
 737 ~~the parameterisation E6 is used following Klassen et al (1998), where T is the temperature in K, and~~  
 738  ~~$\eta$  is the viscosity of sulfuric acid that given by E7.  $c_{HOBr} = 6.2 \cdot 10^8$  for HOBr,  $B = 425$ ,  $n = -1.43$ , A and  $T_0$~~   
 739 ~~are functions of the wt% $H_2SO_4$ , (wt):  $A = 279.4 - 8.8 \cdot wt + 0.358 \cdot wt^2$ ,  $T_0 = 203 - 2.6 \cdot wt + 0.0287 \cdot wt^2$ ,~~  
 740 ~~where the wt% $H_2SO_4$  was determined using the E-AIM thermodynamic model. This parameterisation~~  
 741 ~~is valid for 30 wt % to 72 wt % sulfuric acid at temperatures between 220 and 300 K.  $D_i$  at lower wt%~~  
 742 ~~sulphuric acid (high RH) was estimated by interpolation across the RH and Temperature parameter~~  
 743 ~~space, and extrapolation to high RH, yielding a diffusion rate comparable to that of water at very~~  
 744 ~~high humidity, i.e.  $1.42 \cdot 10^{-5} m^2 s^{-1}$ .~~

745 ~~E6 
$$D_{i,HOBr} = \frac{c_{HOBr} \cdot T}{\eta}$$~~

746 ~~E7 
$$\eta = A \cdot T^n \cdot \text{Exp} \left[ \frac{B}{T - T_0} \right]$$~~

747  
 748 ~~HOBr solubility in weakly acidified sea-salt aerosol is represented using the value for water,  $6.1 \cdot 10^3$~~   
 749  ~~$M atm^{-1}$  at 291 K, (Frenzel et al., 1998), which we apply directly to this study at 298 K, consistent~~  
 750 ~~with the value of  $> 1.9 \cdot 10^3 mol L^{-1} atm^{-1}$  at 298 K estimated by Blatchley et al., (1991). For HOBr~~  
 751 ~~solubility in  $H_2SO_{4(aq)}$  we use a parameterisation derived by Iraci et al. (2005) based on~~  
 752 ~~measurements over 201-252 K in 45-70 wt%  $H_2SO_4$ . In application of this parameterisation, E8, to the~~  
 753 ~~troposphere, we note that the wt% $H_2SO_4$  only exceeds 45% in the troposphere if relative humidity is~~  
 754 ~~less than  $\sim 40-50\%$ . However, Iraci et al. (2005) report that the dependence of solubility,  $H^*$ , on acid~~  
 755 ~~concentration is relatively weak. The parameterisation yields an RH-independent HOBr solubility in~~  
 756 ~~sulphuric acid of  $4 \cdot 10^3 M atm^{-1}$  at 298 K (i.e. an order of magnitude lower than that assumed for~~  
 757 ~~water at this temperature), rising to  $10^3 M atm^{-1}$  at 273 K and  $10^4 M atm^{-1}$  at 253 K.~~

758 ~~E8 
$$\text{LOG}_{10} \left( H_{HOBr-H_2SO_4(aq)}^* \right) = \frac{2349}{T} - 5.27$$~~

759

### 760 **3.3 — Aerosol composition estimated using the E-AIM thermodynamic model**

761 The E-AIM (Extended Aerosol Inorganic Model) thermodynamic model was used to predict the  
762 composition of both acidified sea salt and volcanic aerosol and in particular the halide  
763 concentration,  $X_{\text{aq}}^-$ . We used E-AIM version I that considers the  $\text{H}^+$ – $\text{SO}_4^{2-}$ – $\text{NO}_3^-$ – $\text{Cl}^-$ – $\text{Br}^-$ – $\text{H}_2\text{O}$   
764 system between 200 to 330 K (Carslaw et al. (1995)), and model version III that considers the  $\text{H}^+$ –  
765  $\text{NH}_4^+$ – $\text{Na}^+$ – $\text{SO}_4^{2-}$ – $\text{NO}_3^-$ – $\text{Cl}^-$ – $\text{H}_2\text{O}$  system at 298K (Clegg et al. (1998)).

766 Inputs to E-AIM include the temperature, relative humidity and total  $\text{SO}_4^{2-}$ ,  $\text{Cl}^-$ ,  $\text{Br}^-$ ,  $\text{Na}^+$ , and  $\text{H}^+$  in the  
767 system defined in  $\text{mol}\cdot\text{m}^{-3}$  volume of atmosphere. Outputs include the number of moles per  $\text{m}^3$  of  
768 atmosphere of  $\text{Na}^+_{(\text{aq})}$ ,  $\text{SO}_4^{2-}_{(\text{aq})}$ ,  $\text{HSO}_3^-_{(\text{aq})}$ ,  $\text{H}^+_{(\text{aq})}$ ,  $\text{Br}^-_{(\text{aq})}$ ,  $\text{Cl}^-_{(\text{aq})}$ ,  $\text{HCl}_{(\text{g})}$ ,  $\text{HBr}_{(\text{g})}$ , the activity coefficients for  
769 these species, and the total aerosol volume ( $\text{cm}^3$  per  $\text{m}^3$ ). It was thereby possible to calculate the  
770 aqueous phase concentrations and activities of halides and  $\text{H}^+_{(\text{aq})}$  in the aerosol, in  $\text{mol}\cdot\text{L}^{-1}$ .

771 Because E-AIM model versions cannot predict the composition of aerosol which contains all four  
772 components:  $\text{Na}^+$ ,  $\text{SO}_4^{2-}$ ,  $\text{Br}^-$  and  $\text{Cl}^-$ , calculations for sea salt aerosol were performed with E-AIM  
773 version III (see composition above), with bromide concentration calculated subsequently. For  
774 simplicity we ignore other possible sea salt ions (e.g.  $\text{Mg}^{2+}$ ,  $\text{Ca}^{2+}$ ,  $\text{NH}_4^+$ ,  $\text{NO}_3^-$ ) therefore our assumed  
775 Na:Cl ratio (1:1) is slightly higher than that of actual sea water (0.4685:0.5459 = 0.86:1), Wilson  
776 (1975). The aerosol  $\text{Br}^-_{(\text{aq})}$  concentration was then predicted as follows: total Br concentration was  
777 calculated assuming a Br:Na molar ratio corresponding to that of sea water (0.000842:0.4685  
778 =0.0018), Wilson (1975). The relative concentrations of  $\text{HBr}_{(\text{g})}$  and  $\text{Br}^-_{(\text{aq})}$  were described using the  
779 effective Henry's solubility for HBr,  $\text{H}^{\ddagger}(\text{E9})$ .  $\text{H}^{\ddagger}$  is a function of the acid dissociation constant ( $K_a = 10^9$   
780 M, Schweitzer et al., 2000), and  $\text{H}^+_{(\text{aq})}$  concentration (determined from the E-AIM model output,  
781 noting that HBr contributes negligibly to aerosol acidity compared to  $\text{H}_2\text{SO}_4$ ). For a closed system,  
782 the partitioning between  $\text{HBr}_{(\text{g})}$  and  $\text{Br}^-_{(\text{aq})}$  also depends on the total aerosol volume, and was  
783 calculated using E10, (Seinfeld and Pandis, 2006), involving the HBr solubility,  $\text{H}^{\ddagger}$  ( $\text{mol}\cdot\text{L}^{-1}\cdot\text{atm}^{-1}$ ) the  
784 total bromine concentration Br in the system (in moles per  $\text{L}^{-1}$  of air), the gas constant, R defined  
785 earlier), Temperature T in Kelvin, and the liquid water content,  $w_L = L\cdot 10^{-6}$ , where L is the total  
786 aerosol volume density ( $\text{g}/\text{m}^3$ ) determined from the E-AIM output (for a specified sea salt  
787 concentration in moles/ $\text{m}^3$  and degree of acidification). E-AIM model simulations were performed  
788 for aerosol under reported laboratory conditions of experiments quantifying the HOBr uptake  
789 coefficient (see section 4.4.2 and 4.4.3), and for a 'simple' model sea salt aerosol to demonstrate the  
790 effect of progressive  $\text{H}_2\text{SO}_4$  acidification (section 4.4.1 and 5.1). This 'simple' model sea salt aerosol  
791 composition does not include carbonate buffering (or the effect of other potential impurities such as

792 ammonium). The model aerosol composition is independent of the particle radius,  $r$  (which  
793 nevertheless affects the uptake coefficient calculated according to E2).

794 ~~E9~~ 
$$H_{HBr}^* = \frac{1.3 \cdot 10^9}{K_a} \left(1 + K_a / [H_{(aq)}^+]\right)$$

795 ~~E10~~ 
$$[Br_{(aq)}^-] = H_{HBr}^* \frac{[Br_i] \cdot R \cdot T}{1 + H_{HBr}^* \cdot w_L \cdot R \cdot T}$$

796

797 E-AIM model version I was used to predict volcanic aerosol composition, particularly concentrations  
798 of both  $Br_{(aq)}^-$  and  $Cl_{(aq)}^-$  over a range of tropospheric RH (0.4-0.99) and temperature (300-230 K).  
799 We assumed a volcanic composition of  $(SO_2):Cl:Br:SO_4^{2-}$  of 1:0.5:0.00075:0.01 that is typical for an  
800 Arc (subduction zone) volcano such as Etna (note  $SO_2$  simply listed as a reference volcanic gas but is  
801 not included in the E-AIM calculation). We also consider an evolved plume situation where  
802 significant BrO chemistry has taken place, causing  $[Br_{(aq)}^-]$  to become depleted to  $Br:Cl = 7 \cdot 10^{-5}$   
803 (according to the equilibria of Wang et al., (1994)). Anions were balanced by  $H^+$  as the cation. The  
804  $SO_4^{2-}:SO_2$  ratio assumed here is based on crater rim measurements that indicate sulphate: $SO_2$  molar  
805 ratio of  $\sim 1:100$  (e.g. Mather et al., 2003). This 'quasi-direct' volcanic emission of sulfate is believed to  
806 be caused by high-temperature production of  $SO_3$  in the near-vent plume (Mather et al., 2003)  
807 followed by lower temperature reaction with  $H_2O$  (Roberts et al., 2009). For the abovementioned  
808 volcanic emission composition, the absolute concentrations required for the E-AIM input (in moles  
809  $m^{-3}$ ) were calculated for three different plume strengths equivalent to an  $SO_2$  gas concentration of  
810 30, 3, and  $0.3 \mu mol/m^3$  which is equivalent to approximately 1, 0.1 and 0.01 ppmv  $SO_2$  at 4km  
811 altitude (US standard atmosphere).

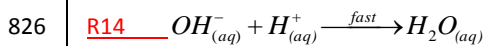
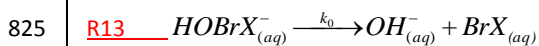
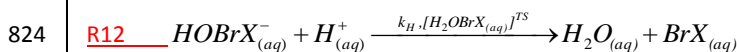
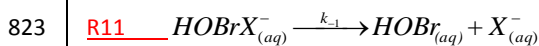
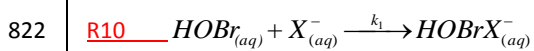
812

813 **4.3 Results**

814 **3.1 The second-order rate constant for aqueous-phase reaction of HOBr with halide ions**

Formatted: Font: Bold

815 In the general acid-assisted mechanism - whereby the rate of reaction of HOBr<sub>(aq)</sub> (needed in E2)  
816 follows a second-order kinetics – an equilibrium is established between HOBr<sub>(aq)</sub> and HOBr  
817 according to the rate constants of R10 and R11,  $k_1$  and  $k_{-1}$  (Eigen and Kustin, 1962). The formation of  
818 products, R12, involves a transition-state, [H<sub>2</sub>OBrX<sub>(aq)</sub>]<sup>TS</sup> that is stabilised by proton-donation to the  
819 oxygen, with overall rate constant  $k_H$ . Moreover, formation of products can also occur at low acid  
820 concentrations via a slower pathway, R13, followed by fast reaction R14, with overall rate constant  
821  $k_0$ .



827 According to R10-R14, the rate of reaction of HOBr<sub>(aq)</sub> can be quantified in terms of a 2<sup>nd</sup> order rate  
828 constant (following E3 and E5) where  $k^{\text{II}}$  is a function of pH, as described by equation E6, whose  
829 derivation is provided in Supplementary Material.

Formatted: Subscript

Formatted: Superscript

Formatted: Superscript

830 In this section we present our parameterisation of the second-order rate coefficient as a function of  
831 aerosol acidity, using both existing experimental data and the E-AIM.

832 E6  $k^{\text{II}} = \frac{k_1 \cdot (k_0 + k_H \cdot [\text{H}_{(aq)}^+])}{k_{-1} + k_0 + k_H \cdot [\text{H}_{(aq)}^+]}$

833 In the limits of high and low acidity (E7 and E8),  $k^{\text{II}}$  is independent of aerosol acidity. For a mid-range  
834 acidity ( $k_H \cdot [\text{H}_{(aq)}^+] \ll k_{-1} + k_0$ ),  $k^{\text{II}}$  becomes linearly dependent on  $[\text{H}_{(aq)}^+]$  i.e. is acid-dependent (E9). In  
835 this mid-acidity regime (only), the acid-dependence is equal to the three-body or termolecular rate  
836 constant,  $k_1 \cdot k_H / (k_{-1} + k_0) = k_{\text{ter}}$ .

Formatted: Superscript

Formatted: Subscript

837 E7  $k^{\text{II}} = k_1$  at high acidity (the limit as  $\text{H}_{(aq)}^+$  tends to infinity)

838 ~~E8~~  $k'' = \frac{k_1 \cdot k_0}{k_{-1} + k_0}$  at very low acidity (the limit as  $H^+_{(aq)}$  tends to zero)

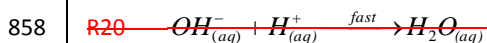
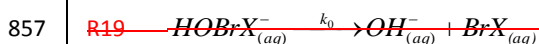
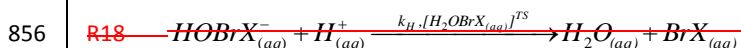
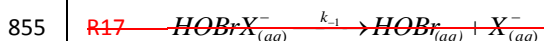
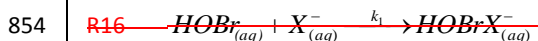
839 ~~E9~~  $k'' = \frac{k_1 \cdot k_0}{k_{-1} + k_0} + \frac{k_1 \cdot k_H \cdot [H^+_{(aq)}]}{k_{-1} + k_0}$

840 Equations E6-E9 describe  $k''$  in terms of four underlying rate constants ( $k_1, k_{-1}, k_0, k_H$ ) and the aerosol  
 841 acidity. However, quantifying these underlying rate constants using published data is somewhat  
 842 challenging given the limited experimental data. This is now attempted below.

843

844 **~~4.1 The kinetics of HOBr+X<sup>-</sup> according to the general acid assisted mechanism~~**

845 ~~The HOBr reaction with X<sup>-</sup> in acidic aerosols has been described using the general acid assisted~~  
 846 ~~mechanism (Eigen and Kustin, 1962), summarized below (reactions R16-20), in which an equilibrium~~  
 847 ~~is established between HOBrX<sup>-</sup><sub>(aq)</sub> and HOBr according to the rate constants of R16 and R17,  $k_1$  and  $k_{-1}$ .~~  
 848 ~~The formation of products, R18, involves a transition state,  $[H_2OBrX_{(aq)}]^{TS}$  that is stabilised by~~  
 849 ~~proton donation to the oxygen, with overall rate constant  $k_H$ . Moreover, formation of products can~~  
 850 ~~also occur at low acid concentrations via a slower pathway, R19, followed by fast reaction R20, with~~  
 851 ~~overall rate constant  $k_0$ . We first derive an expression for  $k''$  according to combined mechanism, in~~  
 852 ~~terms of the underlying rate constants  $k_1, k_{-1}, k_0$  and  $k_H$ , which we will then apply to an analysis of~~  
 853 ~~reported reactive uptake coefficients.~~



859 ~~The combination of R16-R19 leads to E11. Assuming  $[HOBrX^-_{(aq)}]$  is in equilibrium leads to E12.~~

860 ~~E11~~

$$\frac{d[\text{HOBrX}_{(aq)}^-]}{dt}$$

861  $= k_1 \cdot [\text{HOBr}_{(aq)}] \cdot [\text{X}_{(aq)}^-] - k_{-1} \cdot [\text{HOBrX}_{(aq)}^-] - k_H \cdot [\text{HOBrX}_{(aq)}^-] \cdot [\text{H}_{(aq)}^+] - k_0 \cdot [\text{HOBrX}_{(aq)}^-]$

862  $= 0$

862 ~~E12~~  $\frac{k_1 [\text{HOBr}_{(aq)}] [\text{X}_{(aq)}^-]}{k_1 + k_0 + k_H [\text{H}_{(aq)}^+]}$

863 The rate of reaction of  $\text{HOBr}_{(aq)}^-$  is equal to the rate of production of  $\text{BrX}_{(aq)}$ , given by E13. Substitution  
 864 of the equation for  $[\text{HOBrX}_{(aq)}^-]$ , E12, into the rate equation E13, yields E14, enabling the second-  
 865 order rate constant,  $k^{\text{II}}$ , to be defined in terms of  $k_1, k_0, k_H$  and  $[\text{H}_{(aq)}^+]$ , E15.

866 ~~E13~~  $\frac{d[\text{BrX}_{(aq)}]}{dt} = k_1 [\text{HOBr}_{(aq)}] [\text{X}_{(aq)}^-] - k_{-1} [\text{HOBrX}_{(aq)}^-] - k_H [\text{HOBrX}_{(aq)}^-] [\text{H}_{(aq)}^+] - k_0 [\text{HOBrX}_{(aq)}^-]$

867 ~~E14~~  $\frac{d[\text{BrX}_{(aq)}]}{dt} = \frac{k_1 [\text{HOBr}_{(aq)}] [\text{X}_{(aq)}^-]}{k_1 + k_0 + k_H [\text{H}_{(aq)}^+]}$

867  $= \frac{k_1 [\text{HOBr}_{(aq)}] [\text{X}_{(aq)}^-]}{k_1 + k_0 + k_H [\text{H}_{(aq)}^+]}$

868 ~~E15~~  $k^{\text{II}} = \frac{k_1 k_0}{k_1 + k_0 + k_H [\text{H}_{(aq)}^]}$

869 Simplifications to E15 can be made in the limits of high and low acidity (E16 and E17), finding  $k^{\text{II}}$  is  
 870 independent of aerosol acidity in both cases. For a mid range acidity ( $k_H [\text{H}_{(aq)}^+] \ll k_1 + k_0$ ), we can  
 871 show by rewriting E15 to yield E18 that  $k^{\text{II}}$  becomes linearly dependent on the acidity. In this mid-  
 872 acidity regime (only), the acid-dependence is equal to the three-body or termolecular rate constant,  
 873  $k_1 \cdot k_H / (k_1 + k_0) = k_{\text{ter}}$ .

874 ~~E16~~  $k^{\text{II}} = k_1$  at high acidity (the limit as  $\text{H}_{(aq)}^+$  tends to infinity)

875 ~~E17~~  $k^{\text{II}} = \frac{k_1 \cdot k_0}{k_1 + k_0}$  at very low acidity (the limit as  $\text{H}_{(aq)}^+$  tends to zero)

876 ~~E18~~  $k^{\text{II}} = \frac{k_1 k_0}{k_1 + k_0} + \frac{k_1 k_H [\text{H}_{(aq)}^+]}{k_1 + k_0}$



877 ~~Equations E15-E18 describe  $k^{\text{II}}$  in terms of four underlying rate constants ( $k_1$ ,  $k_{-1}$ ,  $k_0$ ,  $k_H$ ) and the~~  
878 ~~aerosol acidity. However, quantifying these underlying rate constants using published data is~~  
879 ~~somewhat challenging given the limited experimental data. This is now attempted below.~~

880

### 881 **4.3.2 Estimating the underlying rate constants ( $k_1$ , $k_{-1}$ , $k_0$ , $k_H$ ) for HOBr+Br<sup>-</sup> and HOBr+Cl<sup>-</sup>**

882 A number of aqueous-phase rate constants for the reaction of HOBr+X<sup>-</sup>+H<sup>+</sup> have been reported: For  
883 HOBr+Br<sup>-</sup><sub>(aq)</sub>, Eigen and Kustin (1952) and Beckwith et al. (1996) report termolecular rate constants  
884 of  $k_{\text{ter}} = 1.6 \cdot 10^{10} \text{ M}^{-2} \text{ s}^{-2}$  over a pH range of 2.7-3.6 and 1.9-2.4 at 298 K, respectively. These  
885 experiments quantified the rate of reaction in the termolecular regime only, although Eigen and  
886 Kustin (1962) used a consideration of relative stability constants (e.g. for equilibrium molarity of  
887 ternary compounds  $X_3^-$  or  $X_2OH^-$  relative to  $X^-$ ,  $X_2^-$  or  $XOH$ ) across the halogen series: HOCl+Cl<sup>-</sup>,  
888 HOBr+Br<sup>-</sup> and HOI+I<sup>-</sup> to attempt to estimate underlying rate constants.

889

890 Using the reported experimental data,  $k^{\text{II}}$  parameterisations (in terms of the underlying rate  
891 constants ( $k_1$ ,  $k_{-1}$ ,  $k_0$  and  $k_H$ ) and acidity according to E15-E6 derived above) are estimated as follows.

892

#### 893 **3.2.1 HOBr+Br<sup>-</sup>**

894 For HOBr+Br<sup>-</sup>, ~~the underlying rate constants are based on~~ Eigen and Kustin (1962), ~~who~~ proposed  
895 order of magnitude estimates of  $k_1 = 5 \cdot 10^9 \text{ M}^{-1} \text{ s}^{-1}$ ,  $k_{-1} = 5 \cdot 10^9 \text{ s}^{-1}$ ,  $k_H = 2 \cdot 10^{10} \text{ M}^{-1} \text{ s}^{-1}$ , and  $k_0 = 10^4 \text{ s}^{-1}$ .  
896 ~~However, The following modification is made, on the basis of data from Beckwith et al. (1996). In~~  
897 ~~figure-Figure 4 of Beckwith et al. (1996), we observethere are~~ indications of acid-saturation in their  
898  $k^{\text{II}}$  rate constant data for HOBr+Br<sup>-</sup>, seen as curvature in the plots of observed  $k^{\text{II}}$  versus acidity. This  
899 is also seen in their Figure 5 where  $k^{\text{II}}_{\text{observed}} \geq 2.3 \cdot 10^8 \text{ M}^{-1} \text{ s}^{-1}$ . We therefore suggest acid-saturation of  
900 the reaction between HOBr and Br<sup>-</sup> may ~~occur around an order of magnitude lower than Eigen and~~  
901 ~~Kustin's estimate of limit  $k^{\text{II}} \sim 5 \cdot 10^9 \text{ M}^{-1} \text{ s}^{-1}$  for HOBr+Br<sup>-</sup><sub>(aq)</sub>, i.e. potentially  $k^{\text{II}}$  to  $\sim 5 \cdot 10^8 \text{ M}^{-1} \text{ s}^{-1}$ . We~~  
902 ~~therefore estimate  $k_1 \sim 5 \cdot 10^8 \text{ M}^{-1} \text{ s}^{-1}$  (E16) and also adjust  $k_{-1}$  to  $k_{-1} \sim 5 \cdot 10^8 \text{ s}^{-1}$  noting theon the basis of~~  
903 ~~the~~ reported stability constant  $k_1/k_{-1} \sim 1 \text{ M}^{-1}$ , ~~according to~~ Eigen and Kustin, ~~(1962)~~. ~~HoweverWhile,~~  
904 any evidence for acid-saturation lays within the reported error bars for the data points ~~this-In any~~  
905 ~~case the abovementioned~~ adjustment does not affect ~~the-our~~ general conclusions about  $\gamma_{\text{HOBr+Br}}$  in  
906 this study.

907

Formatted: Subscript

Formatted: Superscript

Formatted: Subscript

Formatted: Superscript

Formatted: Superscript

Formatted: Subscript

Formatted: Superscript

### 908 3.2.1 HOBr+Cl<sup>-</sup>

909  
910 For HOBr+Cl<sup>-</sup><sub>(aq)</sub>, Liu and Margareum (2001) report a three-body rate constant of  $2.3 \cdot 10^{10} \text{ M}^{-2} \text{ s}^{-2}$  in  
911 buffered aerosol at pH = 6.4 and 298K. Pratte and Rossi (2006) also ~~derived report~~ estimates for first-  
912 order rate constants for reaction of HOBr<sub>(aq)</sub> ~~derived~~ from their uptake coefficient experiments. ~~Their~~  
913 ~~We re-evaluate these reported experimental data is re-interpretted~~ below to ~~contribute~~  
914 ~~furtherimprove~~ quantification ~~to of~~ the reaction kinetics of HOBr+Cl<sup>-</sup>.

915 For HOBr+Cl<sup>-</sup>, the underlying rate constants ( $k_1$ ,  $k_{-1}$ ,  $k_H$ ,  $k_0$ ) are estimated as follows. The rate  
916 constant  $k_1$  is derived from the estimation of  $k^{\text{II}}$  at acid saturation (E746). For this, we estimated  $k^{\text{II}}$  at  
917 pH -1 to 0 from experiments of Pratte and Rossi (2006), Table 2. ~~These~~ new ~~k<sup>II</sup>~~ estimates ~~of k<sup>II</sup>~~ are  
918 derived from first order  $k^{\text{I}}$  rate constants for the reaction of HOBr<sub>(aq)</sub>, reported by Pratte and Rossi  
919 (2006), ~~based on their uptake experiments on H<sub>2</sub>SO<sub>4</sub>-acidified sea salt aerosol at H<sub>2</sub>SO<sub>4</sub>:NaCl of~~  
920 ~~1.45:1, 296 K and RH = 0.77-0.9. Our derivation of k<sup>II</sup> from the reported k<sup>I</sup> requires aerosol chloride~~  
921 ~~concentration to be known, as k<sup>II</sup> = k<sup>I</sup>/[Cl<sup>-</sup><sub>(aq)</sub>]. We utilise the estimates of where [Cl<sup>-</sup><sub>(aq)</sub>] under the~~  
922 ~~experimental conditions as predicted by~~ calculated by the E-AIM model ~~from experimental~~  
923 ~~conditions, that E-AIM~~ predicts chloride concentrations are reduced under the experimental  
924 conditions as consequence of acid-displacement of HCl<sub>(g)</sub> (see further discussion in ~~Section~~  
925 ~~4.4Supplementary Material~~). ~~Our evaluation of rate constants from the experimental data reported~~  
926 ~~by Pratte and Rossi (2006) yields~~ We find  $k^{\text{II}} \sim 10^4 \text{ M}^{-1} \text{ s}^{-1}$  over pH -1 to 0, see Table 2 for details. We  
927 note that in their reporting of  $k^{\text{I}}$  rate constants from their uptake experiments, Pratte and Rossi,  
928 (2006) assumed an accommodation coefficient of either  $\alpha_{\text{HOBr}} = 0.2$  or  $\alpha_{\text{HOBr}} = 0.02$ . Given that  
929 experiments on NaBr<sub>(aq)</sub> aerosol have identified an accommodation coefficient for HOBr on NaBr<sub>(aq)</sub>  
930 particles of 0.6 (Wachsmuth et al. 2002), the  $k^{\text{II}}$  data derived assuming  $\alpha_{\text{HOBr}}=0.2$  are likely more  
931 representative. Nevertheless, either case yields estimate for  $k^{\text{II}} \sim 10^4 \text{ M}^{-1} \text{ s}^{-1}$  over pH = 0 to -1. A ~~further~~  
932 ~~second~~ estimate for  $k^{\text{II}}$  is ~~derived made~~ from the reported three-body rate constant of  $2.3 \cdot 10^{10} \text{ M}^{-2} \text{ s}^{-2}$   
933 at pH = 6.4, by setting  $k^{\text{II}} = k_{\text{ter}} \cdot [\text{H}^+_{(\text{aq})}]$ . This yields  $k^{\text{II}} = 9 \cdot 10^3 \text{ M}^{-1} \text{ s}^{-1}$  at pH 6.4.

934 Thus, collectively these two datasets at pH = 6.4 and 0 to -1 suggest that  $k^{\text{II}}$  is acid saturated at  $\sim 10^4$   
935  $\text{M}^{-1} \text{ s}^{-1}$  at pH  $\leq 6$ . Based on this value for  $k^{\text{II}}$  at acid saturation (where  $k^{\text{II}} = k_1$ ) we set  $k_1 = 1.2 \cdot 10^4 \text{ M}^{-1} \text{ s}^{-1}$ ,  
936 as an average estimate, ~~which~~ ~~This k<sub>1</sub> estimate for HOBr+Cl<sup>-</sup>~~ is less than  $k_1$  for HOBr+Br<sup>-</sup>, ~~and which~~  
937 ~~is~~ consistent with the greater nucleophile strength of Br<sup>-</sup> compared to Cl<sup>-</sup>. ~~A number of choices for~~  
938 ~~k<sub>0</sub>, k<sub>-1</sub> and k<sub>H</sub> might be made, but we~~ We choose to fix  $k_H = 2 \cdot 10^{10} \text{ M}^{-1} \text{ s}^{-1}$  ~~to be~~ equal to that  
939 estimated by Eigen and Kustin (1961) for HOBr+Br<sup>-</sup>, noting this reaction likely close to the diffusion  
940 limit. ~~Our value of~~ We expect that  $k^{\text{II}}$  for HOBr+Cl<sup>-</sup> at low acidity ( $= (k_1 k_0) / (k_0 + k_1)$ ) is ~~of a~~ similar order

Formatted: Not Superscript/ Subscript

941 of magnitude to the  $k^{\text{II}}$  estimate for HOCl+Cl<sup>-</sup> ( $\leq 0.16 \text{ M}^{-1} \text{ s}^{-1}$ , see Gerritsen and Margarem, 1989) or  
942 perhaps slightly higher (because the less electronegative Br of HOBr may be more susceptible to  
943 nucleophilic attack than HOCl), but is substantially less than the  $k^{\text{II}}$  estimate for HOBr+Br<sup>-</sup> ( $10^4 \text{ M}^{-1} \text{ s}^{-1}$ ,  
944 Eigen and Kustin, 1962) at low acidity, and consistent with given Cl<sup>-</sup> is being a weaker nucleophile  
945 than Br<sup>-</sup>. Overall, a value for the Here, we set the low acidity  $k^{\text{II}}$  rate constant;  $(k_0 \cdot k_1)/(k_1 + k_{-1}) = 10^1 \text{ M}^{-1}$   
946  $\text{s}^{-1}$  seems reasonable.

947 A similar analysis based on the further constraint is the reported three-body rate constant of  $2.3 \cdot 10^{10}$   
948  $\text{M}^2 \text{ s}^{-1}$  (Liu and Margarem, 2002). This is commonly interpreted as a termolecular rate constant,  $k_{\text{ter}}$ ,  
949 although the experimental data do not prove that this rate constant is in fact in the termolecular  
950 regime. Nevertheless, assuming  $k_{\text{ter}} = 2.3 \cdot 10^{10} \text{ M}^2 \text{ s}^{-1} = k_{\text{H}} \cdot k_1 / (k_0 + k_{-1})$  and setting the low acidity  $k^{\text{II}}$   
951 rate constant,  $(k_0 \cdot k_1)/(k_1 + k_{-1}) = 10^1 \text{ M}^{-1} \text{ s}^{-1}$  as mentioned above, with  $k_{-1} = 1.2 \cdot 10^4 \text{ M}^{-1} \text{ s}^{-1}$ , yielding yields  
952  $k_0 = 2 \cdot 10^1 \text{ M}^{-1} \text{ s}^{-1}$  and  $k_1 = 1.1 \cdot 10^4 \text{ s}^{-1}$ . Alternatively, setting the low acidity  $k^{\text{II}}$  rate constant to  
953  $(k_0 \cdot k_1)/(k_1 + k_{-1}) = 10^0 \text{ M}^{-1} \text{ s}^{-1}$  (i.e. closer to the estimate for HOCl+Cl<sup>-</sup> (aq)) yields  $k_0 = 10^0 \text{ M}^{-1} \text{ s}^{-1}$  and  $k_{-1} =$   
954  $1.0 \cdot 10^4 \text{ s}^{-1}$ . These estimates for the underlying rate constants for HOBr+Cl<sup>-</sup> are rather uncertain,  
955 nevertheless the most important result is the occurrence of acid-saturation of  $k^{\text{II}}$  for HOBr+Cl<sup>-</sup>, which  
956 the experimental data suggests occurs at limits  $k^{\text{II}}$  to  $\sim 10^4 \text{ M s}^{-1}$  at pH  $\leq 6$ .

Formatted: Superscript

957

### 958 **43.3 A new parameterisation for the $k^{\text{II}}$ for HOBr+Br<sup>-</sup> and HOBr+Cl<sup>-</sup>**

959 The underlying rate constants ( $k_1$ ,  $k_{-1}$ ,  $k_{\text{H}}$ ,  $k_0$ ) for reaction of HOBr+Br<sup>-</sup> and HOBr+Cl<sup>-</sup> estimated above  
960 are summarized in Table 3. Our parameterisation for  $k^{\text{II}}$  based on these data, with  $k^{\text{II}}$  defined by  
961 equation E15-E6 is shown in Figure 1 as a function of aerosol acidity, alongside the experimental  
962 values for  $k^{\text{II}}$  derived from the reported experimental data from Eigen and Kustin (1962), Beckwith et  
963 al. (1996), Liu and Margarem (2001) and Pratte and Rossi (2006) (see Table 2). As expected, the  $k^{\text{II}}$   
964 parameterisations for HOBr+Br<sup>-</sup> and HOBr+Cl<sup>-</sup> exhibit three distinct regimes:  $k^{\text{II}}$  is independent of  
965 acidity at high pH.  $k^{\text{II}}$  is dependent on acidity for a medium pH range, where the rate constant  $k^{\text{II}} =$   
966  $k_{\text{ter}} \cdot [\text{H}^+_{(\text{aq})}]$ , and in this regime the rate constant is termolecular. At high acidity,  $k^{\text{II}}$  becomes acid-  
967 independent ( $k^{\text{II}} = k_1$ ), yielding an acid-saturated  $k^{\text{II}}$  that is lower for HOBr+Cl<sup>-</sup> than HOBr+Br<sup>-</sup> given  
968 the weaker nucleophile strength.

969 Also shown in Figure 1 is the the termolecular approach to HOBr kinetics assumed to date, which  
970 predicts acid-dependent  $k^{\text{II}}$  over all parameter space. Clearly, the termolecular assumption for HOBr  
971 kinetics is only valid in the termolecular regime, between pH 1-6 for HOBr+Br<sup>-</sup>, and  $> \text{pH } 6$  for  
972 HOBr+Cl<sup>-</sup>. At high acidity, the termolecular approach overestimates the rate constant compared to

973 the  $k^{\text{II}}$  parameterisation by several orders of magnitude. The disagreement is greatest for HOBr+Cl<sup>-</sup>,  
974 where the termolecular approach overestimates the  $k^{\text{II}}$  rate constant by a factor of  $10^3$  at pH = 3  
975 and  $10^5$  at pH = 0 (~~overestimations respectively equivalent to ~100 thousand and ~100 million~~  
976 ~~percent of the revised rate constant value~~). Of interest is the effect of our revised parameterisation  
977 on the HOBr reactive uptake coefficient. Below we compare the reactive uptake coefficients of HOBr  
978 calculated ~~use~~ our revised  $k^{\text{II}}$  parameterisation to evaluate ~~experimental~~ uptake coefficients  
979 reported under laboratory ~~experimental~~ conditions. In section 5 we present calculations of we  
980 evaluate the HOBr reactive uptake coefficient ~~in the for~~ marine ~~environment~~ and volcanic plume  
981 conditions and discuss implications for reactive halogen chemistry in these environments.

982

### 983 **4.3.4 Comparison of our model with experimental uptake coefficient data**

984 As discussed in the introduction, discrepancies exist in the reported reactive uptake coefficients for  
985 HOBr on acidified sea-salt aerosol. Abbatt and Waschewsky (1998) observed a strong pH  
986 dependence of the uptake onto sodium chloride aerosol, being  $1.5 \cdot 10^{-3}$  for neutral, unbuffered  
987 sodium chloride aerosol, rising to  $> 0.2$  for aerosols acidified to pH 0.3 by the addition of HCl, i.e.  
988 close to the accommodation coefficient ( $\alpha = 0.6 \pm 0.2$ , Wachsmuth et al., 2002). The role of H<sup>+</sup>  
989 species in the reactive uptake process was further demonstrated by the high uptake coefficient of  $>$   
990  $0.2$  on aerosols buffered to pH 7 by a NaH<sub>2</sub>PO<sub>4</sub>/ Na<sub>2</sub>HPO<sub>4</sub> buffer. In contrast, Pratte and Rossi (2006)  
991 measured reactive uptake coefficients on H<sub>2</sub>SO<sub>4</sub>-acidified sea-salt aerosol to be  $\sim 10^{-2}$  at H<sub>2</sub>SO<sub>4</sub>:NaCl =  
992 1.45:1, with an RH-dependence (finding  $\gamma_{\text{HOBr}} \sim 10^{-3}$  at RH < 70%).

993 We have calculated the reactive uptake coefficients for HOBr for the conditions of these two  
994 laboratory experiments using our new parameterisation for  $k^{\text{II}}$  and the E-AIM model to determine  
995 aerosol composition.

996 Here Below we show that the origin for this wide discrepancy between measured HOBr uptake onto  
997 acidified bromide aerosol and chloride aerosol lies partly in the difference in reactivity of HOBr  
998 towards Br<sup>-</sup> and Cl<sup>-</sup>, but also in the different differences in aerosol composition in the two studies:  
999 HCl-acidified sea-salt aerosol retains high  $\text{Cl}^-_{(\text{aq})}$  concentrations, whereas H<sub>2</sub>SO<sub>4</sub>-acidified sea-salt  
1000 aerosol undergoes HCl-displacement, lowering  $\text{Cl}^-_{(\text{aq})}$  concentrationseases. This acid-displacement of  
1001 HCl leads to a lowering of the reactive uptake coefficient for HOBr on H<sub>2</sub>SO<sub>4</sub>-acidified aerosol.

1002

#### 1003 **4.4.1 Composition of acidified sea-salt aerosol**

Formatted: Superscript

Formatted: Subscript

Formatted: Subscript

Formatted: Subscript

Formatted: Superscript

Formatted: Subscript

Formatted: Subscript

Formatted: Subscript

1004 ~~The uptake experiments of Abbatt and Waschewsky (1998) and Pratte and Rossi (2006) respectively~~  
1005 ~~involve HCl and H<sub>2</sub>SO<sub>4</sub> as acidifying agents of the sea salt aerosol. These are known to exert~~  
1006 ~~contrasting impacts on the aerosol composition, as summarized below.~~

1007 ~~General results for a model sea salt aerosol that undergoes progressive H<sub>2</sub>SO<sub>4</sub> acidification are given~~  
1008 ~~in Figure 2, based on a single mode sea salt aerosol, with a PM10 concentration of 10 μg m<sup>-3</sup>~~  
1009 ~~(Seinfeld and Pandis, 2006), which is equivalent to 0.1 μmoles/m<sup>3</sup> Na<sup>+</sup> at 80% RH and 298 K according~~  
1010 ~~to E-AIM calculations of NaCl(aq). Having set [Cl] = [Na], we vary the H<sub>2</sub>SO<sub>4</sub>:Na molar ratio from 0.05~~  
1011 ~~to 400 and use E-AIM to determine the equilibrium aerosol composition, with bromide and HBr~~  
1012 ~~partitioning determined using Henry's law (see Methods).~~

1013 ~~The H<sub>2</sub>SO<sub>4</sub> acidification induces acid displacement of HCl<sub>(g)</sub>, which occurs around H<sub>2</sub>SO<sub>4</sub>:Na ≥ 0.4 for~~  
1014 ~~the model aerosol, depleting Cl<sup>-</sup><sub>(aq)</sub> concentrations. Further addition of H<sub>2</sub>SO<sub>4(aq)</sub> acts to increase the~~  
1015 ~~total aerosol volume but does not in fact dilute [Cl<sup>-</sup><sub>(aq)</sub>] given the presence of a HCl<sub>(g)</sub> reservoir that~~  
1016 ~~responds by increased HCl<sub>(g)</sub> to Cl<sup>-</sup><sub>(aq)</sub> partitioning. Conversely, acid displacement of HBr<sub>(g)</sub> is less~~  
1017 ~~effective due to the higher solubility of HBr (e.g. Sander, 1999), and the increasing aerosol volume~~  
1018 ~~(as consequence of the additional H<sub>2</sub>SO<sub>4(aq)</sub>) acts to dilute Br<sup>-</sup><sub>(aq)</sub> (as well as Na<sup>+</sup><sub>(aq)</sub>) at high H<sub>2</sub>SO<sub>4</sub>:Na.~~  
1019 ~~Note that in our model aerosol HBr temporarily partitions to the gas phase upon addition of~~  
1020 ~~H<sub>2</sub>SO<sub>4(aq)</sub> but returns to the aqueous phase at higher H<sub>2</sub>SO<sub>4</sub>:Na ratios as consequence of the~~  
1021 ~~increasing total aerosol volume. However, in a real marine environment with multiple aerosol~~  
1022 ~~modes, bromide might largely remain in the aqueous phase. In any case, there exists no HBr<sub>(g)</sub>~~  
1023 ~~reservoir at high H<sub>2</sub>SO<sub>4</sub>:Na ratios; bromide concentrations are diluted but the bromide:sodium ratio~~  
1024 ~~in the aerosol still reflects that of sea salt. In summary, halide concentrations are reduced in H<sub>2</sub>SO<sub>4</sub>-~~  
1025 ~~acidified sea salt aerosol both by acid displacement of HCl<sub>(g)</sub> and by dilution of Br<sup>-</sup><sub>(aq)</sub> by the~~  
1026 ~~additional H<sub>2</sub>SO<sub>4(aq)</sub> volume upon a high degree of H<sub>2</sub>SO<sub>4</sub> acidification. Similar HCl displacement is~~  
1027 ~~expected to occur for HNO<sub>3</sub> acidification of sea salt aerosol, but not for acidification of sea salt~~  
1028 ~~aerosol by HCl.~~

1029

#### 1030 **43.4.2.1 High uptake coefficient on HCl-acidified sea-salt aerosol**

1031 ~~In contrast to the H<sub>2</sub>SO<sub>4</sub> acidified sea salt aerosol case shown above, HCl acidification of sea salt~~  
1032 ~~aerosol does not induce significant acid displacement of HCl<sub>(g)</sub>. Here we illustrate how Cl<sup>-</sup><sub>(aq)</sub>~~  
1033 ~~concentrations in HCl acidified sea salt aerosol remain high so as to yield a high uptake coefficient~~

1034 ~~E-AIM model III calculations were performed for HCl acidified sea salt aerosol at HCl:NaCl = 0.1:1,~~  
1035 ~~298 K and 80% RH (above deliquescence), according to experimental conditions of Wachewsky and~~

1036 ~~Abbatt, 1998. Whilst the experimental aerosol consisted of a bimodal distribution of both large (few~~  
1037  ~~$\mu\text{m}$ ) and small ( $< \mu\text{m}$ ) particles, the larger particles (range 1–5  $\mu\text{m}$  diameter, number density  $1 \cdot 10^4$ –~~  
1038  ~~$4 \cdot 10^4 \text{ cm}^{-3}$ , surface area  $1 \cdot 10^3$ – $6 \cdot 10^3 \text{ cm}^2/\text{cm}^3$ ) were reported to dominate the observed HOBr~~  
1039 ~~uptake. For our calculations we assumed aerosol of 2  $\mu\text{m}$  diameter and number density of  $1 \cdot 10^4 \text{ cm}^{-3}$ ,~~  
1040 ~~which yields a surface area density of  $1.2 \cdot 10^3 \text{ cm}^2/\text{cm}^3$  and volume density of  $4.1 \cdot 10^{-8} \text{ cm}^3/\text{cm}^3$ .~~  
1041 ~~This aerosol volume density is approximately equivalent to a pure deliquesced sea-salt concentration~~  
1042 ~~of 0.2  $\mu\text{moles}/\text{m}^3$  Na at 76% RH and 298 K according to E-AIM. Addition of 0.02  $\mu\text{moles}/\text{m}^3$  HCl~~  
1043 ~~(HCl:NaCl = 0.1:1) yields a predicted aerosol composition with activities of 6.6  $\text{Mol L}^{-1}$  for  $\text{Cl}^-_{(\text{aq})}$  and~~  
1044 ~~2.3  $\text{Mol L}^{-1}$  for  $\text{H}^+_{(\text{aq})}$  (equivalent to a pH of 0.3) for RH = 76%. As might be expected, acidification of~~  
1045  ~~$\text{NaCl}_{(\text{aq})}$  aerosol by HCl leads to an increased acidity without causing a significant reduction in  $\text{Cl}^-_{(\text{aq})}$~~   
1046 ~~concentration through acid-displacement (given the use of HCl as the acidifying agent).~~

1047 On HCl-acidified  $\text{NaCl}_{(\text{aq})}$  aerosol, Abbatt and Wachowsky (1998) measured the uptake coefficient of  
1048 HOBr to be  $> 0.2$ . We calculate the uptake coefficient for  $\text{HOBr} + \text{Cl}^-_{\text{aq}}$  under these experimental  
1049 conditions for which a ~~assuming a temperature of 298 K, a chloride concentration of 6.6 M is~~  
1050 ~~predicted according to E-AIM (see details in Section 3.1.1 of Supplementary Material and Table 4).~~  
1051 ~~For~~ particles of 1  $\mu\text{m}$  radius at 298 K, ~~using both our new parameterisation for  $k^{\text{II}}$  and the~~  
1052 ~~termolecular approach to  $\text{HOBr} + \text{Cl}^-_{\text{aq}}$  kinetics yield high uptake coefficient.~~ Both the approaches to  
1053 ~~calculating the uptake coefficient on HCl-acidified aerosol predict an  $\gamma_{\text{HOBr} + \text{Cl}^-} \sim 0.6$ , thus are consistent~~  
1054 ~~with the experimental findings, see the comparison in Table 4.~~

Formatted: Superscript

Formatted: Superscript

1055

#### 1056 **4.3.2 Low uptake coefficient on $\text{H}_2\text{SO}_4$ -acidified sea-salt aerosol with RH dependence**

1057 ~~From their measured uptake coefficients, Pratte and Rossi (2006) derived first order rate constants~~  
1058 ~~for the reaction of  $\text{HOBr}_{(\text{aq})}$  finding  $k^{\text{I}} \sim 10^3 \text{ s}^{-1}$ . We used these data together with the E-AIM to~~  
1059 ~~derive  $k^{\text{II}}$  estimates from reported  $k^{\text{I}}$ , and also to investigate the RH-dependence of the reported~~  
1060 ~~uptake coefficients.~~

1061 ~~E-AIM model III calculations were performed for  $\text{H}_2\text{SO}_4$ -acidified sea-salt aerosol at  $\text{H}_2\text{SO}_4$ :NaCl =~~  
1062 ~~1.45:1, and 50 and 80% RH, to predict aerosol composition under the experimental conditions of~~  
1063 ~~Pratte and Rossi (2006), where the E-AIM model III temperature of 298.15 K is close to the reported~~  
1064 ~~experimental conditions of 296 K. An estimated sea-salt concentration of 8  $\mu\text{mol}/\text{m}^3$  Na was~~  
1065 ~~assumed, based on the product of the NaCl molarity (e.g. 2.9 M at 70% RH) initially estimated by~~  
1066 ~~Pratte and Rossi (2006) and the reported measured aerosol volume density ( $2.7 \cdot 10^{-9} \text{ cm}^3/\text{cm}^3$ ). To~~

1067 reach the reported experimental  $\text{H}_2\text{SO}_4:\text{NaCl} = 1.45:1$ , an additional  $11.6 \mu\text{M}/\text{m}^3$   $\text{H}_2\text{SO}_4$  was added to  
1068 the E-AIM input. For simplicity the same input estimate is used for E-AIM calculations across all RH.

1069 The output of our E-AIM calculations gives good general agreement between the predicted E-AIM  
1070 aerosol volume density (e.g.  $0.67 \cdot 10^{-9}$ ,  $2.2 \cdot 10^{-9}$  and  $5.5 \cdot 10^{-9} \text{ cm}^3 \text{ cm}^{-3}$  at RH = 40, 70 and 90%,  
1071 respectively) to that reported from their experimental observations ( $1.01 \cdot 10^{-9}$ ,  $2.7 \cdot 10^{-9}$  and  $5.56 \cdot 10^{-9}$   
1072  $\text{ cm}^3 \text{ cm}^{-3}$  at RH = 40, 70 and 90%, respectively). However, the E-AIM data suggest the aerosol  
1073 composition differs to that estimated by Pratte and Rossi (2006).

1074 The E-AIM model predicts that  $\text{Cl}^-_{(\text{aq})}$  concentrations are  $6.8 \cdot 10^{-10}$  and  $1.5 \cdot 10^{-7}$  moles  $\text{ m}^{-3}$  at 50 and 80  
1075 % RH respectively, equivalent to  $0.004 \text{ M L}^{-1}$  and  $0.08 \text{ M L}^{-1}$ . The corresponding  $\text{HCl}_{(\text{g})}$  concentrations  
1076 are  $8.0$  and  $7.9 \mu\text{moles m}^{-3}$ . Thus, E-AIM predicts that the addition of  $\text{H}_2\text{SO}_{4(\text{aq})}$  causes substantial  
1077 acid displacement of  $\text{HCl}_{(\text{g})}$  from the sea salt under the experimental conditions. The  $\text{HCl}_{(\text{g})}$   
1078 displacement acts to lower the aerosol  $\text{Cl}^-_{(\text{aq})}$  concentration, and the effect is more pronounced at  
1079 low relative humidity where wt% $\text{H}_2\text{SO}_4$  of the acidic aerosol solution is higher, hence HCl solubility  
1080 lower.

1081 Pratte and Rossi (2006) did not measure aerosol composition during their experiment, but make the  
1082 assumption that chloride remained entirely in the aerosol phase in their discussion of their data,  
1083 noting that they not detect any  $\text{HCl}_{(\text{g})}$ . However, the predicted  $\text{HCl}_{(\text{g})}$  concentrations by E-AIM e.g.  
1084  $\sim 8 \cdot 10^{-6} \text{ mol m}^{-3}$ , equivalent to  $\sim 5 \cdot 10^{12} \text{ molec cm}^{-3}$  are below the  $\sim 2 \cdot 10^{13} \text{ molec cm}^{-3}$  detection limit  
1085 reported by Pratte and Rossi (2006). This can also be shown directly from the aerosol properties  
1086 estimated by Pratte and Rossi (2006). For example, at the reported aerosol volume of  $2.7 \cdot 10^{-9}$   
1087  $\text{ cm}^3/\text{cm}^3$  at 70% RH would yield a maximum  $\text{HCl}_{(\text{g})}$  concentration if HCl exsolution from the  
1088 (estimated)  $2.9 \text{ M L}^{-1}$  NaCl concentration was complete, of  $2.9 \cdot 10^{-3} \cdot 2.7 \cdot 10^{-9} \cdot (6.023 \cdot 10^{23}) = 4.7 \cdot 10^{12}$   
1089  $\text{ molec cm}^{-3}$ , i.e. below their reported detection limit.

1090 In the following, we show the depletion of chloride due to HCl displacement reactions in  $\text{H}_2\text{SO}_4$ -  
1091 acidified sea salt aerosol (as predicted by E-AIM) to be a plausible explanation for the low uptake  
1092 coefficients for  $\text{HOBr}+\text{Cl}^-$  on this experimental aerosol, and the reported RH dependence.

1093 On  $\text{H}_2\text{SO}_4$ -acidified sea salt aerosol, Pratte and Rossi (2006) measured the uptake coefficient of HOBr  
1094 to be  $\sim 10^{-2}$  at  $\text{H}_2\text{SO}_4:\text{NaCl} = 1.45:1$ , with an RH-dependence (finding  $\gamma_{\text{HOBr}} \sim 10^{-3}$  at RH < 70%). Using  
1095 our parameterisation, we calculate the uptake coefficient for  $\text{HOBr}+\text{Cl}^-$  under these experimental  
1096 conditions, at 298 K, and with variable RH ([see details in Section 3.1.2 of Supplementary Material](#)  
1097 [and Table 4](#)). We assume a solubility of HOBr in sulphuric acid of  $363 \text{ M atm}^{-1}$  at 296 K (following  
1098 Pratte and Rossi, 2006 based on Iraci et al. 2005), and calculate a HOBr ~~rate constant of~~ diffusion

1099 ~~coefficient~~ in sulphuric acid of  $5.5 \cdot 10^{-6} \text{ cm}^2 \text{ s}^{-1}$  and  $1.0 \cdot 10^{-5} \text{ cm}^2 \text{ s}^{-1}$  at 50 and 80 % RH (-48 and 29  
1100 wt% $\text{H}_2\text{SO}_4$ ) respectively. ~~We assume the abovementioned~~ E-AIM predicts the aerosol  $\text{Cl}^-_{(\text{aq})}$   
1101 concentrations ~~predicted by E-AIM (to be~~  $0.004 \text{ M L}^{-1}$  and  $0.08 \text{ M L}^{-1}$  at 50 and 80 % RH respectively),  
1102 see Table 4.

Formatted: Superscript

Formatted: Superscript

Formatted: Superscript

Formatted: Superscript

1103 ~~Our~~ The new parameterisation for  $k^{\text{II}}$  yields uptake coefficients for  $\text{HOBr}+\text{Cl}^-$  of  $4.4 \cdot 10^{-3}$  at 50% RH  
1104 and  $7.6 \cdot 10^{-2}$  at 80% RH, in broad agreement to the low uptake coefficients reported by Pratte and  
1105 Rossi (2006);  $1.0 \pm 10^{-2}$  at  $\text{RH} \geq 76\%$ . Such agreement is to some extent not surprising, given the  
1106 usage of  $k^{\text{I}}$  reported at  $\text{RH} = 77\text{-}90\%$  from the same Pratte and Rossi (2006) experiments to derive an  
1107 estimate for  $k^{\text{II}}$  at acid saturation (see Section 3 and Figure 1). Nevertheless, the uptake calculations  
1108 confirm and provide a first explanation for the RH dependence of the uptake coefficient as reported  
1109 by Pratte and Rossi (2006). The model indicates that the underlying cause of this trend is greater  $[\text{Cl}^-_{(\text{aq})}]$   
1110 at higher RH, given higher solubility of HCl at the lower wt% $\text{H}_2\text{SO}_4$  at high RH. This is further  
1111 shown by Figure 3-2 that compares the modelled and observed RH dependence of the uptake  
1112 coefficient of HOBr across all reported data from 40 – 90 % RH, demonstrating broad agreement in  
1113 the trend (noting discrepancies may result from impurities within the sea-salt solution or  
1114 uncertainties within the parameterisations used in the uptake model).

1115 ~~We contrast~~ These findings are in contrast to the termolecular approach to  $k^{\text{I}}$  that yields an  
1116 uptake coefficient of 0.6 at both RH values, substantially overestimating  $\gamma_{\text{HOBr}}$  (by at least a factor of  
1117 20 (see Table 4)). This is because the termolecular approach assumes acid-dependent  $k^{\text{II}}$  across all  
1118 pH, leading to an extremely high rate constant for the reaction of  $\text{HOBr}+\text{Cl}^-$  at pH -1 to 0, and a very  
1119 fast rate of reaction of HOBr with  $\text{Cl}^-$ : even though  $\text{Cl}^-$  concentrations are depleted by acid-  
1120 displacement, the assumed increased rate constant at low pH overcompensates for this effect.

1121 In conclusion, our new  $k^{\text{II}}$  parameterisation for the kinetics of  $\text{HOBr}+\text{X}^-$  yields uptake coefficients in  
1122 agreement with reported laboratory data, and -for the first time- reconciles differences between  
1123 reported uptake on HCl-acidified and  $\text{H}_2\text{SO}_4$ -acidified sea-salt aerosols, within a single framework.

Formatted: Subscript

Formatted: Subscript

1124

## 1125 5-4 Atmospheric implications for BrO chemistry in the marine and volcanic environments

### 1126 54.1 Declining uptake coefficients on progressively $\text{H}_2\text{SO}_4$ -acidified sea-salt aerosol

1127 Using ~~our~~ the revised HOBr reaction kinetics (Figure 1), ~~we now re-evaluate~~ the  $\text{HOBr}+\text{Br}^-$  and  
1128  $\text{HOBr}+\text{Cl}^-$  reactive uptake coefficients are now re-evaluated for a model sea-salt aerosol that  
1129 undergoes progressive  $\text{H}_2\text{SO}_4$ -acidification (Figure 3) and compared to calculations using the  
1130 termolecular approach (~~Figure 4~~). We investigate how the reductions in halide ion concentrations



1131 caused by the  $\text{H}_2\text{SO}_{4(\text{aq})}$  addition (through both acid-displacement reactions that deplete  $[\text{Cl}^-_{(\text{aq})}]$ , and  
1132 dilution of  $[\text{Br}^-_{(\text{aq})}]$  by  $\text{H}_2\text{SO}_{4(\text{aq})}$  volume), [see Figure 2](#)) impact  $\gamma_{\text{HOBr}}$  at low pH.

1133 ~~We assume a~~ particle radius of 1 or 0.1  $\mu\text{m}$  [is assumed](#) in the uptake calculation. Temperature is set  
1134 to 298 K and RH = 80% (above deliquescence). For aerosol that is alkaline or only weakly acidic (pH  
1135 12 to pH 4), uptake coefficients were calculated assuming a fixed sea-salt composition with  $[\text{Cl}^-_{(\text{aq})}] =$   
1136  $5.3 \text{ Mol L}^{-1}$  and  $[\text{Br}^-_{(\text{aq})}] = 0.008 \text{ Mol L}^{-1}$ , with pH varied between 4 and 12 (E-AIM was not used given  
1137 very low degree of  $\text{H}_2\text{SO}_4$ -acidification). For more strongly acidified sea-salt, across  $\text{H}_2\text{SO}_4:\text{Na}$  ratios  
1138 from 0.05 to 400 (pH 4 to -0.87 for the model aerosol conditions), E-AIM was used to determine the  
1139 extent of acid-displacement of HCl from acidified  $\text{NaCl}_{(\text{aq})}$  aerosol, with aerosol  $\text{Br}^-_{(\text{aq})}$  determined  
1140 using an effective Henry's law solubility for HBr (see predicted composition in [Figure 2 Supp. Material](#)  
1141 [Section 3.2](#)).

Formatted: Superscript

1142 Figure 4 shows the calculated reactive uptake for  $\text{HOBr}+\text{Br}^-$  and  $\text{HOBr}+\text{Cl}^-$  increase with increasing  
1143 acidity over pH 4-12 for the uptake coefficient for 0.1 and 1  $\mu\text{m}$  radius particles, similar to that  
1144 previously reported using the termolecular approach. The alkaline to acid transition in  $\gamma_{\text{HOBr}}$  reflects  
1145 the increase in the underlying  $\text{HOBr}_{(\text{aq})}$   $k^{\text{II}}$  rate constant with acidity due to the onset of the acid  
1146 assisted mechanism, Figure 1 as well as the decrease of HOBr partitioning to  $\text{BrO}^-$ .  $\gamma_{\text{HOBr}+\text{Cl}^-}$  reaches  
1147 values close to the accommodation limit by  $\text{pH} \leq 8$  (for 1  $\mu\text{m}$  radius particles) or  $\text{pH} \leq 7$  (for 0.1  $\mu\text{m}$   
1148 radius particles) while  $\gamma_{\text{HOBr}+\text{Br}^-}$  reaches values close to the accommodation limit by  $\text{pH} \leq 5$  (for 1  $\mu\text{m}$   
1149 radius particles) or  $\text{pH} \leq 4$  (for 0.1  $\mu\text{m}$  radius particles).

1150 In the high acidity regime, the acid-saturation of  $k^{\text{II}}$  can cause  $\gamma_{\text{HOBr}}$  to plateau at a level slightly lower  
1151 than  $\alpha_{\text{HOBr}}$  (e.g. in  $\gamma_{\text{HOBr}+\text{Cl}^-}$  at  $\text{pH} \sim 4$ ), in contrast to the termolecular approach. Overall, for slightly-  
1152 acidified sea-salt aerosol, reactive uptake of HOBr is driven primarily by  $\gamma_{\text{HOBr}+\text{Cl}^-}$ .  $\gamma_{\text{HOBr}+\text{Br}^-}$  reaches  
1153 similar values to  $\gamma_{\text{HOBr}+\text{Cl}^-}$  at  $\text{pH} \sim 3-4$  for the specific model aerosol conditions of this study.

1154 However, as the degree acidification by  $\text{H}_2\text{SO}_4$  increases, the uptake coefficient for  $\text{HOBr}+\text{Cl}^-$  begins  
1155 to decline at  $\text{pH} < 4$ . This is due to acid-displacement reactions that convert  $\text{Cl}^-_{(\text{aq})}$  into  $\text{HCl}_{(\text{g})}$ , thereby  
1156 lowering  $[\text{Cl}^-_{(\text{aq})}]$ . This leads to  $\gamma_{\text{HOBr}+\text{Cl}^-} < \gamma_{\text{HOBr}+\text{Br}^-}$ , i.e. HOBr reactive uptake becomes driven by  
1157  $\text{HOBr}+\text{Br}^-$  below a pH of  $\sim 2$  for the specific aerosol conditions of this study. As  $\text{H}_2\text{SO}_4:\text{Na}$  ratio  
1158 increases further and pH decreases further, the uptake coefficient for  $\text{HOBr}+\text{Br}^-_{(\text{aq})}$  also begins to  
1159 decline. This is principally due to the dilution of  $\text{Br}^-_{(\text{aq})}$  by the additional volume of  $\text{H}_2\text{SO}_{4(\text{aq})}$  that  
1160 becomes important particularly at very high  $\text{H}_2\text{SO}_4:\text{Na}$  ([see E-AIM calculations in Supplementary](#)  
1161 [Materials](#)).

1162 Notably, the declines in uptake coefficients are greatest for smaller particles, for which there is a  
1163 greater probability that  $\text{HOBr}_{(\text{aq})}$  may diffuse across the particle and be released to the gas phase,  
1164 without any aqueous-phase reaction occurring.

1165 The uptake coefficients are also further reduced if parameterisations for the solubility of HOBr in  
1166  $\text{H}_2\text{SO}_{4(\text{aq})}$  is assumed in the uptake equation rather than that for water. The exact point of transition  
1167 between these two parameterisations is not well constrained, but it is clear that the  $\text{H}_2\text{SO}_{4(\text{aq})}$   
1168 parameterisations become more applicable than water with greater acidification, and must certainly  
1169 be more relevant at high  $\text{H}_2\text{SO}_4:\text{Na}$  ~~e.g. at 400:1~~. The lower solubility of HOBr in  $\text{H}_2\text{SO}_{4(\text{aq})}$  acts to  
1170 decrease the uptake coefficient, and is found to have a stronger impact on  $\gamma_{\text{HOBr}}$  than the slower rate  
1171 of diffusion of  $\text{HOBr}_{(\text{aq})}$  in  $\text{H}_2\text{SO}_4$ .

1172 In summary, following a rise over the alkaline-acid transition, our revised HOBr kinetics yields HOBr  
1173 reactive uptake coefficients that subsequently decline on progressively  $\text{H}_2\text{SO}_4$ -acidified sea-salt  
1174 aerosol. For the aerosol concentration assumed, the uptake coefficient on the 0.1  $\mu\text{m}$  radius  
1175 particles declines to  $\gamma_{\text{HOBr}+\text{Br}} < 0.03$  at a  $\text{H}_2\text{SO}_4:\text{Na}$  ratio of 400:1, indicating that the reactive uptake of  
1176 HOBr on highly acidified sub-micrometer particles is extremely low, Figure 43. These decreases in  
1177 uptake coefficient with increasing aerosol acidity are not captured by calculations that assume  
1178 termolecular kinetics. As stated in the previous section, this is because the termolecular approach  
1179 assumes the HOBr rate constant is acid-dependent across all pH, and does not consider acid-  
1180 saturation of the rate constant.

1181

## 1182 4.2 Implications for BrO chemistry in the marine boundary layer

Formatted: Font: Bold

1183

Formatted: Font: Bold

1184 Figure 4 shows clearly that higher acidity does not necessarily lead to faster production of reactive  
1185 bromine. It is well-known that acidity is required for reactive bromine formation to occur. We note  
1186 that  $\text{H}^+$  <sub>(aq)</sub> is consumed in the reaction, therefore a source of acidity is required to sustain prolonged  
1187 BrO formation chemistry. Further, under alkaline conditions HOBr dissociates into less reactive OBr<sup>-</sup>.  
1188 However, the  $\gamma_{\text{HOBr}}$  dependency on acidity shown here suggests that ~~excessive-additional~~ aerosol  
1189 acidification by  $\text{H}_2\text{SO}_{4(\text{aq})}$  ~~exerts a~~ can act as a limitation ~~on the extent of~~ the formation of reactive  
1190 bromine ~~formation~~ via HOBr uptake, particularly for small particle sizes.

1191 This leads to the following implications for BrO chemistry in the marine environment, where both  
1192 supra-micron and sub-micron particles are reported, the former typically being moderately acidified  
1193 perhaps with some Cl-depletion, and the latter being dominated by  $\text{H}_2\text{SO}_4$  with only a trace quantity

Formatted: Subscript

Formatted: Subscript

1194 of sea-salt (e.g. Keene et al., 2002); Further implications for BrO chemistry in the marine boundary  
1195 layer are now discussed.

1196 Firstly, the reactive uptake of HOBr is driven by reaction with Br<sub>2</sub> as  $v_{\text{HOBr+Cl}}$  is reduced on H<sub>2</sub>SO<sub>4</sub>-  
1197 acidified (Cl<sup>-</sup>-depleted) sea-salt aerosol. This leads to a negative feedback in the uptake coefficient  
1198 for HOBr with BrO chemistry evolution over time, as the conversion of Br<sub>(aq)</sub><sup>-</sup> to Br<sub>2(g)</sub> acts to decrease  
1199 aerosol [Br<sub>(aq)</sub><sup>-</sup>], reducing subsequent values of  $v_{\text{HOBr+Br}}$ .

Formatted: Font: Not Bold

Formatted: Superscript

Formatted: Font: Not Bold

1200 This negative feedback for  $v_{\text{HOBr+Br}}$  will play a much more significant role for overall HOBr reactive  
1201 uptake according our revised HOBr kinetics than has been assumed by model studies to date based  
1202 on the termolecular approach (for which  $v_{\text{HOBr+Cl}} \geq v_{\text{HOBr+Br}}$ ).

Formatted: Not Superscript/ Subscript

Formatted: Not Superscript/ Subscript

1203 Secondly, very low reactive uptake coefficients for both HOBr+Br<sup>-</sup> and HOBr+Cl<sup>-</sup> are predicted for  
1204 sub-micron particles at high H<sub>2</sub>SO<sub>4</sub>:Na ratios (e.g.  $v_{\text{HOBr}} < 0.03$ , see Figure 4). Such low  $v_{\text{HOBr}}$  is  
1205 proposed as a first explanation for the absence of observable Br<sub>(aq)</sub><sup>-</sup> depletion in sub-micron H<sub>2</sub>SO<sub>4</sub>-  
1206 dominated particles in the marine environment, in contrast to supra-micron particles where Br<sub>(aq)</sub><sup>-</sup>  
1207 depletion is observed and interpreted as evidence of HOBr reactive uptake to form reactive bromine  
1208 (Sander et al., 2003). Indeed, observations find the submicron H<sub>2</sub>SO<sub>4</sub>-dominated aerosol to be  
1209 enriched in Br<sub>(aq)</sub><sup>-</sup> relative to expected concentrations based on the particle Na<sup>+</sup> content (Sander et  
1210 al., 2003). A plausible explanation is that the release of Br<sub>2(g)</sub> from the supra-micron particles leads to  
1211 the continual formation of gas-phase reactive bromine species of which a proportion will ultimately  
1212 be deposited back to (both types of) marine aerosols as a source of Br<sub>(aq)</sub><sup>-</sup>. The net effect is for Br<sub>(aq)</sub><sup>-</sup>  
1213 concentrations to become enhanced (relative to Na) in the sub-micron aerosol where  $v_{\text{HOBr}}$  is low  
1214 simultaneous to becoming depleted in the supra-micron aerosol where  $v_{\text{HOBr}}$  is high. For the former,  
1215 an upper limit must exist to the extent Br-enrichment can occur whilst maintaining the relatively low  
1216  $v_{\text{HOBr+Br}}$ . Importantly, this argumentation is only possible using our new uptake calculations based on  
1217  $k^{\text{I}}$  calculated using revised HOBr kinetics in terms of  $k^{\text{II}}$ , as the termolecular approach predicts high  
1218 HOBr reactive uptake for both particle types. We encourage our new rate constants calculations for  
1219 HOBr reactive uptake to be incorporated into numerical models to test and quantify potential  
1220 submicron aerosol Br<sub>(aq)</sub><sup>-</sup> enrichment via this proposed mechanism.

Formatted: Adjust space between Latin and Asian text, Adjust space between Asian text and numbers

Formatted: Font: Not Bold

Formatted: Subscript

Formatted: Subscript

Formatted: Superscript

Formatted: Subscript

Formatted: Subscript

Formatted: Subscript

Formatted: Subscript

Formatted: Superscript

Formatted: Superscript

Formatted: Subscript

Formatted: Subscript

Formatted: Subscript

Formatted: Subscript

Formatted: Superscript

Formatted: Subscript

Formatted: Superscript

Formatted: Superscript

Formatted: Subscript

Formatted: Not Superscript/ Subscript

Formatted: Not Superscript/ Subscript

Formatted: Superscript

1221 We further suggest both of the abovementioned factors may also contribute underlying reasons for  
1222 the reported over-prediction by numerical models of BrO cycling in the marine environment (Sander  
1223 et al., 2003; Smoydzin and von Glasow, 2007; Keene et al., 2009). Inclusion of the new HOBr kinetics  
1224 into such models will allow this hypothesis to be tested and quantified.

## 1226 **5.2 Reduced BrO cycling in the marine boundary layer (MBL)**

1227 The MBL typically contains a multi-modal aerosol size distribution, including slightly acidic supra-  
1228 micron particles and substantially acidified submicron particles (e.g. Keene et al., 2002). Whilst fresh  
1229 sea-salt aerosol is alkaline, acids of natural or anthropogenic origin, such as  $\text{H}_2\text{SO}_4$  or  $\text{HNO}_3$  may  
1230 interact with the aerosol with acid-displacement reactions leading to release of  $\text{HCl}_{(g)}$  and depletion  
1231 of aerosol  $\text{Cl}^-_{(aq)}$ . The  $\text{HCl}_{(g)}$  released acts as a gas-phase reservoir of acidity (Von Glasow and Sander,  
1232 2001). Observations find that the sub-micron particles are typically highly acidified by  $\text{H}_2\text{SO}_{4(aq)}$  and  
1233 thus contain relatively low concentrations of sea-salt components.  $\text{Cl}^-_{(aq)}$  is depleted in these  
1234 particles. The supra-micron particles are acidified to a lesser extent, but can also exhibit a degree of  
1235 chloride depletion. For example, Keene et al. (2002) report aerosol pH in Bermuda in 1997 under  
1236 moderately polluted conditions of pH 3–4 for supramicron-sized particles, and pH 1–2 for finer sized  
1237 fractions, with all particle pH buffered by the  $\text{H}^+ + \text{SO}_4^{2-} \leftrightarrow \text{HSO}_4^-$  equilibrium. Sulfate dominated the  
1238 submicrometer size fraction, for example  $\text{Na}^+ < 2.4 \text{ nmol m}^{-3}$  for the 0.3  $\mu\text{m}$  diameter particles  
1239 sampled whilst the maximum  $\text{SO}_4^{2-} \sim 69.8 \text{ nmol m}^{-3}$  and median  $\text{SO}_4^{2-} = 5.93 \text{ nmol m}^{-3}$ .

1240 To date, it has been assumed that HOBr reactive uptake is rapid on both the sub- and supra-micron  
1241 fractions of acidified marine aerosol (e.g. Sander et al., 2003). However, our re-evaluation of HOBr  
1242 reactive kinetics (Figure 1) indicates HOBr reactive uptake to be low on the highly acidified sub-  
1243 micron particles ( $\gamma_{\text{HOBr}} < 0.03$ ). Thus the contribution of the submicron aerosol fraction to HOBr  
1244 uptake is much smaller than has been assumed to date.

1245 Furthermore, a negative feedback exists in the reactive uptake of HOBr+Br<sup>-</sup> as the BrO formation  
1246 chemistry progresses: Given  $\gamma_{\text{HOBr+Br}^-}$  is a function of  $[\text{Br}^-_{(aq)}]$ , the conversion of  $\text{Br}^-_{(aq)}$  to  $\text{Br}_{2(g)}$  acts to  
1247 decrease aerosol  $[\text{Br}^-_{(aq)}]$ , reducing subsequent values of  $\gamma_{\text{HOBr+Br}^-}$ . As already mentioned,  $\gamma_{\text{HOBr+Cl}^-}$  is  
1248 reduced on  $\text{H}_2\text{SO}_4$ -acidified ( $\text{Cl}^-$ -depleted) sea-salt aerosol, such that uptake is driven by HOBr+Br<sup>-</sup>,  
1249 Figure 4. Therefore this negative feedback for  $\gamma_{\text{HOBr+Br}^-}$  will play a much more significant role for  
1250 overall HOBr reactive uptake according our revised HOBr kinetics than has been assumed by model  
1251 studies to date.

1252 We suggest both of the abovementioned factors (the reduced uptake coefficient on highly acidified  
1253 sea-salt particles, and the HOBr+Br<sup>-</sup> negative feedback loop) as potential underlying reasons for the  
1254 over-prediction by numerical models of BrO cycling in the marine environment (Sander et al., 2003;  
1255 Smoydzin and von Glasow, 2007; Keene et al., 2009). Inclusion of the new HOBr kinetics into such  
1256 models will allow our hypothesis to be tested and quantified.

1257

1258 **5.3 — A first explanation for Br enriched sub-micron aerosol in the marine environment**

1259 An atmospheric phenomenon that is observed to be relatively widespread but has not previously  
1260 been explained is the occurrence of Br enrichment in highly acidified sub-micron sea-salt particles  
1261 simultaneous to Br depletion in supramicron sea-salt particles, see Sander et al. (2003) and  
1262 references therein). For example, inorganic aerosol bromine depletion often exceeds 50% in the  
1263 supramicron particle size fraction whereas bromide enrichment may reach 10's % in the  
1264 submicrometer fraction. Whilst reactive halogen chemistry can readily explain the occurrence of Br  
1265 depletion in sea-salt aerosols, a review by Sander et al. (2003) asks the open question "How can  
1266 bromine accumulate in submicrometer particles instead of being recycled back into the gas phase?".

1267 From Figure 4, we can propose a mechanism for Br enrichment. The acidified supra-micron particles  
1268 support reactive uptake of HOBr, with release of reactive bromine leading to Br depletion in these  
1269 particles. However, HOBr uptake coefficients on the highly acidified sub-micron particles are low:  
1270 the HOBr+Cl<sup>-</sup> coefficient is reduced due to acid displacement of HCl<sub>(g)</sub> and the HOBr+Br<sup>-</sup> coefficient is  
1271 reduced due to dilution of [Br<sup>-</sup><sub>(aq)</sub>] at high H<sub>2</sub>SO<sub>4</sub>:Na ratios (note that Na is also diluted so does not  
1272 change relative Br:Na, or the Br enrichment factor). Thus there is a high overall probability that  
1273 HOBr<sub>(aq)</sub> diffuses across and out of the sub-micrometer particles without reaction occurring, yielding  
1274 low  $\gamma_{\text{HOBr}}$ . As consequence, the submicron particles do not readily become depleted in Br<sup>-</sup><sub>(aq)</sub>.  
1275 Moreover, the release of Br<sub>2(g)</sub> from the supra-micron particles leads to the continual formation of  
1276 gas-phase reactive bromine species (such as BrO) in the MBL, of which a proportion will be  
1277 converted to HBr<sub>(g)</sub> (e.g. via reaction of Br with HCHO, or reaction of BrO with OH). Deposition of gas-  
1278 phase bromine species like HBr to the submicron aerosol yields a source of Br<sup>-</sup><sub>(aq)</sub>. The net effect is  
1279 for Br<sup>-</sup><sub>(aq)</sub> concentrations to become enhanced (relative to Na) in the sub-micron aerosol  
1280 simultaneous to becoming depleted in the supra-micron aerosol. Note that this argumentation is  
1281 only possible using our new uptake calculations based on  $k^{\dagger}$  calculated using revised HOBr kinetics in  
1282 terms of  $k^{\text{II}}$  as the termolecular approach predicts high HOBr uptake for both particle types. We  
1283 encourage our new rate constants calculations for HOBr reactive uptake to be incorporated into  
1284 numerical models to test and quantify submicron aerosol Br enrichment via our proposed  
1285 mechanism.

1287 **5.4.4.3 Reactive uptake of HOBr on volcanic aerosol**

1288 HOBr reactive uptake coefficients are now calculated for the first time onto aerosol in a halogen-rich  
1289 volcano plume, using the  $k^{\text{II}}$  parameterisations for  $\text{HOBr}+\text{Br}^-$  and  $\text{HOBr}+\text{Cl}^-$ , ~~and E-AIM predictions of~~  
1290 ~~the volcanic aerosol composition.~~

1291 ~~The predicted aerosol and plume composition for Etna is shown in Figure 5 for two of the three~~  
1292 ~~plume dilution scenarios, at three different temperatures. Whilst the Etna emission~~  
1293 ~~(( $\text{SO}_2$ ): $\text{HCl}$ : $\text{H}_2\text{SO}_4$ : $\text{HBr}$  at molar ratios 1:0.5:0.01:0.00075) contains substantially less HBr than HCl, the~~  
1294 ~~higher solubility of HBr relative to HCl leads to relatively similar aqueous phase concentrations for  $\text{Cl}^-$~~   
1295 ~~( $\text{aq}$ ) and  $\text{Br}^-$ ( $\text{aq}$ ). Both aqueous phase halide concentrations are more elevated in the stronger (30~~  
1296  ~~$\mu\text{mol}/\text{m}^3$   $\text{SO}_2$ ) plume than the dilute (0.3  $\mu\text{mol}/\text{m}^3$   $\text{SO}_2$ ) plume scenarios as a consequence of the~~  
1297 ~~greater HX partial pressures promoting gas to aerosol partitioning in the concentrated plume~~  
1298 ~~scenario. Temperature exerts a significant control on  $[\text{X}^-_{(\text{aq})}]$  through the inverse dependence of~~  
1299 ~~halide solubility on temperature. Relative humidity (RH) also exerts a control on  $[\text{X}^-_{(\text{aq})}]$ ; the~~  
1300 ~~dependence of  $[\text{X}^-_{(\text{aq})}]$  on RH is initially positive, as HX solubility is greater at higher pH (thus, higher~~  
1301 ~~RH). However, in the more concentrated plume scenario the increase in aerosol volume with RH can~~  
1302 ~~lead to complete removal of  $\text{HX}_{(\text{g})}$  followed by dilution of  $[\text{X}^-_{(\text{aq})}]$ . The decline in  $[\text{X}^-_{(\text{aq})}]$  is more~~  
1303 ~~pronounced and occurs earlier for  $\text{Br}^-_{(\text{aq})}$  than  $\text{Cl}^-_{(\text{aq})}$  given higher solubility and lower gas phase~~  
1304 ~~concentrations. These declines in  $[\text{X}^-_{(\text{aq})}]$  are only seen for the strong plume scenario as gas to~~  
1305 ~~aerosol partitioning is much lower for the dilute plume scenario such that HX is not depleted. The Br~~  
1306 ~~composition used here for Etna is based on an average volcanic Br/S emission reported by Aiuppa et~~  
1307 ~~al. (2006), as used in the modelling study of Roberts et al. (2013), and a factor of two and three~~  
1308 ~~lower than that assumed by Roberts et al. (2009) and von Glasow (2010) respectively. Our assumed~~  
1309 ~~volcanic aerosol composition also differs to that reported by Martin et al. (2012) in an E-AIM study of~~  
1310 ~~the Masaya volcano emission, due to differences in the volcano specific gas and aerosol emission,~~  
1311 ~~although both of our E-AIM applications predict similar tendencies for aerosol compositional~~  
1312 ~~changes as a function of temperature and RH.~~

1313 Using the volcanic aerosol composition predicted by E-AIM (based on Etna emission scenario, see  
1314 section 3.3 of Supplementary Material), uptake coefficients for  $\text{HOBr}+\text{Br}^-$  and  $\text{HOBr}+\text{Cl}^-$  are  
1315 calculated across tropospheric temperature and relative humidity, for ~~three two different~~ plume  
1316 dilutions (30, ~~3~~ and 0.3  $\mu\text{mol}/\text{m}^3$ , which are equivalent to  $\sim 1$  ppmv, ~~0.1 ppmv~~, and 0.01 ppmv  $\text{SO}_2$  at  
1317 4 km altitude in US standard atmosphere), and assuming a particle radius of 1  $\mu\text{m}$ , Figure 64. ~~Also~~  
1318 ~~shown is the uptake coefficient for an evolved volcanic plume composition, where it is assumed a~~  
1319 ~~substantial conversion of  $\text{Br}^-_{(\text{aq})}$  to reactive bromine has occurred.~~ There exists no experimental  
1320 information regarding the temperature dependence of  $k^{\text{II}}$  for  $\text{HOBr}+\text{X}$ . Here it is assumed the

Formatted: Superscript

Formatted: Superscript

1321 variation  $k''$  with temperature over 230-300 K is small compared to the temperature dependence of  
1322 the HOBr and HX solubilities (which vary by several orders of magnitude over the parameter space).

1323 High HOBr uptake coefficients are predicted at low tropospheric temperatures:  $\gamma_{\text{HOBr}+\text{Br}^-} \approx \gamma_{\text{HOBr}+\text{Cl}^-} \approx$   
1324 0.6. The uptake coefficient decreases markedly with increasing temperature for  $\gamma_{\text{HOBr}+\text{Cl}^-}$  and also  
1325 decreases for  $\gamma_{\text{HOBr}+\text{Br}^-}$  in the most dilute plume scenario. The inverse temperature trend in  $\gamma_{\text{HOBr}}$   
1326 (~~particularly for  $\gamma_{\text{HOBr}+\text{Cl}^-}$~~ ) is caused by a lower solubility of H~~X~~Cl in sulphuric acid particles at higher  
1327 tropospheric temperatures (~~particularly for HCl~~), augmented by a similar temperature trend in the  
1328 solubility of HOBr<sub>(aq)</sub>. The variation with plume dilution is explained by the fact that lower gas-to-  
1329 aerosol partitioning yields lower  $[X_{\text{(aq)}}]$  in the dilute plume scenarios thus a lower  $k' = k'' \cdot [X_{\text{(aq)}}]$  in the  
1330 uptake equation, hence a reduced  $\gamma_{\text{HOBr}}$ .

1331 Figure 6-4 also illustrates a weak dependence of the uptake coefficients on relative humidity. This is,  
1332 due to increasing solubility of the halides with RH or lower wt%H<sub>2</sub>SO<sub>4</sub> (see Figure 5 and Section 3.7,  
1333 ~~any potential RH-dependence of HOBr solubility is not considered in the parameterisations here~~, see  
1334 ~~Supplementary Material Methods~~). As for the marine aerosol study, reductions in  $\gamma_{\text{HOBr}}$  are more  
1335 pronounced for particles of smaller radii (data not shown), as the probability for diffusion across the  
1336 particle without reaction is higher. According to Figure 6-4,  ~~$\gamma_{\text{HOBr}+\text{Br}^-}$~~  is equal to or exceeds  $\gamma_{\text{HOBr}+\text{Cl}^-}$   
1337 under all temperature and humidity scenarios for the composition of the Etna emission. This is  
1338 driven by ~~higher  $k'$  in the uptake calculation (where  $k' = k'' \cdot [X]$  with  $k''$  a function of pH), due to the~~  
1339 greater ~~saturation value  $k''$  for HOBr+Br<sup>-</sup> at high acidity~~, and the higher solubility of HBr compared to  
1340 HCl. ~~However, the evolved plume scenario where it is assumed Br<sup>-</sup><sub>(aq)</sub> concentrations reduced (as~~  
1341 ~~consequence of reactive bromine release to the gas phase) yields a much lower uptake coefficient~~  
1342 ~~for HOBr+Br<sup>-</sup>.~~

1343 ~~Again it is important to note that this uptake re-evaluation using revised HOBr kinetics differs from~~  
1344 ~~that As in the case of sea salt aerosol, uptake coefficient calculations using the  $k''$  parameterisation~~  
1345 ~~differ markedly from that calculated using the termolecular approach (also shown in Figure 4) to~~  
1346 ~~HOBr kinetics which yields high and typically accommodation limited HOBr uptake coefficients~~  
1347 ~~throughout the parameter space (also shown in Figure 6).~~

1348 ~~Indeed, this is due to the fact that with the termolecular approach ( $k' = k_{\text{ter}} \cdot [\text{H}^+_{\text{(aq)}}] \cdot [X_{\text{(aq)}}]$ ) the~~  
1349 ~~increased value of  $k_{\text{ter}}$  at high acidity more than compensates for the acidity-driven decreases in  $X$ ,~~  
1350 ~~thus yielding high  $k'$  and high  $\gamma_{\text{HOBr}}$ .~~

1351

1352 5.5 Implications for reactive halogen chemistry in volcano plumes

Formatted: Superscript  
Formatted: Not Superscript/ Subscript  
Formatted: Superscript  
Formatted: Superscript  
Formatted: Superscript  
Formatted: Superscript

Formatted: Superscript  
Formatted: Subscript  
Formatted: Superscript  
Formatted: Subscript  
Formatted: Superscript  
Formatted: Subscript  
Formatted: Superscript  
Formatted: Font: Not Bold

1353 ~~We conclude that important factors governing the HOBr reactive uptake coefficient in volcanic~~  
1354 ~~plumes are: plume composition (particularly halogen:sulphate ratios), plume strength or dilution~~  
1355 ~~(through its effect on halogen gas-aerosol partitioning), aerosol size, ambient temperature and~~  
1356 ~~relative humidity, for which the emission altitude and season exert primary controls. The overall rate~~  
1357 ~~of reactive uptake of HOBr in a volcano plume depends also on the concentration of HOBr<sub>(g)</sub> and~~  
1358 ~~aerosol surface area density, as well as the uptake coefficient (see E1).~~

1359 Figure 6-4 shows that in concentrated plumes near to the volcanic source, the aqueous-phase halide  
1360 concentrations are sufficiently high that  $\gamma_{\text{HOBr+Br}^-}$  is accommodation-limited. Rapid formation of BrO is  
1361 expected to occur. This is consistent with observations of volcanic BrO at numerous volcanoes  
1362 globally (e.g. Bobrowski et al., 2007b, Boichu et al., 2011, and references therein), including  
1363 emissions from both low and high altitude volcanoes, explosive eruptions and from passive  
1364 degassing. However, it is anticipated that the reactive uptake coefficient for HOBr+Br<sup>-</sup> will be  
1365 reduced as BrO chemistry progresses causing Br<sub>(aq)<sup>-</sup> concentrations to decline (due to conversion of</sub>  
1366 HBr into reactive bromine). This will likely slow the BrO cycling in the more evolved plume. Plumes  
1367 will also become more dilute over time due to dispersion. Figure 4 predicts this will lead to a  
1368 reduction in the HOBr reactive uptake coefficient particularly in plumes confined to the lower  
1369 troposphere, which may contribute to a slower rate of BrO cycling. For plumes in the mid-upper  
1370 troposphere,  $\gamma_{\text{HOBr}}$  is predicted to remain high.

1371 ~~As the volcanic plume disperses into the troposphere the HOBr gas and aerosol concentration~~  
1372 ~~(hence surface area density) decline. Therefore the rate of HOBr reactive uptake is expected to~~  
1373 ~~decline with plume dilution, which is further reinforced by the predicted decline in  $\gamma_{\text{HOBr}}$  as the plume~~  
1374 ~~disperses and dilutes, particularly for  $\gamma_{\text{HOBr+Cl}^-}$ , which is low at temperatures representative of the~~  
1375 ~~lower troposphere. As a result of this decline, the HOBr reactive uptake becomes driven by  $\gamma_{\text{HOBr+Br}^-}$  in~~  
1376 ~~dispersed plumes under most tropospheric conditions, and in low-altitude plumes. Under these~~  
1377 ~~circumstances a negative feedback exists as the BrO chemistry progresses: the conversion of Br<sub>(aq)<sup>-</sup> to</sub>~~  
1378 ~~Br<sub>2(aq)</sub> acts to deplete [Br<sub>(aq)<sup>-</sup>], and consequently reduces the HOBr+Br<sup>-</sup> uptake coefficient, as shown</sub>~~  
1379 ~~in Figure 6 for the evolved plume scenario (with maximum possible Br<sub>(aq)<sup>-</sup> depletion).</sub>~~

1380 These reductions in  $\gamma_{\text{HOBr+Br}^-}$  and  $\gamma_{\text{HOBr+Cl}^-}$  with plume dispersion and evolution will act to slow the rate  
1381 of reactive bromine cycling in the dispersed plume. However, for plumes injected into the mid-upper  
1382 troposphere, at low ambient temperatures (hence high solubility for HOBr, and HX and low rate of  
1383 diffusion of HOBr<sub>(aq)</sub>),  $\gamma_{\text{HOBr}}$  values remain relatively high. Therefore continued BrO cycling in the  
1384 downwind plumes from eruptions into the mid-troposphere (e.g. Eyjafjallajökull) or in plumes from  
1385 quiescently degassing volcanoes with elevated summits (e.g. Etna, Italy, ~3.3 km asl) is expected. For

Formatted: Superscript

Formatted: Subscript



1386 ~~volcanoes emitting at low altitudes at high ambient tropospheric temperatures, BrO cycling is~~  
1387 ~~expected to be initially rapid (given high plume gas and aerosol concentrations as well as high~~  
1388  ~~$\gamma_{\text{HOBr}+\text{Br}^{\cdot}}$ ), but the decreased uptake coefficient in the dispersed plume may limit the extent of BrO~~  
1389 ~~cycling further downwind.~~

1390 To date, numerical model studies of the impacts of volcanic halogens reactive halogen chemistry in  
1391 the troposphere have either used a fixed uptake coefficient (Roberts et al., 2009; 2014, Kelly et al.,  
1392 2013) or the termolecular approach to HOBr kinetics (Bobrowski et al., 2009; von Glasow, 2010).  
1393 Figure 6-4 illustrates both of these approaches will lead to modelling inaccuracies, particularly in the  
1394 downwind plume. ~~We recommend~~ incorporation of more realistic HOBr kinetics in these models,  
1395 using the parameterisations proposed here, is recommended in order to accurately simulate the  
1396 reactive bromine chemistry and plume impacts.

1397

## 1398 **6-5 Conclusions**

1399 This study introduces a new evaluation of HOBr reactive uptake coefficients on aerosol of different  
1400 compositions, in the context of the general acid assisted mechanism. We emphasise that the  
1401 termolecular kinetic approach assumed in numerical model studies of tropospheric reactive bromine  
1402 chemistry to date is strictly only valid for a specific pH range. Rather, according to the general acid  
1403 assisted mechanism, the reaction kinetics for HOBr becomes independent of pH at high acidity. By  
1404 re-evaluation of reported rate constant data from uptake experiments on acidified sea-salt aerosol,  
1405 and consideration of relative reaction rates according to nucleophile strength, we identify the  
1406 kinetics of HOBr+Cl<sup>-</sup> may saturate below pH 6 to yield a second-order rate constant of  $k^{\text{II}} \sim 10^4 \text{ M s}^{-1}$ .  
1407 The kinetics of HOBr+Br<sup>-</sup> saturates at  $k^{\text{II}} \sim 10^8\text{-}10^9 \text{ M s}^{-1}$  at pH < ~1 based on experimental data and  
1408 kinetics estimates of Eigen and Kustin (1962) and Beckwith et al. (1996).

1409 This study reconciles for the first time the different reported uptake reactive coefficient from  
1410 laboratory experiments. The new  $k^{\text{II}}$  parameterisation yields uptake coefficients that are consistent  
1411 with reported uptake experiments:  $\gamma_{\text{HOBr}} = 0.6$  on super-saturated NaBr aerosol (Wachsmuth et  
1412 al.2002);  $\gamma_{\text{HOBr}} > 0.2$  on HCl-acidified sea-salt aerosol (Abbatt and Wachsewsky 1998),  $\gamma_{\text{HOBr}} = 10^{-2}$  on  
1413 H<sub>2</sub>SO<sub>4</sub>-acidified sea-salt aerosol, with an RH dependence (Pratte and Rossi, 2006). The variation in  
1414 uptake coefficient across the alkaline-aerosol transition is similar to that previously predicted using  
1415 the termolecular approach but uptake calculations using our revised kinetics of HOBr show much  
1416 lower uptake coefficients for HOBr in highly acidified sea-salt aerosol, particularly for small particle  
1417 radii. This is due to acid-displacement of HCl<sub>(g)</sub> at high acidity slowing the rate of reaction of HOBr+Cl<sup>-</sup>

1418 , thus lowering  $\gamma_{\text{HOBr+Cl}}$ , with dilution of  $[\text{Br}^-_{(\text{aq})}]$  at very high  $\text{H}_2\text{SO}_4$ :sea-salt ratios slowing the rate of  
1419 reaction of  $\text{HOBr}+\text{Br}^-$ , thus lowering  $\gamma_{\text{HOBr+Br}^-}$ . This finding ~~is in contrast~~ to the existing termolecular  
1420 approach previous to uptake calculations ~~that assumed high  $\gamma_{\text{HOBr}}$  at high acidity based on~~  
1421 ~~termolecular reaction kinetics~~ in which the higher rate constant  $k^{\text{H}}$  increases with acidity and which  
1422 overcompensates for the decrease in halide concentration with increasing acidity. Thus, the  
1423 termolecular approach, as currently used in numerical models of tropospheric BrO chemistry, may  
1424 cause HOBr reactive uptake to be substantially over estimated in aerosol at high acidity.

Formatted: Superscript

1425 Implications for BrO chemistry in the marine boundary layer have been discussed. Firstly, the HOBr  
1426 uptake coefficient is predicted to be high on slightly acidified supra-micron particles but extremely  
1427 low on highly-acidified sub-micron particles. A first explanation for the observed Br-enrichment in  
1428 the sub-micron particles simultaneous to Br-depletion in supra-micron particles is thereby proposed,  
1429 as reactive bromine release from the supra-micron fraction may deposit and accumulate in the  
1430 submicron fraction, that does not undergo significant Br- depletion. Secondly, because the  
1431 HOBr+Br- uptake coefficient is a function of  $\text{Br}^-_{(\text{aq})}$  concentrations, a negative feedback can occur as  
1432 the marine BrO chemistry evolves, and supramicron particle  $\text{Br}^-_{(\text{aq})}$  concentrations are lowered by the  
1433 release of reactive bromine. According to our revised HOBr kinetics (yielding  $\gamma_{\text{HOBr+Br}^-} > \gamma_{\text{HOBr+Cl}}$ ), this  
1434 negative feedback for  $\gamma_{\text{HOBr+Br}^-}$  exerts a stronger overall influence on the rate of HOBr reactive uptake  
1435 than previous studies have assumed.

Formatted: Superscript

Formatted: Subscript

1436 Calculations on volcanic aerosol show that uptake is high and accommodation limited in the  
1437 concentrated near-source plume, enabling BrO formation to rapidly occur. Uptake coefficients are  
1438 reduced in more dilute plumes, particularly for HOBr+Cl-, at high temperatures (typical lower  
1439 tropospheric altitudes), for small particle radii, ~~and for HOBr+Br- in evolved plume composition~~  
1440 ~~scenarios~~. The findings suggest that HOBr uptake on sulphate aerosol directly emitted from  
1441 volcanoes can readily promote BrO cycling in plumes ~~dispersing into the upper or middle throughout~~  
1442 ~~the -troposphere (quiescently degassing from elevated volcano summits e.g. Etna, or explosive~~  
1443 ~~eruptions e.g. Eyjafjallajökull)~~ but that the rate of BrO cycling may be reduced by low uptake  
1444 coefficients in the dispersed downwind plume, particularly at higher tropospheric temperatures (low  
1445 altitude emissions) lower tropospheric altitudes. Inclusion of our revised HOBr reaction kinetics in  
1446 numerical models of volcanic plume chemistry (or uptake coefficients derived therefrom) is required  
1447 to accurately predict the impacts of volcanic halogens on the troposphere.

1448

1449 **Acknowledgements**

1450 | TJR and LJ are grateful for funding from LABEX VOLTAIRE (VOLatils- Terre Atmosphère Interactions -  
1451 | Ressources et Environnement) ANR-10-LABX-100-01 (2011-20). PTG acknowledges the ERC for  
1452 | funding.  
1453

**Formatted:** Line spacing: 1.5 lines

1454 **References**

- 1455 Abbatt J. P. D. and Waschewsky G. C.G.: Heterogeneous Interactions of HOBr, HNO<sub>3</sub>, O<sub>3</sub>, and NO<sub>2</sub>  
1456 with Deliquescent NaCl Aerosols at Room Temperature, *J. Phys. Chem. A*, 102, 3719-3725, 1998.
- 1457 Ammann, M., Cox, R. A., Crowley, J.N., Jenkin, M. E., Mellouki, A., Rossi, M. J., Troe, J., and  
1458 Wallington, T. J.: Evaluated kinetic and photochemical data for atmospheric chemistry: Volume VI –  
1459 heterogeneous reactions with liquid substrates, *Atmos. Chem. Phys.*, 13, 8045 - 8228, 2013, IUPAC  
1460 Task Group on Atmospheric Chemical Kinetic Data Evaluation, <http://iupac.pole-ether.fr/index.html>.
- 1461 Barrie L. A., Bottenheim J. W., Schnell R. C., Crutzen P. J., Rasmussen R. A.: Ozone destruction and  
1462 photochemical reactions at polar sunrise in the lower Arctic atmosphere, *Nature*, 334, 138-141,  
1463 1998.
- 1464 Beckwith R. C., Wang T. X., and Margerum D. W.: Equilibrium and Kinetics of Bromine Hydrolysis,  
1465 *Inorg. Chem.*, 35, 995-1000, 1996.
- 1466 Blatchley, E. R., R. W. Johnson, J. E. Alleman and W. F. McCoy : Effective Henry's law constants for  
1467 free chlorine and free bromine, *Water Research*, 26, 99-106, 1991.
- 1468 Bobrowski, N., Honniger, G., Galle, B. and Platt, U.: Detection of bromine monoxide in a volcanic  
1469 plume. *Nature*, 423, 273-276, doi:10.1038/nature01625, 2003.
- 1470 Bobrowski, N., von Glasow, R., Aiuppa, A., Inguaggiato, S., Louban, I., Ibrahim, O. W. and Platt, U.:  
1471 Reactive halogen chemistry in volcanic plumes, *J. Geophys. Res.*, 112, D06311,  
1472 doi:101029/2006JD007206, 2007a.
- 1473 Bobrowski, N. and Platt, U.: SO<sub>2</sub>/BrO ratios studied in five volcanic plumes. *J.Volcanol. Geoth. Res.*,  
1474 166, 3-4, 147-160, 10.1016/j.jvolgeores.2007.07.003, 2007b.
- 1475 Boichu, M., Oppenheimer C., Roberts T. J., Tsanev V., Kyle P. R.: On bromine, nitrogen oxides and  
1476 ozone depletion in the tropospheric plume of Erebus volcano (Antarctica), *Atmos. Environ.*, 45, 23,  
1477 3856-3866, 2011.
- 1478 Breider T. J., Chipperfield M. P., Richards N. A. D., Carslaw K. S., Mann G. W., Spracklen D. V.: Impact  
1479 of BrO on dimethylsulfide in the remote marine boundary layer, *Geophys. Res. Lett.*, 37, L02807,  
1480 doi:10.1029/2009GL040868., 2010.
- 1481 Carslaw K. S., Clegg S. L. and Brimblecombe P.: A thermodynamic model of the system HCl - HNO<sub>3</sub> -  
1482 H<sub>2</sub>SO<sub>4</sub> - H<sub>2</sub>O, including solubilities of HBr, from <200 K to 328 K. *J. Phys. Chem.* 99, 11557-11574,  
1483 1995.

1484 Clegg S. L., Brimblecombe P. and Wexler A. S., A thermodynamic model of the system  $H^+ - NH_4^+ - Na^+$   
1485  $- SO_4^{2-} - NO_3^- - Cl^- - H_2O$  at 298.15 K. *J. Phys. Chem. A* 102, 2155-2171, 1998.

1486 Eigen M. and Kustin K.: The Kinetics of Halogen Hydrolysis, *J. Am. Chem. Soc.*, 1962, 84 (8), pp 1355–  
1487 1361, DOI: 10.1021/ja00867a005, 1962.

1488 Fickert S., Adams J. W. and Crowley J. N.: Activation of Br<sub>2</sub> and BrCl via uptake of HOBr onto aqueous  
1489 salt solutions, *Journal of Geophysical Research*, 104, D19, 23719-23727, 1999.

1490 Frenzel A., Scheer V., Sikorski R., George Ch., Behnke W., and Zetzsch C.: Heterogeneous  
1491 Interconversion Reactions of BrNO<sub>2</sub>, ClNO<sub>2</sub>, Br<sub>2</sub>, and Cl<sub>2</sub>., *J. Phys. Chem. A*, 102, 1329-1337, 1998.

1492 Gerritsen C.M. and Margare D. W.: Non-Metal Redox Kinetics: Hypochlorite and Hypochlorous Acid  
1493 Reactions with Cyanide, *Inorg. Chem.*, 29, 2757-2762, 1990.

1494 Iraci L. T., Michelsen R. R., Ashbourn S. F. M., Rammer T. A., and Golden D. M.: Uptake of  
1495 hypobromous acid (HOBr) by aqueous sulfuric acid solutions: low-temperature solubility and  
1496 reaction, *Atmos. Chem. Phys.*, 5, 1577–1587, 2005.

1497 Liu Q. and Margare D. W.: Equilibrium and Kinetics of Bromine, *Environ. Sci. Technol.*, 35, 1127-  
1498 1133, 2001.

1499 Keene W.C., Pszenny A.A.P., Maben J.R., and Sander R.: Variation of marine aerosol acidity with  
1500 particle size, *Geophysical research Letters*, 29, 7, 1101, 10.1029/2001GL013881, 2002.

1501 Keene W. C., Long M. S., Pszenny A. A. P. Sander R., Maben J. R., Wall A. J., O'Halloran T. L., Kerkweg  
1502 A., Fischer E. V., and Schrem O.: Latitudinal variation in the multiphase chemical processing of  
1503 inorganic halogens and related species over the eastern North and South Atlantic Oceans, *Atmos.*  
1504 *Chem. Phys.*, 9, 7361–7385, 2009.

1505 Kelly P J., Kern C., Roberts T. J., Lopez T., Werner C., Aiuppa A., Rapid chemical evolution of  
1506 tropospheric volcanic emissions from Redoubt Volcano, Alaska, based on observations of ozone and  
1507 halogen-containing gases, *Journal of Volcanology and Geothermal Research*, Volume 259, Pages 317-  
1508 333, 2013.

1509 Klassen, J. K., Hu, Z. and Williams, L. R.: Diffusion coefficients for HCl and HBr in 30 wt % to 72 wt %  
1510 sulfuric acid at temperatures between 220 and 300 K, *J. Geophys. Res.* 103, 16197-16202, 1998.

1511 Kumar K. and Margare D. W.: Kinetics and Mechanism of General- Acid-Assisted Oxidation of  
1512 Bromide by Hypochlorite and Hypochlorous Acid, *Inorg. Chem.* 26, 2706-2711, 1987.

1513 Martin R.S.,<sup>2</sup>, Wheeler J.C., Ilyinskaya E., Braban C.F. and Oppenheimer C: The uptake of halogen  
1514 (HF, HCl, HBr and HI) and nitric (HNO<sub>3</sub>) acids into acidic sulphate particles in quiescent volcanic  
1515 plumes, *Chemical Geology* 296-297, 19–25, 2012.

1516 Nagy J.C., Kumar K., Margareem D. W.: Non-Metal Redox Kinetics: Oxidation of Iodide by  
1517 Hypochlorous Acid and by Nitrogen Trichloride Measured by the Pulsed-Accelerated-Flow Method,  
1518 *Inorganic Chemistry*, Vol. 27, No. 16, 2773-2780, 1988.

1519 Nagy P. and Ashby M.T.: Reactive Sulfur Species: Kinetics and Mechanisms of the Oxidation of  
1520 Cysteine by Hypohalous Acid to Give Cysteine Sulfenic Acid, *J. Am Chem Soc*, 129, 14082-14091,  
1521 2007.

1522 Parrella J. P., Jacob D. J., Liang Q., Zhang Y., Mickley L. J., Miller B., Evans, M. J., Yang X., Pyle J. A.,  
1523 Theys N., and Van Roozendaal M.: Tropospheric bromine chemistry: implications for present and  
1524 pre-industrial ozone and mercury, *Atmos. Chem. Phys.*, 12, 6723-6740, 2012.

1525 Pratte P. and Rossi M. J.: The heterogeneous kinetics of HOBr and HOCl on acidified sea salt and  
1526 model aerosol at 40–90% relative humidity and ambient temperature, *Physical Chemistry Chemical*  
1527 *Physics*, 8, 3988–4001, 2006.

1528 Read K. A., Mahajan A. S., Carpenter L. J., Evans M. J., Faria B. V. E., Heard D. E., Hopkins J. R., Lee L.  
1529 D., Moller S. J., Lewis A. C., Mendes L., McQuaid J. B., Oetjen H., Saiz-Lopez A., Pilling M. J. and Plane  
1530 J. M. C., Extensive halogen-mediated ozone destruction over the tropical Atlantic Ocean, *Nature*,  
1531 453, doi:10.1038/nature07035, 1232-1235, 2008.

1532 Roberts, T. J., Braban, C. F., Martin, R. S., Oppenheimer, C., Adams, J. W., Cox, R. A., Jones R. L. and  
1533 Griffiths., P. T, Modelling reactive halogen formation and ozone depletion in volcanic plumes. *Chem.*  
1534 *Geol.*, 263,151-163, 2009.

1535 Roberts T.J., Martin R.S, Jourdain L.,: Reactive halogen chemistry in Mt Etna’s volcanic plume: the  
1536 influence of total Br, high temperature processing, aerosol loading and plume dispersion, *ACPD*,  
1537 2014.

1538 Saiz-Lopez A., and von Glasow R., Reactive halogen chemistry in the troposphere, *Chem Soc Rev*,  
1539 41,6448-6472, 2012.

1540 Sander R., Keen W. C., Pszenny A. A. P., Arimoto R., Ayers G. P., Baboukas E., Caine J. M., Crutzen P.  
1541 J., Duce R. A., Hönninger G., Huebert B. J., Maenhaut W., Mihalopoulos N., Turekian V. C., and Van  
1542 Dingenen R.: Inorganic bromine in the marine boundary layer: a critical review, *Atmos. Chem. Phys.*,  
1543 3, 1301-1336, 2003.

1544 Sander R., Baumgaertner A., Gromov S., Harder H., Jöckel P., Kerckweg A., Kubistin D., Regelin E.,  
1545 Riede H., Sandu A., Taraborelli D., Tost H. and Xie Z.-Q.: The atmospheric chemistry box model  
1546 CAABA/MECCA-3.0, *Geosci. Model Dev.*, 4, 373–380, 2011.

1547 Sander R., Compilation of Henry's Law Constants for Inorganic and Organic Species of Potential  
1548 Importance in Environmental Chemistry (Version 3), <http://www.henrys-law.org> accessed November  
1549 2013, 1999.

1550 Schmodzin L. and von Glasow R.: Do organic surface films on sea salt aerosols influence atmospheric  
1551 chemistry? – a model study, *Atmos. Chem. Phys.*, 7, 5555-5567, doi:10.5194/acp-7-5555-2007, 2007.

1552 Schroeder W.H., Anlauf K. G., Barrie L. A., Lu J. Y., Steffen A., Schneeberger D. R. and Berg T.: Arctic  
1553 springtime depletion of mercury, *Nature*, 394, 331-332, doi:10.1038/28530, 1998.

1554 Schweizer F., Mirabel P. and George C., Uptake of hydrogen halides by water droplets, *J. Phys Chem*  
1555 *A.*, 104, 72-76, 2000.

1556 Seinfeld, John H. ; Pandis, Spyros N. *Atmospheric Chemistry and Physics - From Air Pollution to*  
1557 *Climate Change (2nd Edition)*. John Wiley & Sons, accessed November 2013, 2006

1558 Simpson W.R., von Glasow, R., Riedel K., Anderson P., Ariya P., Bottenheim J., Burrows J., Carpenter  
1559 L. J., Friess U., Goodsite M. E., Heard D., Hutterh M., Jacobi H.-W., Kaleschke L., Neff B., Plance J.,  
1560 Platt U., Richter A., Roscoe H., Sander R., Shepson P., Sodeau J., Steffen A., Wagner T., and Wolff E.:  
1561 Halogens and their role in polar boundary-layer ozone depletion, *Atmos. Chem. Phys.*, 7, 4375–4418,  
1562 2007.

1563 Vogt R., Crutzen P. J., and Sander R.: A mechanism for halogen release from sea-salt aerosol in the  
1564 remote marine boundary layer, *Nature*, 383, 327-330, 1996.

1565 Von Glasow R. and Sander R.: Variation of sea salt aerosol pH with relative humidity, *Geophysical*  
1566 *Research Letters*, 28, 2, 247-250, 2001.

1567 Von Glasow R., Sander R., Bott, A., Crutzen P. J.: Modeling halogen chemistry in the marine boundary  
1568 layer 1. Cloud-free MBL, *Journal of Geophysical Research* 107, D17, 4341,  
1569 doi:10.1029/2001JD000942, 2002.

1570 Von Glasow R., von Kuhlmann R., Lawrence M. G., Platt U., and Crutzen P. J.: Impact of reactive  
1571 bromine chemistry in the troposphere, *Atmos. Chem. Phys.*, 4, 2481-2497, 2004.

1572 Von Glasow, R.: *Atmospheric Chemistry in Volcanic Plumes*, *PNAS*, 107, 15, 6594-6599, 2010.

- 1573 Wachsmuth M., Gäggeler H. W., von Glasow R., Ammann M. : Accommodation coefficient of HOBr  
1574 on deliquescent sodium bromide aerosol particles, *Atmos. Chem. Phys.*, 2, 121–131, 2002.
- 1575 Wang T. X. and Margareem D. W.: Kinetics of Reversible Chlorine Hydrolysis: Temperature  
1576 Dependence and General-Acid/ Base-Assisted Mechanisms, *Inorg. Chem.*, 33, 1050-1055, 1994.
- 1577 Wexler A. S. and Clegg S. L.: Atmospheric aerosol models for systems including the ions  $H^+$ ,  $NH_4^+$ ,  $Na^+$ ,  
1578  $SO_4^{2-}$ ,  $NO_3^-$ ,  $Cl^-$ ,  $Br^-$  and  $H_2O$ . *J. Geophys. Res.* 107, No. D14, 4207-4220, 2002.
- 1579 Wilson, T.R.S.: Salinity and the major elements of sea water. In: Riley, J.P., Skirrow, G. (Eds.),  
1580 *Chemical Oceanography* (1, 2 Edition). Academic, Orlando FL, 365 – 413, 1975.
- 1581 Yang, X., Cox R. A., Warwick N. J., Pyle J. A., Carver G. D., O'Connor F. M., and Savage N. H.:  
1582 Tropospheric bromine chemistry and its impacts on ozone: A model study, *J. Geophys. Res.*, 110,  
1583 D23311, doi:10.1029/2005JD006244., 2005.
- 1584



**Table 1. Summary of experimental data reported on HOBr uptake coefficient and HOBr<sub>(aq)</sub> reaction kinetics under tropospheric conditions.**

Aerosol or Solution	Temperature K	$k_{\text{ter}}$ $\text{M}^{-2} \text{s}^{-1}$	$k^{\text{I}}$ $\text{s}^{-1}$	$k^{\text{II}}$ $\text{M}^{-1} \text{s}^{-1}$	$\gamma_{\text{HOBr}}$	$\alpha_{\text{HOBr}}$	Ref.
<b>HOBr + Cl<sup>-</sup><sub>(aq)</sub></b>							
HCl-acidified NaCl aerosol with HCl:NaCl = 0.1:1	298	-	-	-	> 0.2	-	<sup>a</sup>
H <sub>2</sub> SO <sub>4</sub> -acidified sea-salt aerosol with H <sub>2</sub> SO <sub>4</sub> :NaCl = 1.45:1	296	-	10 <sup>3</sup>	-	10 <sup>-3</sup> -10 <sup>-2</sup>	-	<sup>b</sup>
BrCl <sub>(aq)</sub> solution, pH = 6.4	298	2.3·10 <sup>10</sup>	-	-	-	-	<sup>c</sup>
<b>HOBr+Br<sup>-</sup><sub>(aq)</sub></b>							
HOBr uptake onto supersaturated NaBr <sub>(aq)</sub> , Br <sup>-</sup> <sub>(aq)</sub> > 0.2 M, at very low [HOBr <sub>(g)</sub> ]	296 ±2	-	-	-	-	0.6	<sup>d</sup>
Br <sub>2(aq)</sub> solution, pH = 2.7-3.8	298	1.6·10 <sup>10</sup>	-	-	-	-	<sup>e</sup>
Br <sub>2(aq)</sub> solution, pH = 1.9-2.4	298	1.6(±0.2)·10 <sup>10</sup>	-	-	-	-	<sup>f</sup>

<sup>a</sup>Abbatt and Waschewsky (1998)

<sup>b</sup>Pratte and Rossi (2006)

<sup>c</sup>Liu and Margareem (2002)

<sup>d</sup>Wachsmuth et al. (2002)

<sup>e</sup>Eigen and Kustin (1962)

<sup>f</sup>Beckwith et al. (1996)

**Table 2. Extraction of second-order rate constant values,  $k''$  from reported experimental data. For HOBr+Br,  $k''$  is derived from reported termolecular rate constants using  $k'' = k_{\text{ter}} \cdot [\text{H}^+_{(\text{aq})}]$ . For HOBr+Cl-  $k''$  is derived from a reported termolecular rate constant using  $k'' = k_{\text{ter}} \cdot [\text{H}^+_{(\text{aq})}]$  and from reported first-order rate constant data,  $k'$  using  $k'' = k' / [\text{Cl}^-_{(\text{aq})}]$ . Molarity and Activity of  $\text{Cl}^-_{(\text{aq})}$  and  $\text{H}^+_{(\text{aq})}$  were calculated using the E-AIM model at 298.15 K. See Methods.**

Experiment	T K	RH %	wt% H <sub>2</sub> SO <sub>4</sub>	pH	Cl <sup>-</sup> <sub>(aq)</sub> Activity M	k <sub>ter</sub> M <sup>-2</sup> s <sup>-1</sup>	k' s <sup>-1</sup>		k'' M <sup>-1</sup> s <sup>-1</sup>		Ref.
<b>HOBr+Br<sup>-</sup></b>											
Br <sub>2(aq)</sub>	293	-	-	2.7-3.6	-	1.6·10 <sup>10</sup>	-		4·10 <sup>6</sup> - 3.2·10 <sup>7</sup>		a
Br <sub>2(aq)</sub>	298	-	-	1.9-2.4	-	1.6 (±0.2)·10 <sup>10</sup>	-		6.1·10 <sup>7</sup> - 1.9·10 <sup>8</sup>		b
<b>HOBr+Cl<sup>-</sup></b>											
BrCl <sub>(aq)</sub>	298	-	-	6.4	2.0	2.3·10 <sup>10</sup>	-		8.8·10 <sup>3</sup>		c
							(α = 0.2 <sup>*</sup> )	(α = 0.02 <sup>*</sup> )	(α = 0.2 <sup>*</sup> )	(α = 0.02 <sup>*</sup> )	
H <sub>2</sub> SO <sub>4</sub> :NaCl (1.45:1)	296	77	31.7	-0.84	0.056		922	1855	1.6·10 <sup>4</sup>	3.3·10 <sup>4</sup>	d
	296	79	30.00	-0.75	0.069		1050	2510	1.5·10 <sup>4</sup>	3.6·10 <sup>4</sup>	
	296	80	29.1	-0.71	0.076		1140	3010	1.5·10 <sup>4</sup>	3.9·10 <sup>4</sup>	
	296	85	24.2	-0.48	0.127		800	1485	6.3·10 <sup>3</sup>	1.2·10 <sup>4</sup>	
	296	90	17.7	-0.21	0.209		995	2355	4.8·10 <sup>3</sup>	1.1·10 <sup>4</sup>	
H <sub>2</sub> SO <sub>4</sub> :NaCl (1.45:1)NSS	296	77	31.7	-0.84	0.056		1960	44000	3.5·10 <sup>4</sup>	7.8·10 <sup>5</sup>	d
H <sub>2</sub> SO <sub>4</sub> :NaCl (1.45:1) RSS	296	77	31.7	-0.84	0.056		545	795	9.6·10 <sup>3</sup>	1.4·10 <sup>4</sup>	d
	296	79	30.00	-0.75	0.069		720	1225	1.0·10 <sup>4</sup>	1.8·10 <sup>4</sup>	
	296	80	29.1	-0.71	0.076		1090	2600	1.4·10 <sup>4</sup>	3.4·10 <sup>4</sup>	
	296	85	24.2	-0.48	0.127		815	1580	6.4·10 <sup>3</sup>	1.2·10 <sup>4</sup>	
	296	90	17.7	-0.21	0.209		710	1210	3.4·10 <sup>3</sup>	5.8·10 <sup>3</sup>	

<sup>a</sup>Termolecular rate constant reported by Eigen and Kustin (1962)

<sup>b</sup>Termolecular rate constant reported by Beckwith et al. (1996)

<sup>c</sup>Termolecular rate constant reported by Liu and Magarem (2001) for buffered aerosol containing Cl<sup>-</sup><sub>(aq)</sub> at pH = 6.4 at T = 298 K.

<sup>d</sup>First-order rate constant,  $k'_{\text{rxn}}$  data reported by Pratte and Rossi (2005) for aerosol mixture at H<sub>2</sub>SO<sub>4</sub>:NaCl = 1.45, for laboratory sea-salt, natural sea-salt (nss) or recrystallised sea-salt (rss). Pratte and Rossi (2006) assumed two different accommodation coefficients (α = 0.2, α = 0.02) in the derivation of  $k'_{\text{rxn}}$  values from their uptake experiments, the former being closest to α = 0.6 reported on NaBr<sub>(aq)</sub> aerosol by Wachsmuth et al. (2002).

**Table 3. Underlying rate constant data ( $k_1$ ,  $k_{-1}$ ,  $k_0$ ,  $k_H$ ) used in  $k^{\text{II}}$  parameterisations of Figure 1.**

	HOB <sub>r</sub> +Br	HOB <sub>r</sub> +Cl
$k_1, \text{M}^{-1} \text{s}^{-1}$	$5 \cdot 10^8 \text{ b,a}$	$1.2 \cdot 10^4 \text{ c}$
$k_{-1}, \text{s}^{-1}$	$5 \cdot 10^8 \text{ b,a}$	$1.1 \cdot 10^4 \text{ c}$
$k_0, \text{s}^{-1}$	$10^4 \text{ a}$	$2 \cdot 10^1 \text{ c}$
$k_H, \text{M}^{-1} \text{s}^{-1}$	$2 \cdot 10^{10} \text{ a}$	$2 \cdot 10^{10} \text{ c}$

a: estimated in this study

b: derived from Eigen and Kustin (1962)

c: derived from Kumar and Margerum (1987)

**Table 4 Predicted uptake coefficients compared to reported uptake on experimental aerosol**

\* Br<sup>-</sup> concentration prior to aerosol dehumidifying (reported reduction in volume during dehumidifying indicates actual concentration may be a factor of ~3 higher)

\*\* (reported modal radius, although particles >0.2 μm exist within the size spectrum)

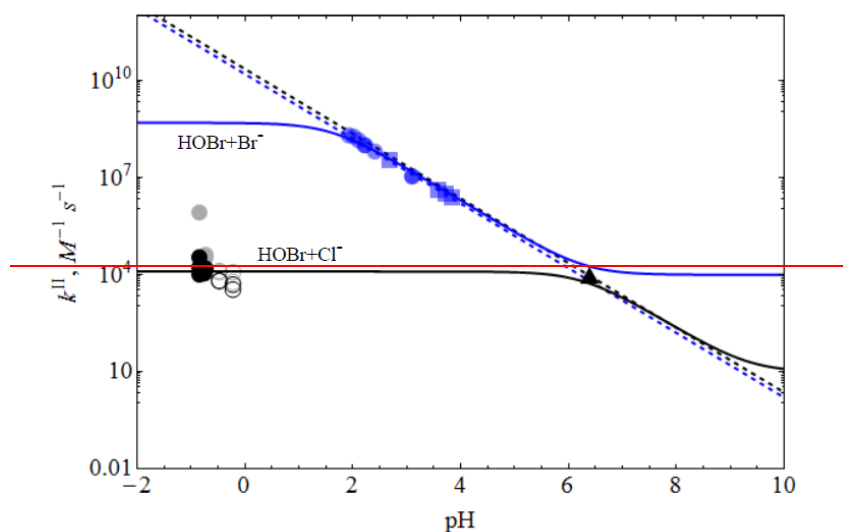
Experimental aerosol:	NaBr aerosol (Wachsmuth et al., 2002) supersaturated NaBr <sub>(aq)</sub>	HCl-acidified NaCl aerosol (Abbatt and Waschewsky, 1998) HCl/NaCl = 0.1:1	H <sub>2</sub> SO <sub>4</sub> -acidified sea-salt aerosol (Pratte and Rossi, 2006) H <sub>2</sub> SO <sub>4</sub> /NaCl = 1.45:1	
γ <sub>H<sub>2</sub>OBr</sub> : observed	0.6 ± 0.2	> 0.2	(0.1-0.3)·10 <sup>-2</sup> at RH 40 to 70 %	(1.0±0.2)·10 <sup>-2</sup> at RH ≥ 76 %
<b>Uptake Model Parameters:</b>				
Temperature	298.15	298.15	298.15	298.15
α (accommodation coefficient)	0.6	0.6	0.6	0.6
Na concentration (μmol/m <sup>3</sup> )	-	0.2	0.8	0.8
RH, %	80	76	50	80
[Br <sub>(aq)</sub> <sup>-</sup> ], M	> 0.2*	-	-	-
[Cl <sub>(aq)</sub> <sup>-</sup> ], M (E-AIM)	-	6.6	4.4·10 <sup>-3</sup>	7.6·10 <sup>-2</sup>
[H <sub>(aq)</sub> <sup>+</sup> ], M (E-AIM)	~2·10 <sup>-6</sup>	2.3	83	5
pH	~6	-0.3	-1.9	-0.7
k <sup>II</sup> , M <sup>-1</sup> s <sup>-1</sup>	3·10 <sup>4</sup>	10 <sup>4</sup>	10 <sup>4</sup>	10 <sup>4</sup>
k <sub>terr</sub> , M <sup>-2</sup> s <sup>-1</sup>	1.6·10 <sup>10</sup>	2.3·10 <sup>10</sup>	2.3·10 <sup>10</sup>	2.3·10 <sup>10</sup>
Particle radius, μm	>0.03**	1.	~0.17	~0.17
wt%H <sub>2</sub> SO <sub>4</sub>	-	-	48	29
H <sub>2</sub> OBr solubility, M atm <sup>-1</sup>	6.1·10 <sup>3</sup>	6.1·10 <sup>3</sup>	364	364
H <sub>2</sub> OBr Diffusion constant, cm <sup>2</sup> s <sup>-1</sup>	1.42·10 <sup>-5</sup>	1.42·10 <sup>-5</sup>	5.5·10 <sup>-6</sup>	1.0·10 <sup>-5</sup>
γ <sub>H<sub>2</sub>OBr</sub> : old approach (where k <sup>I</sup> = k <sub>terr</sub> ·[X <sub>(aq)</sub> <sup>-</sup> ]·[H <sub>(aq)</sub> <sup>+</sup> ])	0.1 < γ <sub>H<sub>2</sub>OBr</sub> ≤ 0.6	0.6	0.6	0.6
γ <sub>H<sub>2</sub>OBr</sub> : new approach (where k <sup>I</sup> = k <sup>II</sup> ·[X <sub>(aq)</sub> <sup>-</sup> ])	0.1 < γ <sub>H<sub>2</sub>OBr</sub> ≤ 0.6	0.6	2·10 <sup>-4</sup>	7·10 <sup>-3</sup>

1 **Figure 1**

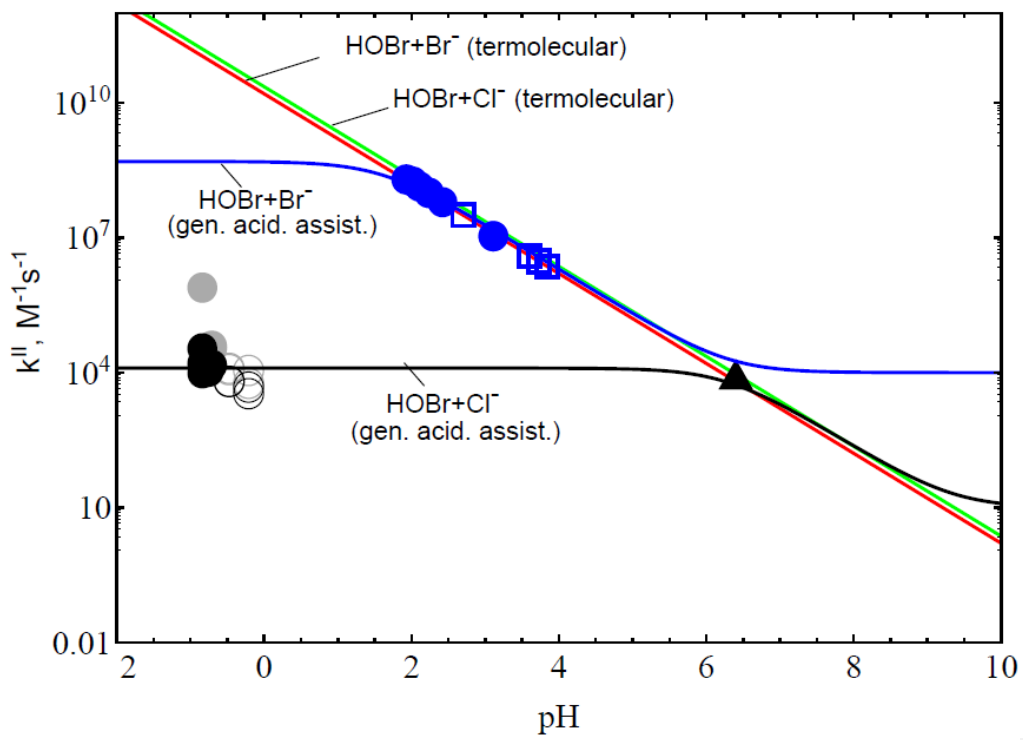
2 Second order rate constants for the reaction of HOBr with Br<sup>-</sup> and Cl<sup>-</sup> as a function of pH.  
3 Experimental estimates for k<sup>II</sup> for HOBr+Br<sup>-</sup> derived from data from Eigen and Kustin (1962) and  
4 Beckwith et al. (1996), (blue squares and circles respectively) are shown alongside model estimate  
5 (blue line) according to the acid-assisted mechanism. The blue-dottedred line denotes the k<sup>II</sup> rate  
6 constant assuming termolecular kinetics across all pH. Experimental estimates for k<sup>II</sup> for HOBr+Cl<sup>-</sup>  
7 derived from data from Liu and Margareum (2001) at pH = 6.4 (black triangle) and Pratte and Rossi  
8 (2006) at pH -1 to 0 (black and grey disks for data at RH = 77-80%, open circles for RH = 85-90%), are  
9 shown alongside model estimate (black line) according to the general acid-assisted mechanism. The  
10 black-green dotted line denotes the k<sup>II</sup> rate constant assuming termolecular kinetics across all  
11 pH. denotes k<sup>II</sup> predicted using the three body approach that assumes termolecular kinetics across all  
12 pH.

Formatted: Superscript

Formatted: Superscript



13



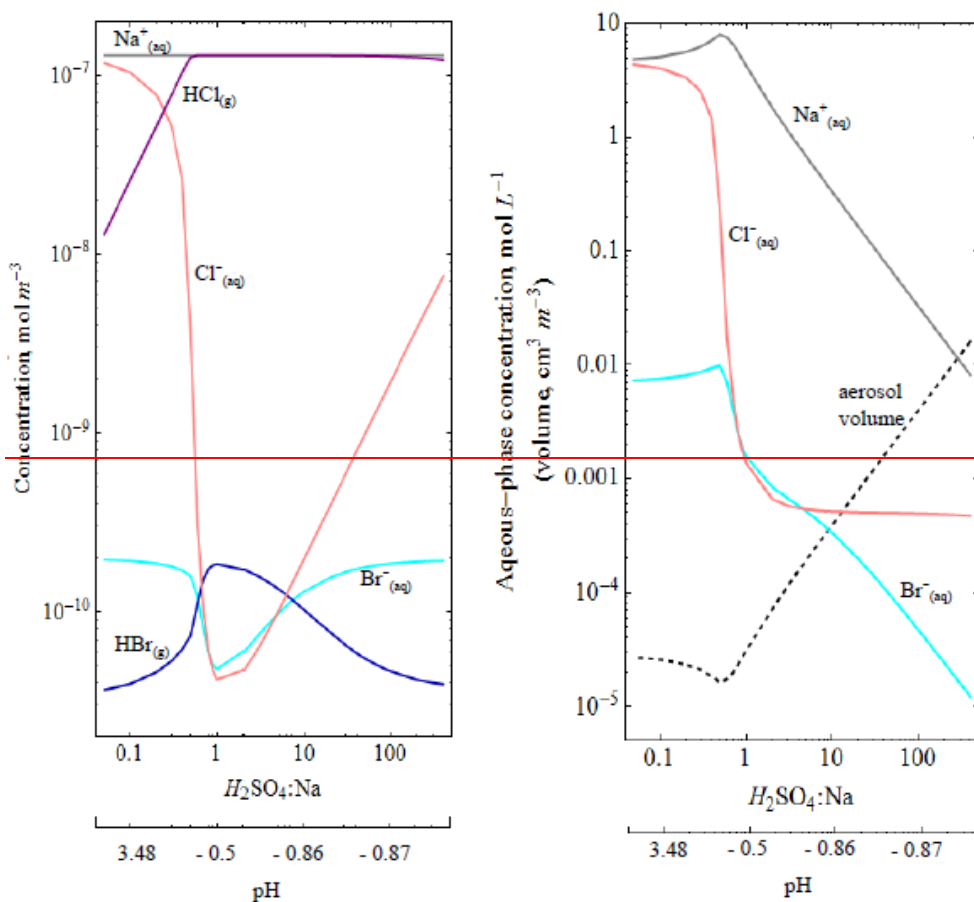
14

15

16 **Figure 2**

17 Gas-aerosol partitioning according to E-AIM thermodynamic model III for a progressively  $H_2SO_4$ -  
18 acidified model sea salt aerosol. Temperature is 298 K, relative humidity is 80%. Na concentration  
19 was set to  $1.3 \cdot 10^{-7}$  moles/ $m^3$ , equivalent to a marine environment PM10 of  $10 \mu g/m^3$  (Seinfeld and  
20 Pandis, 2006) assuming  $NaCl_{(aq)}$ . Molar concentrations (mole/ $m^3$ ) of  $Na^+$  (gray),  $HCl_{(g)}$  (purple),  $Cl^-_{(aq)}$  (pink),  
21  $Br^-_{(aq)}$  (light blue),  $HBr_{(g)}$  (dark blue) are shown as well as aqueous phase concentration (mol  
22  $L^{-1}$ ) as a function of  $H_2SO_4:Na$  for  $Cl^-_{(aq)}$  (pink),  $Br^-_{(aq)}$  (light blue), and  $Na^+_{(aq)}$  (grey). Aerosol volume  
23 ( $cm^3/m^3$ ) is shown by black dotted line.

Formatted: Left



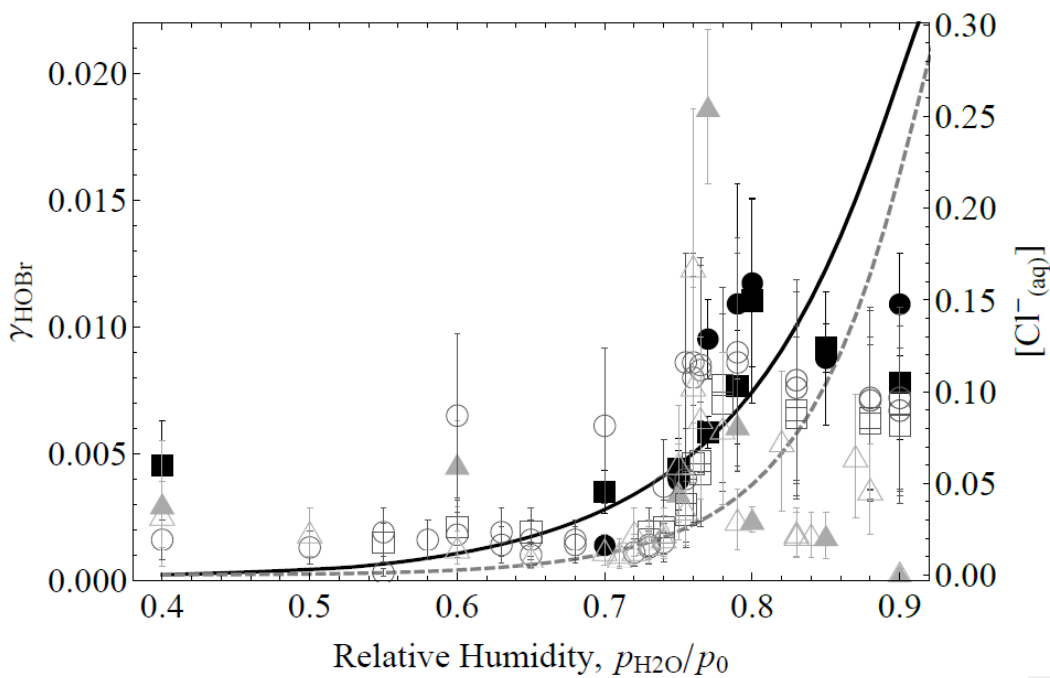
24

25

26 **Figure 32**

27 Dependence of reactive uptake coefficient for HOBr on relative humidity (RH) in the experiments of  
28 Pratte and Rossi (2006) on H<sub>2</sub>SO<sub>4</sub>-acidified sea-salt aerosol (H<sub>2</sub>SO<sub>4</sub>:NaCl = 1.45:1) at 296 K, on  
29 acidified sea-salt (circles), recrystallized sea-salt (squares) and natural sea-salt (triangles), under two  
30 experimental set-ups: (i) the observed rate of HOBr<sub>(g)</sub> decay for a measured aerosol size distribution,  
31 with effective radius ranging over 165-183 nm (filled shapes), and (ii) a survey type mode with HOBr  
32 depletion monitored as a function of RH (unfilled shapes, with reported error estimated at 30-50%)  
33 over a constant reaction time. ~~The Also shown is the modelled uptake coefficient for HOBr (black~~  
34 ~~line), and the Cl<sup>-</sup><sub>(aq)</sub> molarity (dotted line) as used within the uptake calculation.~~

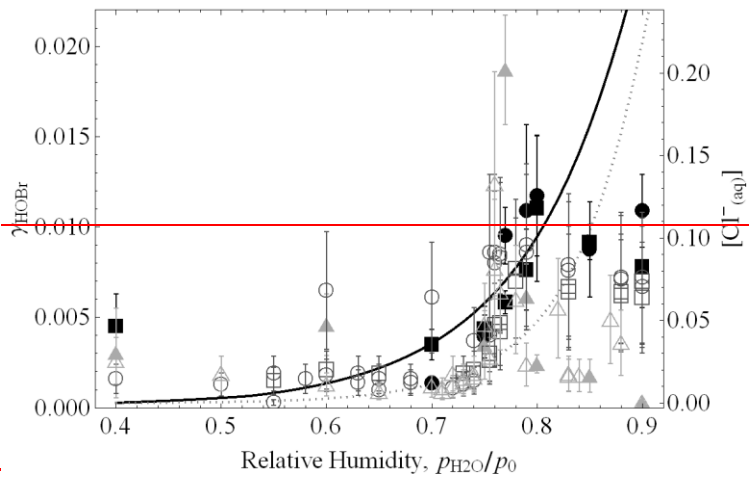
35 ~~was calculated for particles with 170 nm effective radius at the experimental temperature of 296 K,~~  
36 ~~and an aerosol mixture of H<sub>2</sub>SO<sub>4</sub>:NaCl ratio 1.45:1. Within the uptake calculation,  $k^{\dagger} = k^{\#} [\text{Cl}^{-}_{(\text{aq})}]$~~   
37 ~~where  $k^{\#}$  is according to the new parameterisation (Figure 1) and Cl<sup>-</sup><sub>(aq)</sub> molarity (dotted line) and~~  
38 ~~activity coefficients were calculated using the E-AIM thermodynamic model at 298 K.~~



39 ~~Uptake calculations based on the termolecular approach that yield  $\gamma \sim 0.6$  across all RH (not shown).~~



41 -  
42



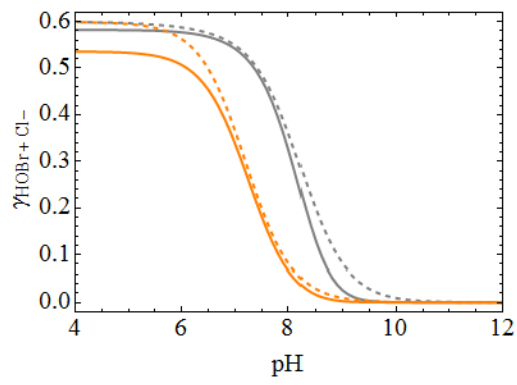
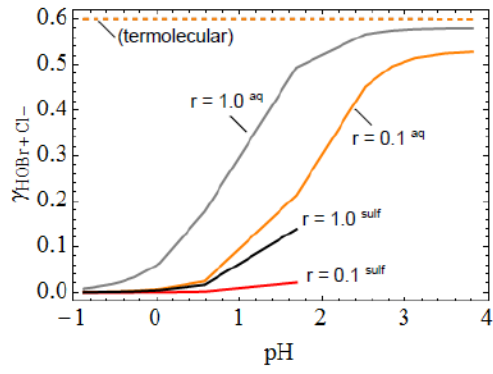
43 | **Figure 43**

44 | Variation in the HOBr uptake coefficient with pH, for reaction of HOBr with (upper) Cl- and (lower)  
45 | Br- on  $\text{H}_2\text{SO}_4\text{-H}_2\text{SO}_4$ -acidified sea-salt aerosol. Grey and orange lines denote uptake onto 1 and 0.1  
46 |  $\mu\text{m}$  radius particles, respectively. Black and red lines denote uptake onto 1 and 0.1  $\mu\text{m}$  radius  
47 | particles calculated using  $\text{H}^+$  and  $\text{D}_1$  parameterisations for sulfuric acid (rather than water), shown  
48 | only for  $\text{H}_2\text{SO}_4\text{:Na}$  ratios greater than 0.5. Relative humidity is set to 80% and Na concentration  
49 |  $1.3 \cdot 10^{-7}$  moles/ $\text{m}^3$  (equivalent to a PM10 of  $10 \mu\text{g}/\text{m}^3$  in the marine environment, Seinfeld and  
50 | Pandis, 2006). For comparison, uptake coefficients calculated assuming termolecular kinetics are  
51 | also shown (dashed lines).

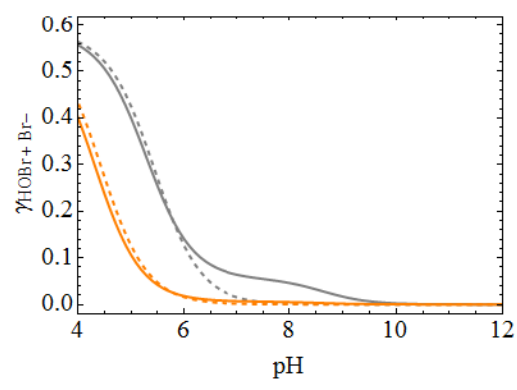
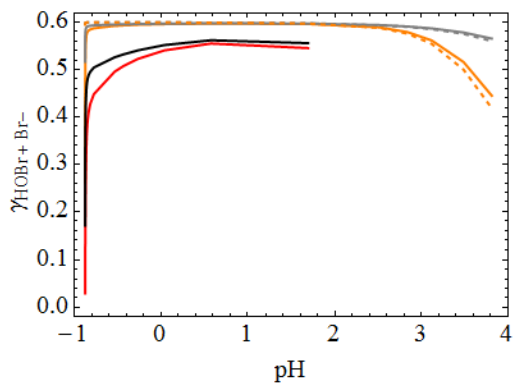
Formatted: Subscript

Formatted: Subscript

HOBr + Cl<sup>-</sup> + H<sup>+</sup>

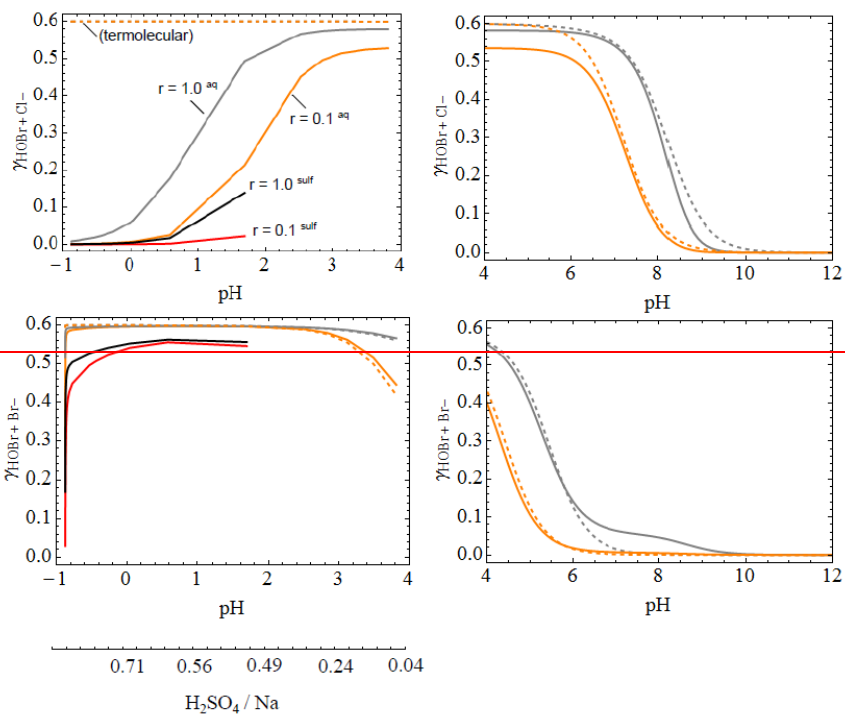


HOBr + Br<sup>-</sup> + H<sup>+</sup>



0.71 0.56 0.49 0.24 0.04

H<sub>2</sub>SO<sub>4</sub> / Na



53

54

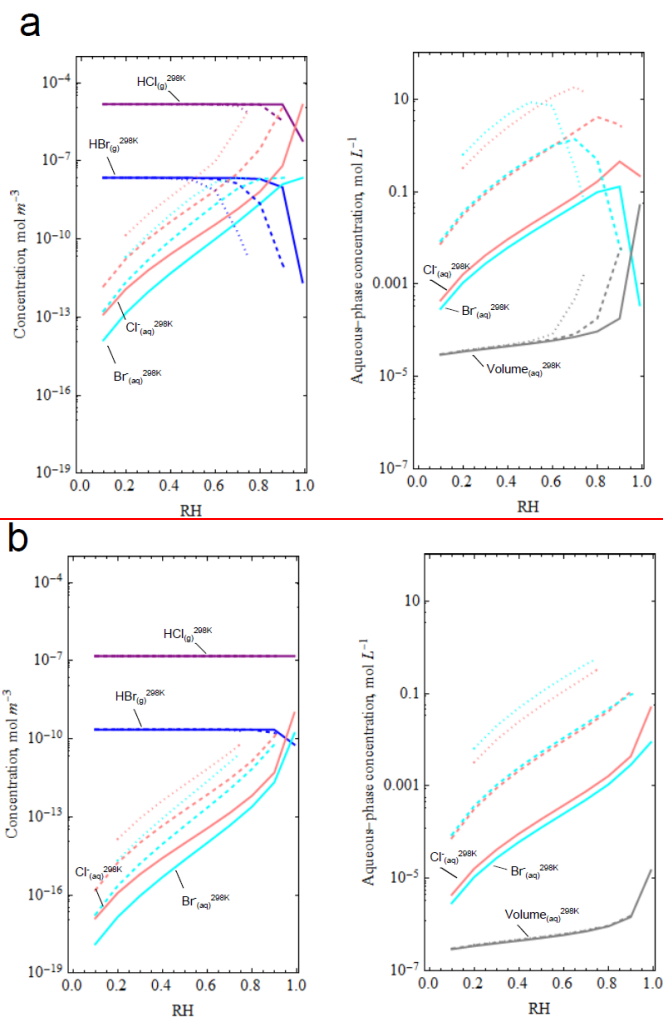
55

56

**Figure 5**

57 Predicted volcanic plume composition for (a) strong plume ( $30 \mu\text{mol}/\text{m}^3$ , corresponding to 1 ppmv  $\text{SO}_2$  at 4 km in a standard atmosphere) and (b) weak plume ( $0.3 \mu\text{mol}/\text{m}^3$ , corresponding to 0.01 ppmv  $\text{SO}_2$ ) strengths. Gas-aerosol partitioning predicted according to E-AIM thermodynamic model for a volcanic plume that has molar composition  $(\text{SO}_2):\text{HCl}:\text{HBr}:\text{SO}_4^{2-} = (1):0.5:0.00075:0.01$ , representing a typical Arc volcano emission such as Etna. Plume halogen composition (in  $\text{mol m}^{-3}$  of atmosphere) and aqueous-phase composition (in  $\text{mol L}^{-1}$ ) are shown as a function of RH, and for three different temperatures: 293, 263 and 243 K (thick, dashed and dotted lines, respectively), for conditions where aerosol is predicted to be purely in liquid form. Concentrations of  $\text{HCl}_{(\text{g})}$  (purple),  $\text{HBr}_{(\text{g})}$  (blue),  $\text{Cl}_{(\text{aq})}^-$  (pink),  $\text{Br}_{(\text{aq})}^-$  (cyan) with aqueous-phase volume density ( $\text{cm}^3$  per  $\text{m}^3$ , grey lines). For clarity, only 298 K model output is labelled.

Formatted: Left



67

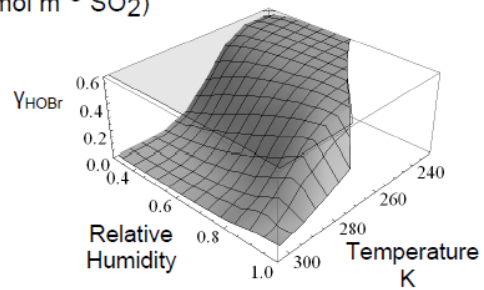
68 | **Figure 64**

69 HOB<sup>+</sup>Cl<sup>-</sup> and HOB<sup>+</sup>Br<sup>-</sup> reactive uptake coefficients onto volcanic sulphate aerosol particles of 1 μm radius, calculated using our revised HOB<sup>+</sup> kinetics.  
70 Calculations are performed for a typical Arc or subduction zone volcanic plume composition containing a (SO<sub>2</sub>):HCl:H<sub>2</sub>SO<sub>4</sub>:HBr molar ratio mixture of  
71 1:0.5:0.01:0.00075. The plume strength is 30, ~~3~~ or 0.3 μmol/m<sup>3</sup>, equivalent to approximately 1 ~~or, 0.1~~ 0.01 ppmv SO<sub>2</sub> at 4 km altitude (US standard  
72 atmosphere). ~~Also shown is the HOB<sup>+</sup>Br<sup>-</sup> uptake coefficient for an evolved plume where significant BrO chemistry is underway, and it is assumed Br~~  
73 ~~concentrations have become depleted to the level: [Br<sup>-</sup><sub>(eq)] = 1.3/(1.8·10<sup>4</sup>) = 7·10<sup>-5</sup>·[Cl<sup>-</sup><sub>(eq)]</sub>. For comparison</sub>~~ Conversely, uptake coefficients calculated using  
74 the termolecular approach, yielding high accommodation-limited values across all parameter space, ~~typically accommodation-limited~~ (light grey).

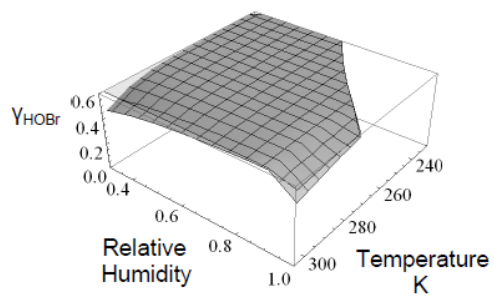
**Strong plume**

( $30 \mu\text{mol m}^{-3} \text{SO}_2$ )

**HOB<sub>r</sub>+Cl<sup>-</sup>**

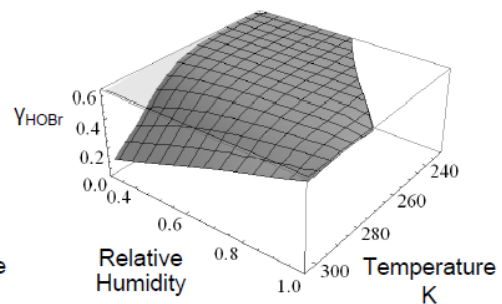
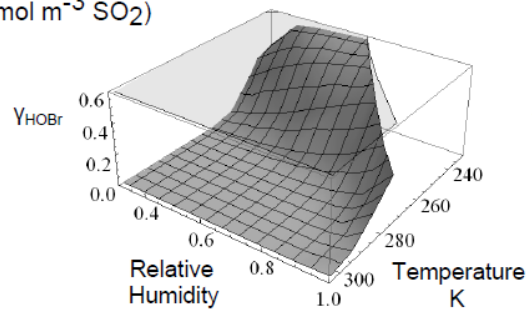


**HOB<sub>r</sub>+Br<sup>-</sup>**



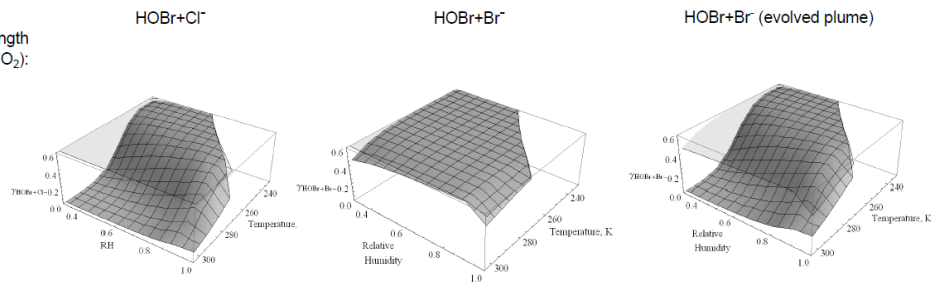
**Weak plume**

( $0.3 \mu\text{mol m}^{-3} \text{SO}_2$ )

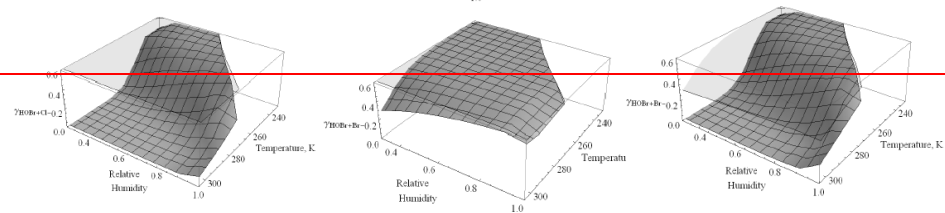


Plume Strength  
( $\mu\text{mol m}^{-3} \text{SO}_2$ ):

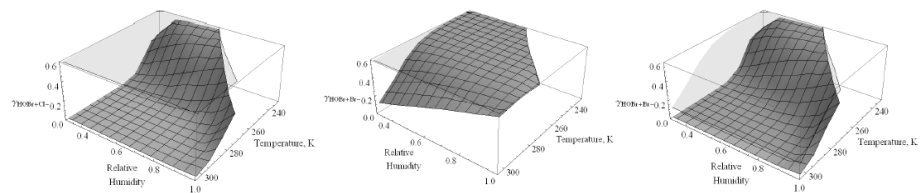
30



3



0.3



Formatted: Justified